UNIVERSITY OF CALIFORNIA, SAN DIEGO

Mechanisms of deprivation-induced map plasticity at layer 4 to layer 2/3 synapses in rat barrel cortex

A dissertation submitted in partial satisfaction of the

requirements for the degree Doctor of Philosophy

in

Biology

by

Kevin James Bender

Committee in charge:

Professor Daniel E. Feldman, Chair
Professor Edward M. Callaway
Professor Jeffry S. Isaacson
Professor William B. Kristan Jr.
Professor Massimo Scanziani

2005

The dissertation of Kevin James Bender is approved, and it is acceptable in quality and form for publication on microfilm:

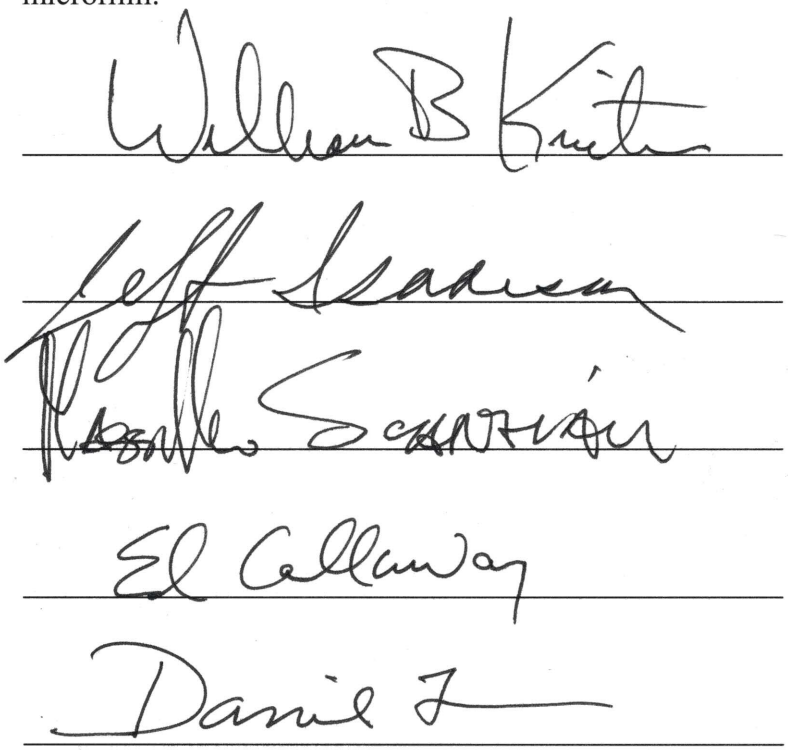

Chair

University of California, San Diego

2005

Acknowledgements

I could not have asked for a better advisor and mentor than Dan Feldman, and I value his example of how science should be done. I would also like to thank members of my thesis committee, Ed Callaway, Jeff Isaacson, Bill Kristan, and Massimo Scanziani, as well as other members of the UCSD neuroscience community, most notably Marla Feller, for their support and guidance. I am indebted to two very talented histologists, Juliana Rangel and Suvarna Deshmukh, for their extremely meticulous and valuable help with anatomical studies. Tansu Celikel provided coding expertise that enriched those same studies. Cara Allen helped train me as a physiologist, and pioneered experiments in the lab that have allowed us to collaborate to this day.

I have been extremely lucky to work in an environment full of friends and family. It continues to be an honor to work with my wife, Vanessa. Her support, both in and out of lab, knows no end. Past and present members of Dan's lab, DJ Brasier, Elisabeth Foeller, Jason Wolfe, Patrick Drew, Shantanu Jadhav, David House, and those mentioned above, have made work a joy.

Special thanks go to my parents, Jim and Michelle, and the rest of my family, which has grown considerably in the last year. My parents, who have been the principal teachers in my life, have always been supportive and encouraging. This work is dedicated to them.

Chapter 3, in full, is a republication of the material as it appears in Bender, K.J., Rangel, J., Feldman, D.E., Development of columnar topography in the

excitatory layer 4 to layer 2/3 projection in rat barrel cortex. *J Neurosci.* 23, 8759-8770 (2003). The dissertation author was the primary investigator and first author of this paper.

Table of Contents

List of Figures and Tables

Chapter 1:

Chapter 2:

Chapter 3:

Vita

2000 B.S., Biology, Biomedical Engineering Systems, Music, *cum laude*, Tufts University, Meford, MA

2005 Ph.D., Biology, University of California, San Diego

Publications

Peer reviewed competitive journals:

Bender VA, Bender KJ, Brasier DJ, Feldman DE. Two coincidence detectors for STDP in somatosensory cortex. Submitted, 2005.

Bender KJ, Rangel J, Feldman DE. Development of columnar topography in the excitatory layer 4 to layer 2/3 projection in rat barrel cortex. J Neurosci. 2003 Sep 24; 23(25):8759-70.

Belanger JH, Bender KJ, Trimmer BA. Context dependency of a limb withdrawal reflex in the caterpillar *Manduca sexta*. J Comp Physiol [A]. 2000 Nov;186(11):1041-8.

Book chapter:

Bender KJ, Deshmukh S, Feldman DE. LTD as a mechanism for map plasticity in rat barrel cortex. *In* Development and Plasticity in Sensory Thalamus and Cortex (Ed: W. Guido, R. Erzurumlu, Z. Molnar). Kluwer Academic/Plenum Publishers, 2005 (in press).

Awards

2002 Fine Science Tools/UCSD travel award, SFN conference
2000 Howard Hughes Undergraduate Research Fellow, Tufts University
2000 Thomas & Emily Carmichael Prize Scholarship in Physiology, Tufts University

ABSTRACT OF THE DISSERTATION

Mechanisms of deprivation-induced map plasticity at

layer 4 to layer 2/3 synapses in rat barrel cortex

by

Kevin James Bender

Doctor of Philosophy in Biology

University of California, San Diego, 2005

Professor Daniel E. Feldman, Chair

Neocortical representations of sensory information are commonly arranged in topographic maps that can be modified and reorganized based on recent sensory experience. This map plasticity is thought to involve both anatomical and physiological changes of cortical circuits. In rat somatosensory cortex, it has been hypothesized that long-term synaptic depression (LTD) is a major mechanism for a common feature of cortical map plasticity, the reduction in cortical responsiveness to deprived sensory inputs. Recent work has shown that whisker deprivation weakens the layer 4 (L4) to L2/3 excitatory projection in columns deprived of their main sensory input, and that this weakening occludes subsequent attempts to induce LTD, suggesting that weakening represent, in part, LTD induced by sensory deprivation *in vivo* (Allen et al., 2003). The specific mechanisms that mediate this reduction in

projection strength, and whether they share features with LTD, remain unclear. In chapter 2, we show that deprivation-induced weakening of L4 to L2/3 inputs represents synaptic weakening, and is mediated by a reduction in presynaptic, but not postsynaptic, efficacy, consistent with known mechanisms of LTD at this synapse. Chapter 3 focuses on the development and plasticity of L4 excitatory axonal arbors, which are the main columnar projection from L4 to L2/3. These arbors develop a high degree of columnar specificity from an initially less precise projection through targeted growth within columnar bounds. This process occurs identically regardless of sensory experience, indicating that deprivation-induced plasticity at this synapse does not involve large-scale axonal reorganization. Chapter 4 shows that whisker deprivation does not alter neuron density in L4, suggesting that whisker deprivation at these ages does not involve elimination of presynaptic neurons. In chapter 5, horizontal, trans-columnar axonal pathways are analyzed for their putative role in a second feature of map plasticity, the expansion of spared cortical representations in sensory maps.

Chapter 1

Introduction

LTP and LTD as cellular mechanisms for sensory map plasticity

The ability of neural circuits to adapt to new experiences and to store information about the environment is central to brain development and learning. An important paradigm for studying this adaptive ability is sensory map plasticity, in which sensory and motor maps are modified based on recent experience, including training on learning tasks. Map plasticity occurs with highly similar functional properties across many brain areas, including primary visual, auditory, somatosensory, and motor cortex (Wiesel and Hubel, 1963; Buonomano and Merzenich, 1998; Sanes and Donoghue, 2000). However, the cellular and synaptic mechanisms that mediate map plasticity are only beginning to be understood.

Long-term potentiation (LTP) and depression (LTD) of cortical synapses emerged as prominent candidate mechanisms for cortical map plasticity relatively soon after the discovery of ocular dominance plasticity in the visual cortex (Stent, 1973; Bear et al., 1987). These mechanisms instantiate Hebbian synaptic plasticity, which can explain many features of cortical map plasticity (Hebb, 1949; Bear et al., 1987; Buonomano and Merzenich, 1998). LTP and LTD are generally hypothesized to mediate rapid components of map plasticity, while anatomical changes that often occur during map plasticity may mediate slower components.

LTD has been hypothesized to play two major roles in map development and plasticity. First, during developmental refinement of topographic projections, LTD is thought to act to weaken aberrant synapses according to Hebbian learning rules, perhaps leading ultimately to synapse elimination (Stent, 1973; Buonomano and Merzenich, 1998). Second, even after maps have formed, patterns of sensory use and

disuse powerfully regulate map topography. During this phase, LTD is thought to be involved in weakening excitatory synapses that are underused or behaviorally irrelevant, thus reducing the representation of these inputs in cortical maps (Bear et al., 1987; Singer, 1995; Buonomano and Merzenich, 1998; Ruthazer and Cline, 2004). Though the capacity for LTD may decline somewhat with age, recent studies have clearly demonstrated LTD in adults, indicating that it may contribute to both developmental and adult plasticity (Heynen et al., 1996; Manahan-Vaughan and Braunewell, 1999).

Though LTD has long been hypothesized to contribute to sensory cortical map plasticity, and despite strong evidence for LTD being involved in cerebellar learning (Boyden et al., 2004), direct evidence for LTD in cortical map plasticity was lacking until recently. In this introduction, I review recent evidence suggesting that LTD is involved in map plasticity in rat primary somatosensory cortex (S1), specifically by weakening layer 4 (L4) to L2/3 excitatory synapses deprived of their primary sensory input. Subsequent chapters explore anatomical and physiological characteristics of this synapse to determine how deprivation-induced weakening is mediated, and to test whether the physiological mechanisms of weakening induced by deprivation represent LTD induced *in vivo*.

Map plasticity in barrel cortex

In the rat primary somatosensory cortex, the ~30 large facial whiskers are represented by clusters of cells in cortical layer 4 (L4) called barrels. Barrels are arranged in a map isomorphic with the whiskers on the rat's snout (Woolsey and Van

der Loos, 1970; Welker and Woolsey, 1974), and neurons in each barrel are driven best by deflection of a single whisker, termed the principal whisker, which corresponds to the identity of the barrel within the map (Fig. 1.1A, B). Excitatory cells in each L4 barrel make a dense, columnar projection onto layer 2/3 (L2/3) neurons in the cortical column surrounding that barrel, termed the barrel column (Fig. 1.1C, D) (Petersen and Sakmann, 2001; Feldmeyer et al., 2002). The vast majority of neurons in each barrel column are driven most strongly by the anatomically appropriate principal whisker, and only weakly by neighboring, surround whiskers (Simons, 1978; Keller, 1995). Thus, an orderly map of whisker receptive fields is present across S1, and the barrels in L4 provide an anatomical reference for this functional whisker map.

The whisker receptive field map in S1 is modifiable by sensory experience. If a whisker is plucked or trimmed for several days or weeks in adolescent animals (7 to ~60 days of age), receptive fields of L2/3 cells within the corresponding column change in two ways. First, L2/3 neurons within the deprived column lose responses to the deprived principal whisker, a phenomenon called principal whisker response depression (PWRD). Second, neurons begin to respond more strongly to neighboring, spared whiskers, termed spared whisker response potentiation (SWRP). These two components of plasticity can be separated genetically and developmentally, indicating that they represent two independent mechanisms for plasticity in S1 (Glazewski and Fox, 1996; Glazewski et al., 2000). Together, PWRD and SWRP cause receptive fields in deprived columns to become dominated by neighboring, spared inputs, rather than deprived principal whisker inputs. This makes the representation of the spared

whisker expand within the whisker map (Fox, 1992; Diamond et al., 1994) (Fig. 1.2A). Highly similar components of plasticity occur in visual cortex during monocular deprivation (Sawtell et al., 2003; Frenkel and Bear, 2004).

In animals older than the first postnatal week, univibrissa rearing drived PWRD and SWRP primarily and most rapidly in L2/3, with little or no receptive field plasticity in L4 (Glazewski and Fox, 1996). This indicates that PWRD and SWRP are mediated by functional changes in intracortical, rather than subcortical, circuits. Substantial progress has been made in identifying the neural basis for PWRD. Fox's group originally hypothesized that PWRD is due to deprivation-induced weakening, perhaps LTD, of the excitatory L4 to L2/3 projection in deprived columns, which normally drives principal whisker responses in L2/3 (Glazewski and Fox, 1996; Fox, 2002) (Fig. 1.2B). Strong evidence now exists for this hypothesis (see below). In contrast, the mechanisms underlying SWRP are less clear. SWRP is likely to involve LTP, since transgenic mice with autophosphorylation-incompetent CaMKII, which lack cortical LTP, have substantially impaired SWRP (Glazewski et al., 2000; Hardingham and Fox, 2004). One possibility is that SWRP involves LTP of excitatory trans-columnar projections, which would increase surround whisker responses in L2/3 neurons However, the site(s) of LTP for SWRP are not yet known, and other mechanisms besides LTP and LTD are likely to contribute to this and other aspects of whisker map plasticity (eg., Lendvai et al., 2000; Knott et al., 2002; Shepherd et al., 2003).

Here we summarize recent work focusing on how LTD at the L4-L2/3 excitatory synapse might contribute to the first component of deprivation-induced

plasticity, PWRD. This work shows that L4-L2/3 synapses are capable of LTD *in vitro*, and that whisker deprivation induces marked LTD-like depression of these synapses *in vivo*. Recordings of spiking patterns in L4 and L2/3 *in vivo* suggest that this LTD is induced by a reversal in the precise, millisecond-scale timing of L4 and L2/3 spikes during deprivation, which is known to induce spike timing-dependent LTD at this synapse *in vitro*.

Deprivation induces LTD-like weakening of L4-L2/3 synapses *in vivo*

To determine if deprivation weakens L4-L2/3 synapses, Allen *et al.* (2003) took advantage of the fact that synaptic and cellular plasticity induced by experience *in vivo* persists and can be measured in acute, *ex vivo* brain slices (McKernan and Shinnick-Gallagher, 1997; Finnerty et al., 1999; Rioult-Pedotti et al., 2000). Rats were raised with one or more rows of whiskers plucked starting at postnatal day (P) 12, and slices were prepared 10-20 days later, after whisker map plasticity had presumably occurred (Fig. 1.3A). Slices were cut in an "across-row" plane that contained one barrel column from each of the 5 rows (termed A-E), so that spared and deprived columns could be identified unambiguously in the slice (Fig. 1.3B). Bulk synaptic strength of the L4-L2/3 projection was assayed using input-output curves in field potential and whole cell recordings, and was found to be 30-40% weaker in deprived columns than either neighboring, spared columns (Fig. 1.3C, D) or control columns from sham-plucked littermates (not shown). Plucking did not affect measures of intrinsic postsynaptic excitability, suggesting that the measured depression was due to synaptic changes (Allen et al., 2003).

To determine whether this deprivation-induced synaptic depression represents a reduction in the strength of preexisting, strong synapses, versus a failure of initially weak synapses to strengthen with development, deprivation was begun at the older age of P20, when synapses are more developed. Four to six days of deprivation starting at P20 caused the same magnitude of synaptic depression as did deprivation from P12, suggesting that deprivation does not simply cause a failure of synaptic development, but actively weakens existing synapses. In addition, the time course of depression was determined by recording in slices made from animals deprived of whiskers for 3, 5, and 7 days, beginning at P12. Significant synaptic depression was observed after 5 days of deprivation, but not 3 days, suggesting that 4-5 days of deprivation are required to alter synaptic strength at these ages (Allen, 2004, and see chapter 2).

To determine whether deprivation-induced synaptic weakening represents LTD, Allen *et al.* tested for occlusion (2003). Because LTD is typically a saturable phenomenon (Dudek and Bear, 1992; Mulkey and Malenka, 1992; Lebel et al., 2001), LTD induced by deprivation *in vivo* should occlude further LTD induction *in vitro*. Results showed that deprivation-induced synaptic weakening profoundly occluded LTD induction by low frequency stimulation (900 pulses at 1 Hz) (Fig. 1.3D). Consistent with the occlusion model, the capacity for LTP was enhanced by deprivation, indicating that deprived synapses were not merely deficient in plasticity. These findings were recently replicated (Hardingham and Fox, 2004). Thus, these experiments suggest that whisker deprivation reduces the physiological strength of L4-L2/3 synapses via LTD or an LTD-like mechanism. Similar results have been found for monocular deprivation, which causes both physiological and biochemical

signatures of LTD at L4 to L2/3 synapses in visual cortex (Heynen et al., 2003). Together, these results suggest that LTD is likely to be an important mechanism for plasticity in S1 and V1. Whether deprivation also weakens circuits through reduction in synapse or neuron number is addressed by experiments below (Chapters 3-4).

How is LTD induced during sensory deprivation *in vivo*?

At L4-L2/3 synapses *in vitro*, like at many excitatory synapses, LTP and LTD can be induced by multiple induction protocols. These include altering presynaptic firing rate (termed rate-dependent plasticity) (Madison et al., 1991; Linden and Connor, 1995), and modulating the relative timing of pre- and postsynaptic spikes on a millisecond timescale, largely independent of firing rate (spike-timing dependent plasticity, STDP) (Dan and Poo, 2004). Most models of experience-dependent cortical plasticity assume rate-dependent induction of LTP and LTD. However, Celikel *et al.* conducted experiments to determine which of these modes of LTP/LTD induction drives LTD at L4-L2/3 synapses in S1 in response to whisker deprivation and found strong evidence that STDP is the relevant mechanism (Celikel et al., 2004).

L4-L2/3 synapses in visual cortex exhibit a standard rate-dependent LTP/LTD learning rule in which presynaptic firing rates of a few Hz drive LTD, and rates > 10 Hz drive LTP (Fig. 1.4A). Though the full learning rule is not known in S1, its basic form is similar, with a cross-over point between LTP and LTD at about 10 Hz (S. Bergquist and D.E. Feldman, unpublished data). To determine whether deprivation alters spike rate in a manner appropriate to drive rate-dependent LTD at L4-L2/3 synapses *in vivo*, Celikel *et al.* made extracellular recordings from L4 and L2/3

neurons in awake, behaving rats. When all whiskers were intact, L4 and L2/3 neurons fired at mean rates of 2.7 and 2.1 Hz, respectively, across several whisker-related behavioral states. Trimming of the principal whisker corresponding to the recorded column caused mean firing rates to reduce, but only modestly, to 2.1 and 1.7 Hz, respectively (Fig. 1.4B). Because 2-4 Hz firing elicits similar, near-maximal LTD at L4-L2/3 synapses in V1, as well as in CA1 hippocampus, it seems unlikely that these modest changes in spike rate could drive rate-dependent LTD *in vivo* (Dudek and Bear, 1992; Bear, 1996; Kirkwood et al., 1996; Huber et al., 1998) (Fig. 1.4A). Indeed, the low frequency of firing observed with all whiskers intact suggests that precise spike timing, rather than firing rate, may be most relevant for plasticity *in vivo*.

How spike timing may drive LTD *in vivo* can be inferred from the precise shape of the STDP learning rule measured *in vitro*. LTP is induced at L4-L2/3 synapses when presynaptic spikes lead postsynaptic spikes by 0-15 ms. In contrast, LTD results when postsynaptic spikes lead presynaptic spikes by a longer interval of 0-50 ms (Fig. 1.4C). The longer temporal window for LTD predicts that LTD can be induced *in vivo* by two means: either by reliable post-leading-pre firing within the LTD window, or by uncorrelated spiking at low rates, which drives net LTD because uncorrelated spike trains contain more interspike delays that fall within the long LTD window than delays that fall within the brief LTP window (Feldman, 2000).

To determine whether deprivation may drive spike timing-dependent LTD *in vivo*, Celikel *et al*. measured the spiking of L4 and L2/3 neurons simultaneously in the same barrel column in anesthetized rats. To mimic normal whisking, all whiskers were deflected together by inserting them into a piezoelectric-driven plastic mesh.

Under this condition, L4 neurons faithfully spiked several milliseconds before neurons in L2/3, a pre-leading-post firing order that is appropriate to drive spike timing-dependent LTP (Fig. 1.5). To simulate whisker deprivation, the principal whisker was cut to narrowly escape the mesh, so that the mesh now deflected all whiskers but the principal whisker. This resulted in two immediate changes in L4 and L2/3 firing correlations in the deprived column. First, mean firing order reversed, with most L2/3 neurons now spiking before L4 neurons (Fig. 1.5). This reversal was most pronounced between L4 and L2 neurons. Second, overall firing correlations between pairs of L4 and L2/3 neurons significantly decreased (not shown). These changes recovered immediately when the principal whisker was reinserted into the mesh. Thus, whisker deprivation acutely altered spike timing at L4-L2/3 synapses in a manner that was exactly appropriate to drive spike timing-dependent LTD (Celikel et al., 2004).

These experiments suggest that spike timing, not spike rate, is the key feature of S1 spike trains that drives deprivation-induced weakening of L4-L2/3 synapses, and that STDP is the relevant mode of LTD induction. However, it will be critical to verify that these use-dependent changes in spike timing occur in awake-behaving, not just anesthetized, rats. In addition, the prevalence of STDP as a learning mechanism *in vivo* needs to be examined. Is it most relevant only in sparsely spiking brain regions, like S1, in which rate-dependent plasticity is unlikely, or is it utilized more generally?

Conclusions

Work presented here suggests that LTD could be an important component of developmental map plasticity in sensory cortex, but it is unclear how similar the mechanisms of experience-induced depression are with LTD. In subsequent chapters, we explore the physiological and anatomical mechanisms of deprivation-induced depression at L4 to L2/3 synapses. Results show that experience weakens these synapses by lowering release probability, and that this decrease in release probability is consistent with known, presynaptic mechanisms of LTD at this synapse (Chapter 2). Anatomical experiments suggest that experience does not alter neural density (Chapter 4) or axonal distribution of L4 neurons (Chapter 3). Thus, experience-dependent plasticity at L4 to L2/3 synapses involves physiological synaptic plasticity but not large-scale anatomical remodeling. These data provide further support for the role of LTD in cortical map plasticity.

References

Allen CB (2004) Synaptic depression induced by whisker deprivation in rat barrel cortex. PhD thesis University of California, San Diego.

Allen CB, Celikel T, Feldman DE (2003) Long-term depression induced by sensory deprivation during cortical map plasticity in vivo. Nat Neurosci 6:291-299.

Bear MF (1996) A synaptic basis for memory storage in the cerebral cortex. Proc Natl Acad Sci U S A 93:13453-13459.

Bear MF, Cooper LN, Ebner FF (1987) A physiological basis for a theory of synapse modification. Science 237:42-48.

Buonomano DV, Merzenich MM (1998) Cortical plasticity: from synapses to maps. Annu Rev Neurosci 21:149-186.

Celikel T, Szostak VA, Feldman DE (2004) Modulation of spike timing by sensory deprivation during induction of cortical map plasticity. Nat Neurosci 7:534-541.

Dan Y, Poo MM (2004) Spike timing-dependent plasticity of neural circuits. Neuron 44:23-30.

Diamond ME, Huang W, Ebner FF (1994) Laminar comparison of somatosensory cortical plasticity. Science 265:1885-1888.

Dudek SM, Bear MF (1992) Homosynaptic long-term depression in area CA1 of hippocampus and effects of N-methyl-D-aspartate receptor blockade. Proc Natl Acad Sci U S A 89:4363-4367.

Feldman DE (2000) Timing-based LTP and LTD at vertical inputs to layer II/III pyramidal cells in rat barrel cortex. Neuron 27:45-56.

Feldmeyer D, Lubke J, Silver RA, Sakmann B (2002) Synaptic connections between layer 4 spiny neurone-layer 2/3 pyramidal cell pairs in juvenile rat barrel cortex: physiology and anatomy of interlaminar signalling within a cortical column. J Physiol 538:803-822.

Finnerty GT, Roberts LS, Connors BW (1999) Sensory experience modifies the short-term dynamics of neocortical synapses. Nature 400:367-371.

Fox K (1992) A critical period for experience-dependent synaptic plasticity in rat barrel cortex. J Neurosci 12:1826-1838.

Fox K (2002) Anatomical pathways and molecular mechanisms for plasticity in the barrel cortex. Neuroscience 111:799-814.

Frenkel MY, Bear MF (2004) How monocular deprivation shifts ocular dominance in visual cortex of young mice. Neuron 44:917-923.

Glazewski S, Fox K (1996) Time course of experience-dependent synaptic potentiation and depression in barrel cortex of adolescent rats. J Neurophysiol 75:1714-1729.

Glazewski S, Giese KP, Silva A, Fox K (2000) The role of alpha-CaMKII autophosphorylation in neocortical experience-dependent plasticity. Nat Neurosci 3:911-918.

Hardingham NR, Fox K (2004) The relationship between spike timing plasticity and experience-dependent plasticity in αCAMKII-T286A Mutants. Soc Neurosci Abstr 857.21.

Hebb DO (1949) Organization of Behavior. John Wiley & Sons, New York.

Heynen AJ, Abraham WC, Bear MF (1996) Bidirectional modification of CA1 synapses in the adult hippocampus in vivo. Nature 381:163-166.

Heynen AJ, Yoon BJ, Liu CH, Chung HJ, Huganir RL, Bear MF (2003) Molecular mechanism for loss of visual cortical responsiveness following brief monocular deprivation. Nat Neurosci 6:854-862.

Huber KM, Sawtell NB, Bear MF (1998) Brain-derived neurotrophic factor alters the synaptic modification threshold in visual cortex. Neuropharmacology 37:571-579.

Keller A (1995) Synaptic organization of the barrel cortex. In: The barrel cortex of rodents (Jones EG and Diamond IT, ed). New York: Plenum:221-262.

Kirkwood A, Rioult MC, Bear MF (1996) Experience-dependent modification of synaptic plasticity in visual cortex. Nature 381:526-528.

Knott GW, Quairiaux C, Genoud C, Welker E (2002) Formation of dendritic spines with GABAergic synapses induced by whisker stimulation in adult mice. Neuron 34:265-273.

Lebel D, Grossman Y, Barkai E (2001) Olfactory learning modifies predisposition for long-term potentiation and long-term depression induction in the rat piriform (olfactory) cortex. Cereb Cortex 11:485-489.

Lendvai B, Stern EA, Chen B, Svoboda K (2000) Experience-dependent plasticity of dendritic spines in the developing rat barrel cortex in vivo. Nature 404:876-881.

Linden DJ, Connor JA (1995) Long-term synaptic depression. Annu Rev Neurosci 18:319-357.

Madison DV, Malenka RC, Nicoll RA (1991) Mechanisms underlying long-term potentiation of synaptic transmission. Annu Rev Neurosci 14:379-397.

Manahan-Vaughan D, Braunewell KH (1999) Novelty acquisition is associated with induction of hippocampal long-term depression. Proc Natl Acad Sci U S A 96:8739-8744.

McKernan MG, Shinnick-Gallagher P (1997) Fear conditioning induces a lasting potentiation of synaptic currents in vitro. Nature 390:607-611.

Mulkey RM, Malenka RC (1992) Mechanisms underlying induction of homosynaptic long-term depression in area CA1 of the hippocampus. Neuron 9:967-975.

Petersen CC, Sakmann B (2001) Functionally independent columns of rat somatosensory barrel cortex revealed with voltage-sensitive dye imaging. J Neurosci 21:8435-8446.

Rioult-Pedotti MS, Friedman D, Donoghue JP (2000) Learning-induced LTP in neocortex. Science 290:533-536.

Ruthazer ES, Cline HT (2004) Insights into activity-dependent map formation from the retinotectal system: a middle-of-the-brain perspective. J Neurobiol 59:134-146.

Sanes JN, Donoghue JP (2000) Plasticity and primary motor cortex. Annu Rev Neurosci 23:393-415.

Sawtell NB, Frenkel MY, Philpot BD, Nakazawa K, Tonegawa S, Bear MF (2003) NMDA receptor-dependent ocular dominance plasticity in adult visual cortex. Neuron 38:977-985.

Shepherd GM, Pologruto TA, Svoboda K (2003) Circuit analysis of experience-dependent plasticity in the developing rat barrel cortex. Neuron 38:277-289.

Simons DJ (1978) Response properties of vibrissa units in rat SI somatosensory neocortex. J Neurophysiol 41:798-820.

Singer W (1995) Development and plasticity of cortical processing architectures. Science 270:758-764.

Stent GS (1973) A physiological mechanism for Hebb's postulate of learning. Proc Natl Acad Sci U S A 70:997-1001.

Welker C, Woolsey TA (1974) Structure of layer IV in the somatosensory neocortex of the rat: description and comparison with the mouse. J Comp Neurol 158:437-453.

Wiesel TN, Hubel DH (1963) Single-Cell Responses in Striate Cortex of Kittens Deprived of Vision in One Eye. J Neurophysiol 26:1003-1017.

Woolsey TA, Van der Loos H (1970) The structural organization of layer IV in the somatosensory region (SI) of mouse cerebral cortex. The description of a cortical field composed of discrete cytoarchitectonic units. Brain Res 17:205-242.

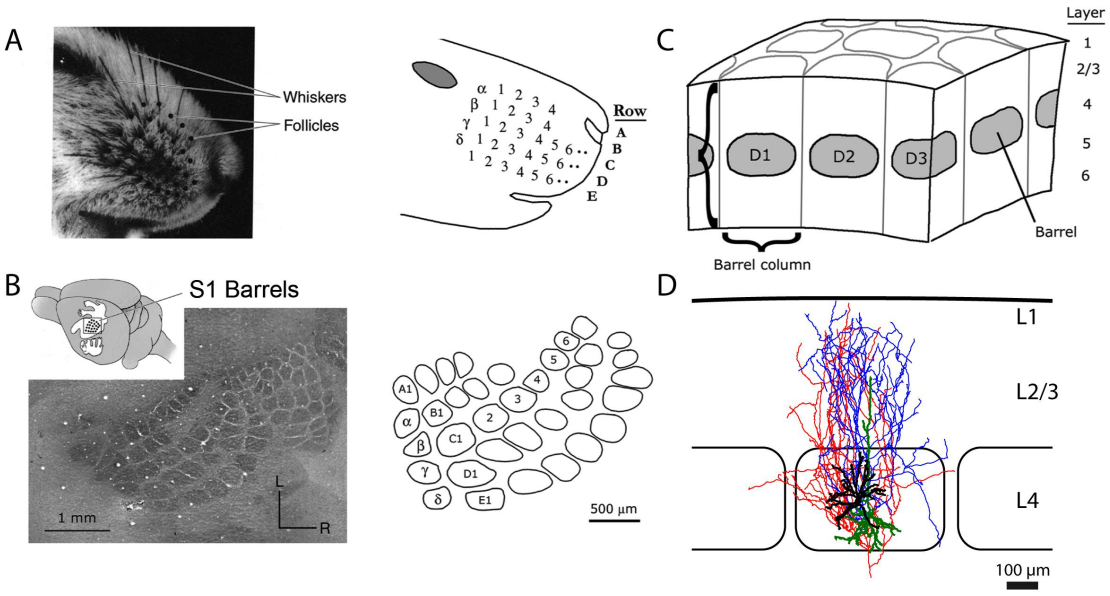

Fig. 1.1: Whisker map in rat S1 cortex. A, Arrangement of large whiskers on mystacal pad. B, Arrangement of corresponding barrels in L4 of S1. C, Barrels in L4 form the center of barrel columns in S1. Neurons within single barrel columns respond preferentially to deflections of one, principal whisker. D, Reconstruction of two L4 excitatory neurons that confer the main, feedforward circuit from L4 to L2/3. Dendrites and soma in black and green, axon in red and blue.

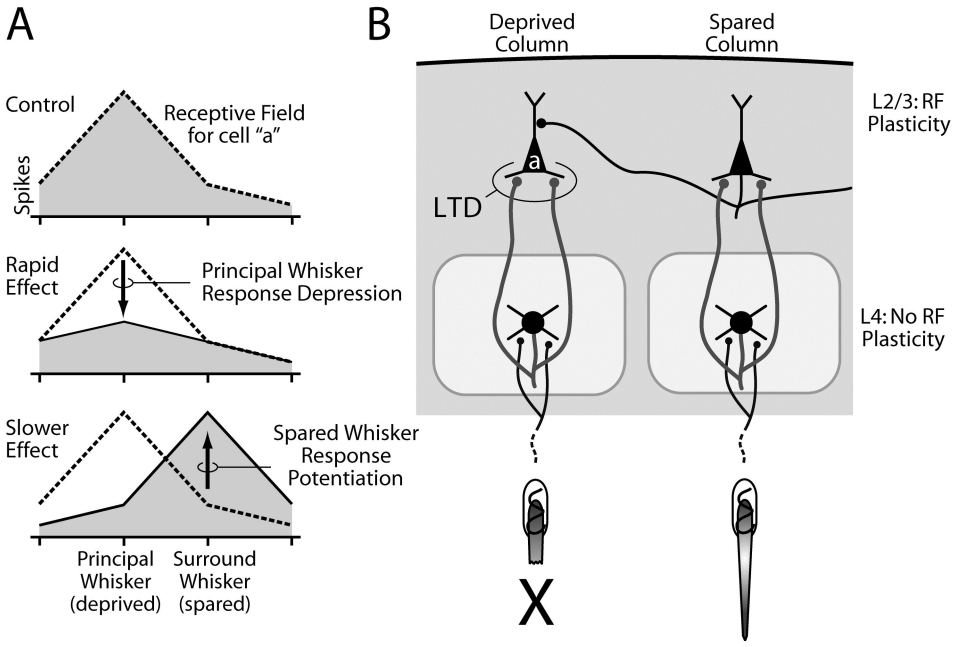

Fig. 1.2: Whisker receptive field plasticity and a possible synaptic basis in rat S1 cortex. A, Receptive field of L2/3 neuron "a". Principal whisker deprivation causes a rapid (7 days) loss of responses to the deprived, principal whisker, and a slower (20 days) increase in responses to spared, surround whiskers. Dashed lines, control receptive field. Data schematized from Glazewski and Fox, 1996. B, Hypothesized site of LTD mediating principal whisker response depression in adolescent rats.

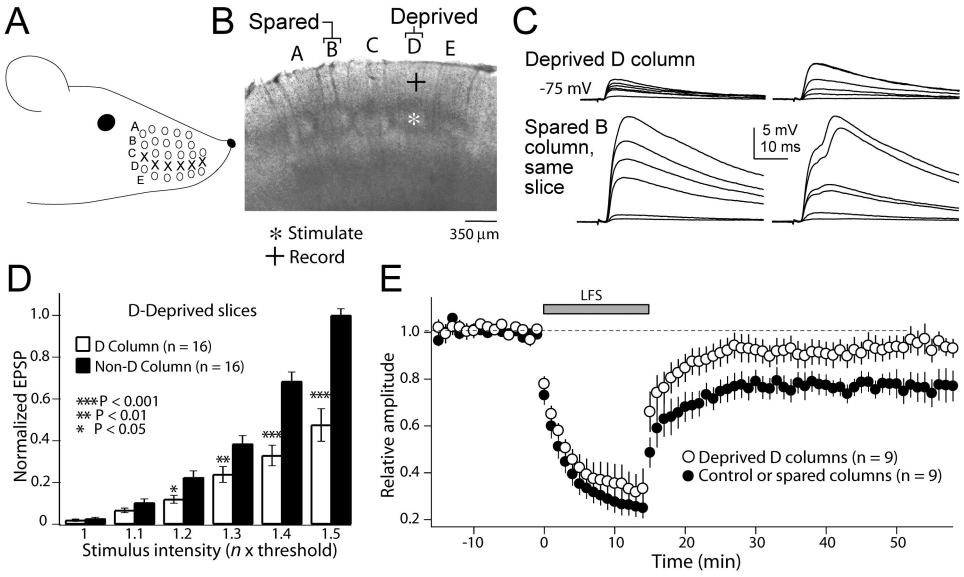

Fig. 1.3: Whisker deprivation causes LTD-like weakening of L4 to L2/3 excitatory synapses. A, Deprivation of D row whiskers on the snout (X's). B, Living S1 slice containing five barrels corresponding to whisker rows A-E, visualized by transillumination. Stimulation and whole-cell recording sites for studying L4-L2/3 synapses are shown. C, Family of EPSPs in response to increasing stimulation intensity in L4, for two cells in a deprived D column, and 2 cells in the spared B column of the same slice. D, Comparison of mean EPSP amplitude between deprived and spared columns. All amplitudes are normalized to the mean maximal amplitude in the non-deprived column of each slice. E, Occlusion of LTD by whisker deprivation. LFS, 900 presynaptic stimuli at 1 Hz. Bars are S.E.M. Data from Allen et al., 2003.

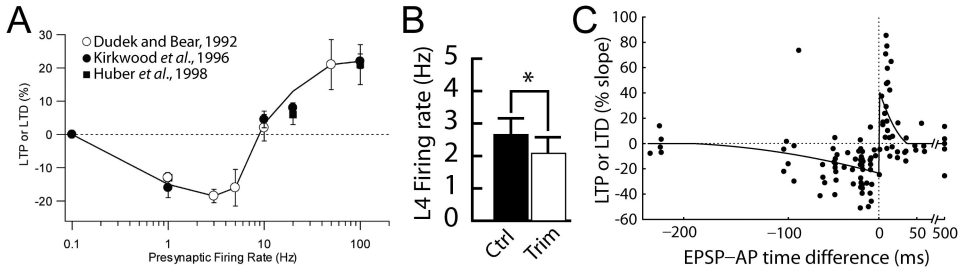

Fig. 1.4: Rate-dependent and spike timing-dependent learning rules for LTP and LTD. A, Summary plot of the learning rule for firing rate-dependent LTP and LTD from Schaffer collateral-CA1 synapses (open symbols) and L4-L2/3 synapses in V1 (filled symbols). Data are from the indicated papers. B, Mean firing rate of L4 neurons in awake behaving rats recording when all whiskers were intact ("ctrl") and immediately after trimming the principal whisker to the level of the fur ("trim"). C, Learning rule for STDP at L4 to L2/3 synapses in S1. Data from Celikel et al., 2004.

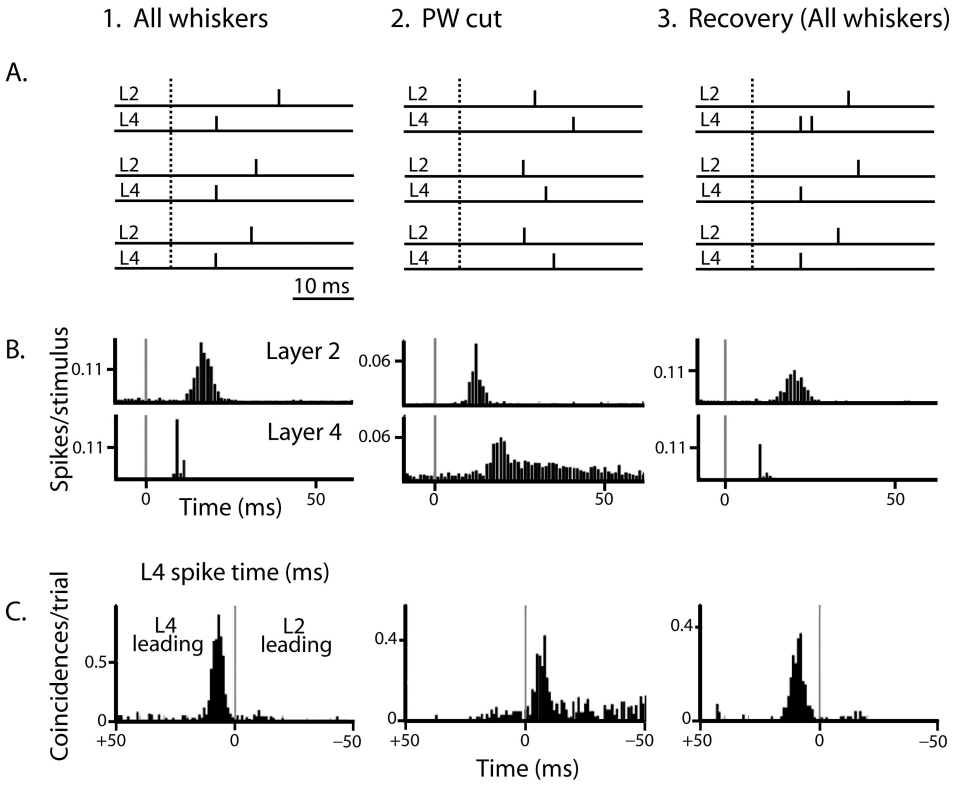

Fig. 1.5: Acute deprivation of a single principal whisker causes a reversal in L4-L2/3 firing order appropriate to drive spike timing-dependent LTD *in vivo*. A, Spike trains of a pair of L4 and L2 neurons, recorded simultaneously in a single S1 column, under 3 sequential conditions: simultaneous deflection of all whiskers, deflection of all but the principal whisker (PW cut, to mimic acute deprivation of one whisker). and all-whisker deflection (recovery). Note reversal in L4-L2 firing order during PW cut. B, Peristimulus time histograms of L4 and L2 responses for each stimulus condition (900 stimulus repetitions). Stimulus onset, 0 ms. C, Cross-correlograms representing relative timing of L4 and L2 spikes during sensory responses in each condition. Data from Celikel et al., 2004.

Chapter 2

Synaptic basis for whisker deprivation-induced synaptic depression in rat somatosensory cortex

Abstract

Whisker deprivation induces weakening of excitatory layer 4 (L4) inputs to L2/3 in rat primary somatosensory (S1) cortex, which is likely to contribute to plasticity of the whisker receptive field map. Prior experiments showed that this weakening occluded subsequent long-term depression (LTD), suggesting that it represented LTD induced by deprivation *in vivo*. Here, we examined the synaptic expression mechanisms for this weakening and assessed its similarity to LTD, which is known to be presynaptically expressed at L4-L2/3 inputs. Whisker deprivation increased paired pulse ratios at presumptive L4-L2/3 synapses, and slowed the use-dependent block of NMDA receptor-mediated transmission by MK-801, indicating that deprivation reduced release probability. In contrast, L4-L2/3 quantal amplitude, assessed by stimulating L4 afferents in the presence of strontium, was not altered by deprivation, indicating that deprivation did not affect postsynaptic responsiveness. Five days of deprivation (begun at P12) were required to significantly weaken L4-L2/3 synapses. Equivalent weakening occurred when deprivation began at older ages (P20), indicating that weakening is not simply a failure of early synaptic maturation. Thus, deprivation weakens L4-L2/3 synapses by decreasing presynaptic function, similar to known LTD mechanisms at this synapse.

Introduction

Topographic sensory maps in primary sensory cortex are modified based on recent sensory experience or deprivation; however, the synaptic and cellular mechanisms that underlie these changes are just beginning to be understood. In classical Hebbian map plasticity, the representations of more active or behaviorally relevant stimuli expand within sensory maps, and the representations of less active or irrelevant stimuli shrink, thus increasing the cortical processing capacity for relevant inputs (LeVay et al., 1980; Buonomano and Merzenich, 1998). A prominent hypothesis is that reduced representation of deprived stimuli within maps involves long term depression (LTD) at specific cortical synapses (Buonomano and Merzenich, 1998; Fox, 2002), but existing evidence is incomplete. Sensory deprivation causes weakening of specific intracortical synaptic projections, measured in *ex vivo* brain slices prepared from deprived animals (Finnerty et al., 1999; Allen et al., 2003; Shepherd et al., 2003). This weakening can occlude subsequent LTD induction, suggesting that it may represent LTD induced *in vivo* (Rioult-Pedotti et al., 2000; Allen et al., 2003; Heynen et al., 2003); however, attempts to block map plasticity by disrupting LTD mechanisms have had mixed results (Hensch and Stryker, 1996; Renger et al., 2002; Fischer et al., 2004). Therefore, it remains unclear whether deprivation-induced synaptic weakening *in vivo* represents LTD, versus other physiological or anatomical modifications.

Here, we characterize synaptic weakening induced by partial sensory deprivation in rat somatosensory (S1) cortex, in order to determine whether this weakening has quantal properties consistent with LTD. Rat S1 is a powerful model

system for studying experience-dependent plasticity of sensory maps (Feldman and Brecht, 2005). The large facial whiskers are represented in S1 by cell clusters, called barrels, in cortical layer 4 (L4), whose arrangement is isomorphic with the whiskers on the rat's snout (Woolsey and Van der Loos, 1970; Welker and Woolsey, 1974). L4 neurons, which receive thalamic input, project to L2/3 neurons within the same radial column, termed a barrel column. Within a barrel column, both L4 and L2/3 neurons are driven most strongly by a single whisker, termed the principal whisker, corresponding to that column. Neurons also respond less strongly to adjacent whiskers.

When a subset of whiskers is deprived by trimming or plucking in post-neonatal, adolescent rats (age P7-P60), L2/3 neurons in deprived columns lose responsiveness to the deprived principal whisker while L4 neuronal responses are unaffected. This weakening of deprived principal whisker responses in L2/3 has been proposed to be due to deprivation-induced weakening of L4-L2/3 synapses (Glazewski and Fox, 1996; Fox, 2002). Supporting this hypothesis, Allen et al. (2003) showed that whisker deprivation reduces the bulk functional efficacy of the L4-L2/3 excitatory projection (measured in *ex vivo* S1 slices). This weakening occluded LTD, suggesting that it may represent LTD induced by deprivation *in vivo*. However, whether deprivation weakens individual synapses (as opposed to reducing synapse number or preventing normal synaptic development) remains unknown.

Here we examined the expression mechanisms for deprivation-induced weakening of L4-L2/3 synapses, and assessed its similarity to LTD, which was recently shown to be presynaptically expressed via retrograde endocannabinoid

signaling at these synapses (Bender et al., submitted). We found that whisker deprivation increased paired pulse ratios (PPR) and slowed use-dependent blockade of NMDA receptor currents by MK-801, suggesting that presynaptic release probability was reduced. In contrast, quantal amplitude measured using strontium (Dodge et al., 1969) was unaltered by deprivation, indicating that postsynaptic sensitivity was unchanged. This apparent presynaptic expression is consistent with known LTD mechanisms at this synapse (Bender et al., submitted). Deprivation depressed synaptic function equally in young (P12) and more mature rats (P20), suggesting that whisker deprivation does not act by preventing normal synaptic maturation, but instead may actively weakens synapses. Thus, deprivation-induced weakening resembles LTD at the synaptic level.

Methods

Whisker deprivation. All procedures were approved by the UCSD Institutional Animal Care and Use Committee. Every 2 days, D1-6 and γ whiskers were plucked from the right side of Long-Evans rats under isofluorane anesthesia (3% in 2 L/min O_2). Deprivation began at postnatal day (P) 12 unless otherwise noted. Sham-plucked littermates were subject to identical levels of anesthesia and handling, and their whiskers were manipulated with forceps but not plucked.

Slice preparation. Rats were anesthetized with isoflurane and the brain was removed in either chilled normal Ringer's solution (P15-22) (in mM: NaCl, 119; KCl, 2.5; $MgSO_4$, 1.3; NaH_2PO_4, 1; $NaHCO_3$, 26.3; D-(+)-glucose, 11; and $CaCl_2$, 2.5, bubbled with 95% O_2/5% CO_2 [pH 7.4]), or low-sodium, low-calcium Ringer's solution (P23-26) (in mM: sucrose, 250; KCl, 2.5; $MgSO_4 \cdot 7H_2O$, 4; $NaH_2PO_4 \cdot H_2O$, 1; HEPES, 15; D(+)glucose, 11; $CaCl_2$, 0.1). "Across row" S1 slices (400 μm) from the left hemisphere were cut 50° from the midsagittal plane on a vibrating microtome (Finnerty et al., 1999; Allen et al., 2003). Slices were incubated 30 min at 30°C in normal Ringer's solution, then at room temperature for 0.5-6 h before recording.

Electrophysiology. Recordings were made at room temperature in normal Ringer's solution. Experiments were performed blind to whisker experience unless noted otherwise. Whisker barrels were identified with transmitted light (Finnerty et al., 1999; Allen et al., 2003). A bipolar stimulating electrode (FHC, Bowdoinham, ME) was placed in the geometric center of a L4 barrel, 200 μm below the surface of the slice. Whole-cell recordings were made from L2/3 pyramidal cells located radially

above the center of the stimulated barrel, approximately 300 μm below the L1-pia border (Fig. 2.1A). Neurons were visualized with differential interference contrast optics and recordings were made with 3–4 MΩ pipettes using Axoclamp-2B, Axopatch 200B, or Multiclamp 700B amplifiers (Molecular Devices, Sunnyvale, CA). For current-clamp recordings, the internal solution contained, in mM: K-gluconate 116; KCl 6; NaCl 2; HEPES 20; EGTA 0.5; MgATP 4; NaGTP 0.3; phosphocreatine 10; pH 7.20-7.25. For voltage-clamp recordings, in mM: D-gluconic acid 118; CsOH 118; HEPES 20; EGTA 0.4;NaCl 2.8; TEA-Cl 5; MgATP 4; NaGTP 0.3; phosphocreatine 10; pH 7.20-7.25. Cells were selected for recording if they had clear pyramidal somata and regular spiking responses to current injection (500 ms) (Connors and Gutnick, 1990). In a previous study, histological confirmation of pyramidal cell morphology was obtained in all (n = 50) L2/3 cells identified with these criteria (Feldman, 2000). For current-clamp recordings, experiments were discarded if initial series resistance (R_s) > 30 MΩ, membrane potential (V_m) > -75 mV, or if V_m changed by more than 20%. R_{in} and R_s were monitored continuously with small hyperpolarizing pulses, and R_s was compensated by bridge balance. Membrane potential was maintained at -75 ± 2 mV by current injection. For voltage-clamp recordings, experiments were discarded if initial V_m > -75 mV, R_s > 25 MΩ and R_{in} < 100 MΩ. R_s was not compensated. R_{in} and R_s were monitored continuously, and experiments were discarded if either changed by 20%. All membrane potential values were adjusted for the measured liquid junction potential (10 mV for current clamp recordings in either normal or high-divalent Ringer's, 11 mV for voltage clamp recordings).

Input-output curves. Current clamp recordings were made in high divalent Ringer's solution (in mM: NaCl, 116; KCl, 2.5; $MgSO_4 \cdot 7H_2O$, 4; $NaH_2PO_4 \cdot H_2O$, 1; $NaHCO_3$, 26.2; D(+)glucose, 8; $CaCl_2$, 4, bubbled with 95% O_2/5%CO_2) to suppress polysynaptic responses. Bicuculline methiodide (BMI, 5 mM) was applied focally via a pipette (5 μm tip internal diameter, located < 100 μm from recorded cell) to block local γ-aminobutyric acid (GABA-A) receptors and isolate excitatory synaptic inputs (Castro-Alamancos et al., 1995; Feldman, 2000). Threshold was defined as the lowest stimulus intensity required to reliably evoke excitatory postsynaptic potentials (EPSPs) during 5 consecutive trials. Threshold was confirmed by the lack of EPSPs at 0.95 times threshold. Significance was determined by a two-way ANOVA of normalized input-output curves (factors: stimulation intensity and sensory experience).

Paired pulse experiments. Recordings were made in normal Ringer's solution. D-(-)-2-amino-5-phosphonopentanoic acid (D-AP5) (50 μM, Tocris) and focal BMI (see above) were used to isolate α-amino-3-hydroxy-5methyl-4-isoxazole-propionate (AMPA) receptor mediated currents. In some experiments, cyclothiazide (50 μM, Tocris, dissolved in DMSO) was added to block AMPA-R desensitization. Cells were voltage-clamped at -70 mV. Paired stimuli with inter-stimulus intervals (ISI) of 12, 20, 40, 80 ms were delivered every 25 sec (6-8 sweeps each). Paired pulse ratios (PPR) were calculated as the ratio of the mean amplitude of the second EPSC to the first. When the second pulse overlapped with the decay of the first, the tail of the first EPSC was subtracted to obtain an accurate amplitude for the second EPSC. For low calcium experiments, $CaCl_2$ was reduced to 1.25 mM and $MgCl_2$ raised to 2.5 mM

to maintain total divalent ion concentration. Slices were incubated in low calcium Ringer's at least 0.5 h before recording.

MK-801 experiments. Recordings were made in normal Ringer's solution. *N*-methyl-D-aspartate (NMDA) currents were isolated by bath application of 6,7-dinitroquinoxaline-2,3-dione (DNQX) (10 μM) and either picrotoxin (100 μM) or local BMI (5 mM). Internal solution included 5 mM BAPTA. Cells were voltage-clamped at +40 mV and EPSCs were elicited every 15 s. Following a stable baseline, stimulation was paused and neurons were voltage clamped at -70 mV while 5 μM (5S,10R)-(+)-5-methyl-10,11-dihydro-5H-dibenzo[a,d]cyclohepten-5,10-imine maleate (MK-801) was added to the perfusate. After 10 minute application (by which time MK-801 was fully equilibrated in the slice), the holding potential was returned to +40 mV and stimulation was resumed. EPSC decay was fit to a double exponential function in Igor Pro (Wavemetrics, Portland, OR). The mean weighted time constant (τ_m) was calculated from fast (τ_f) and slow (τ_s) time constants, scaled by their relative amplitudes (a_f and a_s, respectively) as: $\tau_m = a_f\tau_f + a_s\tau_s$. Decay constants of EPSCs were derived from averages of all 20 baseline responses and the first 20 responses in the presence of MK-801.

Miniature excitatory postsynaptic potentials (mEPSCs). AMPA-mediated mEPSCs were isolated by bath application of tetrodotoxin (0.5 μM), D-AP5 (50 μM), and picrotoxin (100 μM). Cells were voltage-clamped at –70 mV. R_s and R_{in} were measured at the beginning and end of recordings from the response to 5 mV hyperpolarizing pulses. Data were collected (pClamp, Axon Instruments) and stored

on computer for off-line analysis using MiniAnalysis software (Synaptosoft, Decatur, GA). Automated detection of mEPSCs (amplitude ≥ 4.5 pA, 10-90% rise time < 2 ms) was verified by visual inspection. 706 ± 70 mEPSCs were analyzed in each cell (range: 380-1305). Root mean square noise, measured between identified mEPSCs, was 1.90 ± 0.04 pA (n = 12 cells).

Evoked EPSCs in strontium-containing solution (SrEPSCs). D-AP5 (50 μM, Tocris) and focal BMI (5 mM) were applied to isolate AMPA receptor mediated currents. Cells were voltage-clamped at –70 mV. EPSCs (~100 pA) were first elicited in each slice in high divalent Ringer's solution (see above). Ca^{2+} was then replaced by equimolar (4 mM) Sr^{2+}. After 20-30 min of Sr^{2+} perfusion, the initial, synchronous EPSC decreased to ~20-40 pA, and the frequency of miniature, asynchronous EPSCs increased. Stimulation intensity was maintained at initial levels for subsequent recordings in the same slice. SrEPSCs within 40-380 msec of evoked EPSC onset were analyzed in the same manner as mEPSCs, using identical selection criteria. 440 ± 48 events mEPSCs were analyzed in each cell (range 185-1106). Root mean square noise, measured > 500 ms after stimulation, was 1.95 ± 0.05 pA (n = 29 cells).

Statistics. All values are expressed as mean ± standard error. Significance was determined using Student's *t* test unless otherwise noted.

Results

To examine the synaptic mechanisms of deprivation-induced weakening of the L4-L2/3 projection, we made whole cell recordings from L2/3 pyramidal neurons in acute brain slices (400 μm) prepared from rats in which the D row of whiskers had been deprived for up to 9 days (Fig. 2.1A), and from sham-deprived rats. Slices were cut across S1 barrel rows, so that each slice contained one barrel from each of the 5 rows (A-E). Barrels were visualized via transillumination to allow targeted recordings from deprived and spared barrel columns (Allen et al., 2003). Presumptive L4-L2/3 synapses within a column were studied using extracellular stimulation in the geometric center of a L4 barrel and whole-cell recording from radially aligned L2/3 pyramidal cells. Bicuculline methiodide (BMI) was applied focally via a nearby pipette to block GABA-A receptors and isolate excitatory inputs (Fig. 2.1B).

Time course for deprivation-induced depression

Deprivation of the D row of whiskers for 9-14 days beginning at P12 is known to depress EPSPs at L4-L2/3 synapses in the deprived (D) column, measured by input-output curves in S1 slices from whisker-deprived rats (Allen et al., 2003). To determine the time course for this deprivation-induced depression, we performed unilateral D-row whisker deprivation beginning at P12 for 3, 5, 7, and 9 days, and then prepared S1 slices. Input-output curves were measured in multiple cells (range 1-3 cells, mean 2 cells) in the D column and one non-D column (B-row in 20 slices, C-row in 2, E-row in 2) per slice. This experiment was not performed blind to deprivation. For each cell, L4 stimulation intensity was adjusted in 5% increments to find the

lowest stimulation intensity that evoked a detectable excitatory postsynaptic potential (threshold stimulation intensity) and then increased in 10% increments to 1.5 times threshold (x), as previously described (Allen et al., 2003). Input-output curves were constructed from the amplitude of the short-latency component of the EPSP, measured at each stimulus intensity. As observed previously (Allen et al., 2003), deprivation caused depression of the absolute amplitude of input-output curves in the deprived (D) column, relative to spared (non-D) columns (Fig. 2.1C, D).

To control for inter-slice variability, EPSP amplitudes for all cells within each slice were normalized to the mean EPSP amplitude at 1.5 times threshold for all cells in the spared column(s) of that slice. Weakening of the L4-L2/3 projection required at least 4 days of deprivation. No weakening was observed after 3 days of whisker deprivation from P12 (Fig. 2.1E) ($p = 0.9$, two-way ANOVA [see methods], $n = 15$ deprived, 12 spared cells in 7 slices from 4 rats). After 5 days, responses were weaker in deprived columns at a range of stimulus intensities (Fig. 2.1E) ($p < 0.05$, ANOVA, $n = 15$ deprived, 15 spared, 7 slices from 5 rats; $p < 0.02$, Fisher's PLSD for D vs. Non-D values at 1.2-1.5x). Similar depression was observed with 7 d of deprivation ($p < 0.0001$, $n = 9$ deprived, 12 spared, 6 slices from 4 rats, $p< 0.01$ at 1.2-1.5x, Fisher's PLSD) and 9 days of deprivation ($p < 0.001$, $n = 9$ deprived, 8 spared, 4 slices from 3 rats, $p < 0.03$ at 1.3-1.5x, Fisher's PLSD).

To create a scalar index of the magnitude of deprivation-induced depression, we divided the raw (non-normalized) input-output curve of each D-row cell by the mean input-output curve for all cells in the non-D row of the same slice. The mean value of this ratio for stimulation intensities of 1.3-1.5 times threshold was termed the

D:non-D EPSP ratio. (Fig. 2.1G). We calculated the D:non-D EPSP ratio for each D-row cell from whisker-deprived rats, and from control rats from a previous study (Fig. 2.1F) (n= 11 D cells, 11 non-D cells, 6 slices, 5 rats, aged 21-25) (Allen et al., 2003). The D:non-D EPSP ratio in control rats was 1.09 ± 0.14, indicating that D-row EPSP amplitudes were slightly larger than non-D (usually B) row amplitudes. Three days of deprivation did not depress the D:non-D EPSP ratio (Fig. 2.1G). However, 5, 7, and 9 days of deprivation significantly reduced the D:non-D EPSP ratio ($p < 0.01$, ANOVA; $p < 0.05$ for 5, 7, and 9 days, Fisher's PLSD). No correlations were found between deprivation duration and magnitude after five days [$p > 0.1$, $R^2 = 0.05$, with data from (Allen et al., 2003)], suggesting that depression requires at least 3 days to depress this projection and is near maximal after five days. The D:non-D ratio for all cells with at least 5 days of deprivation was 0.64 ± 0.05 (n = 52). Thus, deprivation weakens L4-L2/3 inputs by ~36%.

Whisker deprivation increased paired-pulse ratios

To determine whether deprivation weakens individual L4-L2/3 synapses, as opposed to reducing synapse number, we measured short-term synaptic plasticity, which is commonly used as an indirect measure of release probability (P_r). High P_r synapses tend to exhibit paired pulse depression (PPD), whereas low P_r synapses show paired pulse facilitation (PPF), and experimentally altering P_r (for example, by varying the external calcium concentration) produces corresponding changes in PPR (Zucker and Regehr, 2002).

To measure PPR, AMPA-mediated EPSCs were isolated in voltage clamp recordings by bath application of D-AP5 (50 μM) and local BMI (see methods). Voltage clamp was used to minimize voltage-dependent dendritic boosting of EPSPs and changes in driving force, which can contribute to PPR (Magee and Johnston, 2005). Pairs of closely-timed EPSCs were evoked with inter-stimulus intervals (ISI) of 12, 20, 40 and 80 ms (Fig. 2.2). Stimulus intensity was adjusted so the amplitude of the first EPSC was similar for each cell (D-row sham: 126 ± 7.1 pA, n = 25; B-row sham and deprived: 152 ± 14.5 pA, n = 18; D-row deprived: 131 ± 8.0 pA, n = 29; $p > 0.2$, ANOVA). In B and D columns in slices from sham-deprived rats, L4-L2/3 synapse showed either no paired pulse plasticity [12 ms ISI: 0.92 ± 0.06, n = 19, $p > 0.1$; 20 ms: 0.94 ± 0.04, n = 21, $p > 0.1$; 40 ms ISI: 0.95 ± 0.03, n = 34, $p = 0.058$, vs. a mean of 1.0 (no plasticity) single-tailed t-test], or modest PPD (80 ms: 0.88 ± 0.03, n = 33, $p < 0.0001$, single-tailed t-test) (Fig. 2.2A, Table 2.1), consistent with recordings of unitary L4-L2/3 connections (Feldmeyer et al., 2002).

To determine if whisker deprivation altered PPR at L4-L2/3 synapses, recordings were made from animals that were either sham-deprived or D-row deprived from P12 to P18-21, when slices were made. PPR was significantly elevated in the D-row in whisker deprived animals, as compared to the B-row in the same slice (e.g., 40 ms ISI, D-row: 1.52 ± 0.10, n = 29; B-row: 0.97 ± 0.04, n = 9; $p < 0.0001$, ANOVA; $p < 0.03$ at all ISIs, Fisher's PLSD), or the D-row in sham-deprived littermates (e.g., 40 ms ISI, D-row deprived: 1.52 ± 0.10, n = 29; D-row sham: 0.96 ± 0.02, n = 25; $p < 0.0001$, ANOVA; $p < 0.02$ at all ISIs, Fisher's PLSD). Similar findings occurred at all ISIs tested (Fig. 2.2A, Table 2.1).

To confirm that PPR reflected release probability, we lowered extracellular calcium from 2.5 mM to 1.25 mM, a manipulation known to reduce release probability (Zucker and Regehr, 2002). PPR was significantly increased in low calcium Ringer's (Fig. 2.2B, Table 2.1) (e.g., 40 ms ISI: 1.87 ± 0.09, n = 20; $p < 0.0001$ vs. sham D, ANOVA; $p < 0.0001$ at all ISIs, Fisher's PLSD). To test whether PPR was significantly determined by postsynaptic AMPA receptor desensitization (Otis et al., 1996), we applied the AMPA-R desensitization blocker cyclothiazide (CTZ, 50 μM). CTZ increased AMPA currents, but did not alter PPR at any ISI relative to DMSO vehicle (Fig. 2.2C) (e.g., 40 ms ISI: 0.88 ± 0.07, n = 10; $p > 0.8$, ANOVA, vs. CTZ vehicle). DMSO vehicle did not alter PPR relative to control Ringer's (e.g., 40 ms ISI, normal Ringer's: 1.08 ± 0.08; DMSO: 1.10 ± 0.10; n = 5, $p > 0.3$, ANOVA for all ISIs). These results suggest that PPR primarily reflects release probability at this synapse, and thus that whisker deprivation weakens L4-L2/3 synapses by lowering release probability.

Whisker deprivation decreased release probability measured by MK-801

As an additional, more direct measure of P_r, we applied the irreversible open-channel NMDA receptor blocker MK-801. The rate of progressive block of NMDAR-EPSCs by MK-801 is a standard measure of P_r (Hessler et al., 1993; Rosenmund et al., 1993). Because MK-801 only blocks open, ligand-bound receptors, repetitive presynaptic stimulation in the presence of MK-801 will cause NMDA receptors to be blocked at synapses where a vesicle has been released. If P_r is high, many synapses contribute to each event and a high proportion of NMDARs will be blocked with each

presynaptic stimulus, leading to a fast decrease in transmission. If P_r is low, few receptors will be blocked during each stimulus, leading to a slower block of transmission. Therefore, the speed of MK-801 blockade is inversely related to P_r.

We examined the rate of blockade of synaptically evoked NMDA currents (NMDA-EPSCs) by MK-801 in slices from animals that were either sham-deprived or D-row deprived from P12 to P18-21. NMDA-EPSCs (measured at a holding potential of +40 mV) were isolated with DNQX (10 μM) and either BMI or picrotoxin. After attaining a stable baseline (sham: 107.0 ± 8.7 pA amplitude, n = 10; deprived, 116.4 ± 7.2 pA, n = 10: $p > 0.4$), stimulation was paused and MK-801 (5 μM) was added to the perfusate for 10 minutes. Stimulation was then resumed and the decay in NMDA-EPSCs was measured over 104-227 stimuli (Fig. 2.3A). EPSCs were normalized to the amplitude of the first response in MK-801. The decay after stimulation was resumed was fit with a double exponential for each cell (Fig. 2.3B). Results showed that MK801 blockade was slower in deprived columns, relative to sham-deprived columns (Fig. 2.3B). Correspondingly, the fast time constant increased with deprivation (sham: 5.9 ± 1.0, n = 10; deprived: 12.0 ± 1.4, n = 10; $p < 0.005$), while the slow time constant did not (sham: 59.0 ± 8.8; deprived: 109.6 ± 22.7; $p = 0.053$). This finding suggests that P_r at relatively high release probability synapses [corresponding to the fast time constant (Hessler et al., 1993)] was decreased by deprivation (Kaneko and Takahashi, 2004; Nosyreva and Huber, 2005). The relative amplitude of the fast exponential component of the fit also increased significantly with deprivation (a_f sham: 0.45 ± 0.06; a_f deprived: 0.61 ± 0.04; $p < 0.05$), suggesting that deprivation may have caused some low P_r synapses to become effectively silent. To

obtain a rough estimate of the change in P_r, we calculated the difference in the weighted mean time constant for sham and deprived conditions (see Methods). The weighted mean time constant, which is inversely proportional to P_r (Kaneko and Takahashi, 2004), was increased by 44% in deprived columns relative to sham, suggesting that P_r had decreased by this amount.

Because interpretation of double exponential time constants is difficult when the relative amplitude of each exponential changes, we confirmed this result by asking whether of deprivation altered the number of stimuli required to reach 50% block of NMDA-EPSCs, which is a model-independent measure of the rate of MK-801 block. Deprivation significantly slowed the rate of MK-801 blockade by this measure (sham: 13.0 ± 1.8, deprived 18.2 ± 1.7 events; $p < 0.05$), consistent with a decrease in P_r by deprivation (Fig. 2.2B, D).

To confirm that the decrease in the speed of NMDA-EPSC transmission block in deprived conditions reflects a change in P_r, we lowered extracellular calcium from 2.5 mM to 1.25 mM. This manipulation increased PPR by amounts similar to deprivation (Fig. 2.2). Baseline NMDA-EPSC amplitudes were comparable to sham conditions (126.9 ± 10.8 pA, $n = 9$, $p > 0.15$ vs. sham). As with deprivation, lowering calcium increased fast time constants (15.9 ± 1.8, $p < 0.0001$ vs. sham), but not slow time constants (94.4 ± 16.9, $p > 0.05$ vs. sham) of MK-801 blockade (Fig. 2.3C). The relative amplitude of fast events was comparable to deprived conditions, but not significantly different than sham conditions (a_f low Ca^{2+}: 0.63 ± 0.06, $p = 0.06$, vs. sham). The time to 50% transmission block was longer in low calcium Ringer's (18.4 ± 1.7 events, $p < 0.05$ vs. sham) (Fig. 2.3 D). The weighted mean time constant

changed by 57%, suggesting that reducing extracellular calcium by half reduces P_r at these synapses more powerfully than deprivation.

In principle, MK-801 block may be slowed because of either a decrease in release probability, or if the blocking fraction (the fraction of open NMDA receptors that are blocked by MK-801 during each channel opening) is reduced with deprivation. A reduction in blocking fraction could occur if, for example, NMDAR currents became shorter with deprivation, reducing the time available for MK-801 to enter and block the channel. Our data showed no difference in NMDA-EPSC decay kinetics following deprivation, either in the baseline, before MK-801 addition (Fig. 2.3E) (sham: 143 ± 8 ms, deprived: 145 ± 8, $p > 0.8$), or in the presence of MK-801 (sham: 120 ± 9 ms, deprived: 113 ± 5, $p > 0.5$). We also examined the reduction in NMDA-EPSC duration produced by MK-801, which correlates with the blocking fraction, because it is caused by MK-801 entering naïve NMDA receptors during channel opening (Huettner and Bean, 1988; Huang and Stevens, 1997). MK-801 sped decay kinetics by similar amounts (sham, 16.6 ± 3.9 % reduction in time constant of EPSC decay relative to baseline; deprived: 21.4 ± 2.7 %, $p > 0.3$). This finding strongly suggests that the fractional block of NMDARs by MK-801 is similar between sham and deprived rats. Thus, these results suggest that whisker deprivation reduces P_r at L4-L2/3 synapses.

Deprivation did not affect mEPSCs

To determine if whisker deprivation alters the postsynaptic response to neurotransmitter, we first examined miniature EPSCs (mEPSCs), which represent

postsynaptic responses to single, spontaneously released vesicles (Fatt and Katz, 1952; Paulsen and Heggelund, 1994). Recordings were made from L2/3 pyramidal cells in the D and B rows of slices from rats D-row deprived from P12 fo r 11-13 days, and AMPA-R mediated mEPSCs were isolated by bath application of 0.5 μM tetrodotoxin, 50 μM D-AP5, and 100 μM picrotoxin (Fig. 2.4A) (n = 6 cells/row). mEPSC analyses, but not recordings, were performed blind to sensory experience. Deprivation did not affect mEPSC amplitude (Fig. 2.4B) (deprived D: 8.59 ± 0.36 pA, spared B: 8.30 ± 0.42 pA, $p > 0.6$), decay kinetics (single exponential decay tau, D-row: 4.4 ± 0.2 ms, B-row: 4.6 ± 0.1 ms, $p > 0.4$), or frequency (Fig. 2.4C) (D: 2.78 ± 0.37 Hz, B: 3.06 ± 0.54 Hz, $p = 0.7$). No differences were observed in input resistance (D: 244 ± 7 MΩ, B: 244 ± 18 MΩ, $p > 0.5$), series resistance (D: 13 ± 3 MΩ, B: 13 ± 2 MΩ, $p > 0.9$), or resting membrane potential (D: -72 ± 0.5 mV, B: -71 ± 0.5 mV, $p > 0.5$), suggesting that passive cable properties were not altered by whisker deprivation, consistent with previous results (Allen et al., 2003). These results suggest that whisker deprivation does not alter quantal amplitude, when examined across all synapses onto L2/3 pyramidal neurons (all of which contribute mEPSCs).

Deprivation did not alter quantal amplitude at L4-L2/3 synapses

To examine quantal amplitude at L4-L2/3 synapses specifically, we used the divalent ion strontium. When normal extracellular calcium is replaced with strontium, synchronous vesicle release is suppressed, and prolonged asynchronous release occurs instead. Evoked postsynaptic currents in strontium consist of individual, discrete events presumed to represent postsynaptic responses to single, asynchronously

released vesicles from stimulated afferents (Miledi and Slater, 1966; Dodge et al., 1969; Goda and Stevens, 1994; Oliet et al., 1996). Thus, strontium allows measurement of quantal amplitude at L4-L2/3 synapses specifically, in relative isolation from other inputs.

We recorded EPSCs in extracellular strontium (SrEPSCs) in L2/3 pyramidal cells in deprived and spared columns of slices from rats with D-row whiskers deprived from P12 to P19-24. When calcium was replaced with equimolar strontium, peak EPSC amplitude (representing synchronous release) decreased, while the frequency of small asynchronous EPSCs following stimulation dramatically increased (Fig. 2.5A). We analyzed SrEPSCs occurring 40-380 ms after the onset of residual synchronous EPSCs (analyses, not recordings, performed blind). The number of events observed after stimulation decreased over time, but their amplitude remained largely constant, consistent with the hypothesis that SrEPSCs represent responses to individual quanta of transmitter (Fig. 2.5B). SrEPSCs were similar to mEPSCs in amplitude and kinetics, also consistent with this idea (Fig. 2.5A, D). Whisker deprivation did not affect SrEPSC amplitude (deprived: 8.63 ± 0.18 pA, control: 8.61 ± 0.17, $p > 0.9$), or decay kinetics (single exponential decay tau, D-row: 3.9 ± 0.2 ms, B-row: 3.9 ± 0.2 ms, $p > 0.9$) (Fig. 2.5C), suggesting that deprivation-induced weakening does not involve changes in quantal amplitude at this synapse.

Deprivation-induced synaptic weakening was not simply a failure of development

L4-L2/3 synapses are actively developing through the period of deprivation studied here, with extensive synaptogenesis and axonal and dendritic elaboration

occurring through the second postnatal week (Micheva and Beaulieu, 1996; De Felipe et al., 1997; Bender et al., 2003), and the magnitude of whisker-evoked postsynaptic potentials and spiking responses increasing until ~P20 (Stern et al., 2001). Thus, the decrease in average P_r produced by whisker deprivation may represent either an active reduction in the strength of pre-existing synapses, or a failure of normal developmental strengthening of this synaptic population. To address this question, we examined the effects of D-row whisker deprivation beginning at P20, when L4-L2/3 synapses are more mature. Whiskers were plucked from P20 to P24-26, and input-output curves for subthreshold responses were obtained from deprived (D) and control (non-D) columns, using the same techniques as above. When deprivation was begun at P20, EPSPs recorded in deprived columns were significantly smaller than those in spared columns of the same slice ($p = 0.003$, ANOVA; n = 20 deprived column cells, 16 spared column cells, 10 slices from 6 rats; $p < 0.04$ at 1.3-1.5 times threshold, PLSD) (Fig. 2.6A). The magnitude of depression was calculated using the D:non-D EPSP ratio for each cell recorded in a D column. The D:non-D EPSP ratio in rats deprived for 4-6 d beginning at P20 (0.78 ± 0.10, n= 20 cells) was not significantly different from that observed after 5 days of deprivation from P12 (0.72 ± 0.11, n = 15 cells, $p > 0.6$) (Fig. 2.6B). There was no correlation between D:non-D EPSP ratio and plucking duration within the 4-6 d range ($p>0.9$, $R^2 < 0.001$).

Two days of deprivation from P20 did not alter input-output curves: responses in deprived barrel columns after 2 d of deprivation were not different from responses in spared columns ($p > 0.9$, ANOVA, n = 10 deprived cells, 10 spared cells, 5 slices

from 4 rats) (Fig. 2.6A). Furthermore, the D:non-D EPSP ratio calculated for these animals was not different from age-matched control rats (deprived: 1.13 ± 0.16, n = 10 D-row cells; control: 1.09 ± 0.14, n=11 D-row cells, $p > 0.8$) (Fig. 2.6B), suggesting that two days of deprivation is insufficient for induction of whisker deprivation-induced depression, even at P20. Together, these results show that deprivation-induced synaptic depression occurs with similar magnitude and time course when begun at either P12 or P20. In both cases, 4 days of deprivation are required for significant depression of input-output curves, and this depression requires more than 2 days to occur.

Discussion

These results show that whisker deprivation weakens L4-L2/3 synapses. Input-output curves indicated that the overall efficacy of L4-L2/3 inputs was reduced by 36%. This effect takes at least 4 days to occur, and appears to reflect active weakening of synapses, rather than a delay in normal synaptic maturation, because it occurs to an equal extent when deprivation began at P12 versus at P20, when synaptic connections are more mature (Stern et al., 2001). Deprivation increased PPR and slowed the rate of MK-801 blockade of NMDA-EPSCs, consistent with the hypothesis that deprivation decreased P_r. In contrast, deprivation did not alter the amplitude of either mEPSCs or L4-L2/3 pathway-specific quantal events recorded in strontium, indicating that whisker deprivation does not alter quantal amplitude. Thus, these data argue for a presynaptic locus of expression for deprivation-induced depression of L4-L2/3 synapses.

Evidence that deprivation reduces release probability

We used 2 measures to determine if deprivation reduced presynaptic release probability: PPR, which is classically thought to be inversely related to P_r (Zucker and Regehr, 2002), and the rate of NMDA-EPSC blockade by MK-801 (Hessler et al., 1993; Rosenmund et al., 1993). Deprivation selectively increased PPR in deprived columns. PPR appeared to largely reflect presynaptic function under our conditions, because it was dependent on extracellular calcium concentration but independent of AMPAR desensitization. Interestingly, a slightly different whisker deprivation pattern in which 2-3 adjacent rows of whiskers were deprived caused changes in short-term

depression at a variety of S1 synapses, but not at deprived L4-L2/3 inputs (Finnerty et al., 1999). This suggests that the locus and type of synaptic plasticity induced by experience in S1 is actively controlled by specific patterns of deprivation or use.

Deprivation slowed the progressive block of NMDAR-mediated transmission by MK-801, which is a standard measure of P_r commonly used to examine changes in P_r with plasticity (Weisskopf and Nicoll, 1995; Kullmann et al., 1996; Kaneko and Takahashi, 2004). Since the speed of MK-801 block is directly related to P_r, this indicates that P_r was lower in deprived columns. At many central synapses, the block in transmission by MK-801 can be well fit with a double exponential. Classically, this is thought to represent the progressive blockade of two sets of synapses, one with a relatively high P_r that is blocked quickly, and one with a low P_r (Hessler et al., 1993; Rosenmund et al., 1993), though such a decay could represent the progressive block of a projection with a continuum of P_r at individual synapses (Huang and Stevens, 1997). We did not attempt to assess whether the L4-L2/3 projection forms distinct sets of high and low P_r synapses, or whether a continuum of P_r exists across all synapses. Still, changes in the time course and relative contribution of fast and slow components of decay derived from double exponential fits allowed us to estimate changes in bulk P_r. Changes in the weighted mean time constant, a measure of the overall change in the speed of MK-801 block (Kaneko and Takahashi, 2004), showed that P_r decreased by 44% with deprivation. This result is comparable to the 36% decrease in overall synaptic strength assessed through input-output curves (Fig. 2.1D). Thus, a decrease in P_r alone can account for the weakening of the bulk L4-L2/3 input after whisker deprivation.

This conclusion is critically dependent on the assumption that deprivation does not alter NMDAR properties in a way that changes the ability of MK-801 to enter and block the channel. For example, slower blockade would be expected if deprivation decreased the open time of NMDARs, which would allow less time for MK-801 to block receptors, or if deprivation decreased the ability of NMDARs to bind MK-801. In our data, deprivation did not alter NMDA current kinetics, though a different deprivation protocol (unilateral whisker deprivation from P6 to P13-15) has been shown to affect NMDA current kinetics by delaying the normal developmental loss of NR2B subunits (note that this effect would be in the opposite direction of that required to explain our data) (Mierau et al., 2004). Furthermore, MK-801 reduced NMDA current kinetics similarly in sham and deprived conditions, indicating that the binding affinity of MK-801 is not altered by deprivation. These results suggest that the reduced rate of MK-801 blockade with deprivation does not reflect changes in NMDAR properties, but instead reflects a decrease in P_r at L4-L2/3 synapses.

Deprivation does not appear to reduce postsynaptic responsiveness

Postsynaptically, deprivation-induced depression could be expressed by decreasing quantal amplitude. We examined quantal amplitude at all synapses onto L2/3 neurons by analyzing mEPSCs, and examined L4-L2/3 synapses in isolation by analyzing miniature events in the presence of strontium. In control conditions, average mEPSCs and SrEPSCs had similar amplitudes and initial kinetics. The late component of EPSC decay was slower for SrEPSCs compared to mESPCs, but this can be attributed to the likelihood that an individual SrEPSC was immediately

followed by another SrEPSC. Therefore, our data support the hypothesis that miniature events recorded in strontium represent the postsynaptic response to individual quanta of neurotransmitter. We did not observe any difference in mEPSC or SrEPSC amplitude with deprivation, suggesting that whisker experience does not affect quantal amplitude.

If whisker deprivation weakens L4-L2/3 synapses by reducing P_r, then the frequency of miniature events at L4-L2/3 synapses should be lower (Redman, 1990). We did not observe a change in mEPSC frequency with deprivation, but this might be because changes at L4-L2/3 synapses were masked by the numerous other inputs onto L2/3 neurons, which may not show a similar depression. SrEPSC frequency was not analyzed since the number of fibers stimulated presumably varied across experiments. Thus, it remains unknown whether deprivation alters miniature frequency specifically at L4-L2/3 synapses.

Does deprivation-induced synaptic weakening represent LTD?

Multiple lines of evidence suggest that spike timing-dependent plasticity (STDP) may be the relevant form of LTD and LTD driving experience-dependent plasticity in parmary sensory cortex *in vivo* (Schuett et al., 2001; Yao and Dan, 2001; Fu et al., 2002), and specifically that whisker deprivation may induce STD-LTD at L4-L2/3 synapses in S1 (Celikel et al., 2004; Bender et al., 2005). STD-LTD is expressed presynaptically at L4-L2/3 synapses *in vitro*: STD-LTD increases PPR, requires retrograde cannabinoid signaling, and is mimicked by activation of presynaptic CB1 receptors, which are known to reduce release probability (Bender et

al., submitted). The present results indicate that deprivation weakens synapses by similar presynaptic mechanisms. Combined with previous data showing that deprivation occludes further LTD and enhances LTP (Allen et al., 2003), this suggests that deprivation-induced weakening of L4-L2/3 synapses represents LTD induced *in vivo*; however, it remains important to test the causality of known LTD signaling mechanisms for deprivation-induced weakening. Several attempts have been made to link map plasticity to LTP and LTD, with mixed results. Map plasticity occludes subsequent attempts to induce plasticity at L4-L2/3 synapses in S1 and V1 (Allen et al., 2003; Heynen et al., 2003), and experience can drive AMPAR insertion in S1 (Takahashi et al., 2003). While some experiments show that blocking LTD can also block map plasticity (Fischer et al., 2004), others have shown that map plasticity can persist despite a block of synaptic plasticity (Hensch and Stryker, 1996; Renger et al., 2002), though it is unknown whether other forms of plasticity compensate when one form is removed. A more detailed understanding of the various plasticity mechanisms expressed at different synapses would allow more direct tests for a causal link between LTP, LTD and map plasticity.

LTD is commonly expressed within minutes of induction *in vitro* (Feldman, 2000), and whisker deprivation causes an immediate reversal of L4-L2/3 spike timing in anesthetized animals, which would be predicted to rapidly drive STD-LTD (Celikel et al., 2004). Why then are at least 4-5 days of whisker deprivation required to significantly weaken L4-L2/3 synapses *in vivo*? One possibility is that in behaving animals, spontaneous spikes and spikes driven by whisker self-motion outnumber spikes driven by whisker contact onto objects (Fee et al., 1997), and thus, small

changes in the timing of whisker-driven spikes may produce a relatively minor bias in overall spiking statistics. This condition would be expected to lead to a slow accrual of timing-dependent LTD, compared to LTD induction protocols *in vitro*. Another possibility is that spontaneous network activity, which is known to reverse recently induced LTP and LTD, slows the accrual of experience-dependent plasticity *in vivo* (Xu et al., 1998; Zhou et al., 2003). A third possibility is that our whisker deprivation protocol, in which whole rows of whiskers are deprived or spared, might not be optimal for eliciting L4-L2/3 weakening. Receptive field plasticity is known to be more robust when whiskers are plucked singly or in a checkerboard pattern, so that each deprived column has many spared neighboring columns (Fox, 2002). The precise pattern of receptive field plasticity, as well as the spiking statistics of L4 and L2/3 neurons, remains unknown for row-based deprivation protocols.

Conclusions

While LTP and LTD are expressed postsynaptically at mature hippocampal synapses (Malinow and Malenka, 2002), it is evident that several forms of cortical LTP and LTD have presynaptic expression mechanisms (Markram and Tsodyks, 1996; Sjostrom et al., 2003; Bender et al., submitted). Here, we have shown that whisker deprivation weakens L4-L2/3 synapses in a manner consistent with known presynaptic mechanisms for LTD. Thus, these results provide further support for the hypothesis that synaptic plasticity contributes to the modification of cortical circuits during map plasticity.

References

Allen CB, Celikel T, Feldman DE (2003) Long-term depression induced by sensory deprivation during cortical map plasticity in vivo. Nat Neurosci 6:291-299.

Bender KJ, Rangel J, Feldman DE (2003) Development of columnar topography in the excitatory layer 4 to layer 2/3 projection in rat barrel cortex. J Neurosci 23:8759-8770.

Bender KJ, Deshmukh S, Feldman DE (2005) LTD as a mechanism for map plasticity in rat barrel cortex. Development and Plasticity in Sensory Thalamus and Cortex, (eds) R Erzurumlu, W Guido, and Z Molnar, Springer, NY In press.

Bender VA, Bender KJ, Braiser DJ, Feldman DE (submitted) Two coincidence detectors for STDP in somatosensory cortex.

Buonomano DV, Merzenich MM (1998) Cortical plasticity: from synapses to maps. Annu Rev Neurosci 21:149-186.

Castro-Alamancos MA, Donoghue JP, Connors BW (1995) Different forms of synaptic plasticity in somatosensory and motor areas of the neocortex. J Neurosci 15:5324-5333.

Celikel T, Szostak VA, Feldman DE (2004) Modulation of spike timing by sensory deprivation during induction of cortical map plasticity. Nat Neurosci 7:534-541.

Connors BW, Gutnick MJ (1990) Intrinsic firing patterns of diverse neocortical neurons. Trends Neurosci 13:99-104.

De Felipe J, Marco P, Fairen A, Jones EG (1997) Inhibitory synaptogenesis in mouse somatosensory cortex. Cereb Cortex 7:619-634.

Dodge FA, Jr., Miledi R, Rahamimoff R (1969) Strontium and quantal release of transmitter at the neuromuscular junction. J Physiol 200:267-283.

Fatt P, Katz B (1952) Spontaneous subthreshold activity at motor nerve endings. J Physiol 117:109-128.

Fee MS, Mitra PP, Kleinfeld D (1997) Central versus peripheral determinants of patterned spike activity in rat vibrissa cortex during whisking. J Neurophysiol 78:1144-1149.

Feldman DE (2000) Timing-based LTP and LTD at vertical inputs to layer II/III pyramidal cells in rat barrel cortex. Neuron 27:45-56.

Feldman DE, Brecht M (2005) Map Plasticity in Somatosensory Cortex. Science in press.

Feldmeyer D, Lubke J, Silver RA, Sakmann B (2002) Synaptic connections between layer 4 spiny neurone-layer 2/3 pyramidal cell pairs in juvenile rat barrel cortex: physiology and anatomy of interlaminar signalling within a cortical column. J Physiol 538:803-822.

Finnerty GT, Roberts LS, Connors BW (1999) Sensory experience modifies the short-term dynamics of neocortical synapses. Nature 400:367-371.

Fischer QS, Beaver CJ, Yang Y, Rao Y, Jakobsdottir KB, Storm DR, McKnight GS, Daw NW (2004) Requirement for the RIIbeta isoform of PKA, but not calcium-stimulated adenylyl cyclase, in visual cortical plasticity. J Neurosci 24:9049-9058.

Fox K (2002) Anatomical pathways and molecular mechanisms for plasticity in the barrel cortex. Neuroscience 111:799-814.

Fu YX, Djupsund K, Gao H, Hayden B, Shen K, Dan Y (2002) Temporal specificity in the cortical plasticity of visual space representation. Science 296:1999-2003.

Glazewski S, Fox K (1996) Time course of experience-dependent synaptic potentiation and depression in barrel cortex of adolescent rats. J Neurophysiol 75:1714-1729.

Goda Y, Stevens CF (1994) Two components of transmitter release at a central synapse. Proc Natl Acad Sci U S A 91:12942-12946.

Hensch TK, Stryker MP (1996) Ocular dominance plasticity under metabotropic glutamate receptor blockade. Science 272:554-557.

Hessler NA, Shirke AM, Malinow R (1993) The probability of transmitter release at a mammalian central synapse. Nature 366:569-572.

Heynen AJ, Yoon BJ, Liu CH, Chung HJ, Huganir RL, Bear MF (2003) Molecular mechanism for loss of visual cortical responsiveness following brief monocular deprivation. Nat Neurosci 6:854-862.

Huang EP, Stevens CF (1997) Estimating the distribution of synaptic reliabilities. J Neurophysiol 78:2870-2880.

Huettner JE, Bean BP (1988) Block of N-methyl-D-aspartate-activated current by the anticonvulsant MK-801: selective binding to open channels. Proc Natl Acad Sci U S A 85:1307-1311.

Kaneko M, Takahashi T (2004) Presynaptic mechanism underlying cAMP-dependent synaptic potentiation. J Neurosci 24:5202-5208.

Kullmann DM, Erdemli G, Asztely F (1996) LTP of AMPA and NMDA receptor-mediated signals: evidence for presynaptic expression and extrasynaptic glutamate spill-over. Neuron 17:461-474.

LeVay S, Wiesel TN, Hubel DH (1980) The development of ocular dominance columns in normal and visually deprived monkeys. J Comp Neurol 191:1-51.

Magee JC, Johnston D (2005) Plasticity of dendritic function. Curr Opin Neurobiol 15:334-342.

Malinow R, Malenka RC (2002) AMPA receptor trafficking and synaptic plasticity. Annu Rev Neurosci 25:103-126.

Markram H, Tsodyks M (1996) Redistribution of synaptic efficacy between neocortical pyramidal neurons. Nature 382:807-810.

Micheva KD, Beaulieu C (1996) Quantitative aspects of synaptogenesis in the rat barrel field cortex with special reference to GABA circuitry. J Comp Neurol 373:340-354.

Mierau SB, Meredith RM, Upton AL, Paulsen O (2004) Dissociation of experience-dependent and -independent changes in excitatory synaptic transmission during development of barrel cortex. Proc Natl Acad Sci U S A 101:15518-15523.

Miledi R, Slater CR (1966) The action of calcium on neuronal synapses in the squid. J Physiol 184:473-498.

Nosyreva ED, Huber KM (2005) Developmental switch in synaptic mechanisms of hippocampal metabotropic glutamate receptor-dependent long-term depression. J Neurosci 25:2992-3001.

Oliet SH, Malenka RC, Nicoll RA (1996) Bidirectional control of quantal size by synaptic activity in the hippocampus. Science 271:1294-1297.

Otis T, Zhang S, Trussell LO (1996) Direct measurement of AMPA receptor desensitization induced by glutamatergic synaptic transmission. J Neurosci 16:7496-7504.

Paulsen O, Heggelund P (1994) The quantal size at retinogeniculate synapses determined from spontaneous and evoked EPSCs in guinea-pig thalamic slices. J Physiol 480 (Pt 3):505-511.

Redman S (1990) Quantal analysis of synaptic potentials in neurons of the central nervous system. Physiol Rev 70:165-198.

Renger JJ, Hartman KN, Tsuchimoto Y, Yokoi M, Nakanishi S, Hensch TK (2002) Experience-dependent plasticity without long-term depression by type 2 metabotropic glutamate receptors in developing visual cortex. Proc Natl Acad Sci U S A 99:1041-1046.

Rioult-Pedotti MS, Friedman D, Donoghue JP (2000) Learning-induced LTP in neocortex. Science 290:533-536.

Rosenmund C, Clements JD, Westbrook GL (1993) Nonuniform probability of glutamate release at a hippocampal synapse. Science 262:754-757.

Schuett S, Bonhoeffer T, Hubener M (2001) Pairing-induced changes of orientation maps in cat visual cortex. Neuron 32:325-337.

Shepherd GM, Pologruto TA, Svoboda K (2003) Circuit analysis of experience-dependent plasticity in the developing rat barrel cortex. Neuron 38:277-289.

Sjostrom PJ, Turrigiano GG, Nelson SB (2003) Neocortical LTD via coincident activation of presynaptic NMDA and cannabinoid receptors. Neuron 39:641-654.

Stern EA, Maravall M, Svoboda K (2001) Rapid development and plasticity of layer 2/3 maps in rat barrel cortex in vivo. Neuron 31:305-315.

Takahashi T, Svoboda K, Malinow R (2003) Experience strengthening transmission by driving AMPA receptors into synapses. Science 299:1585-1588.

Weisskopf MG, Nicoll RA (1995) Presynaptic changes during mossy fibre LTP revealed by NMDA receptor-mediated synaptic responses. Nature 376:256-259.

Welker C, Woolsey TA (1974) Structure of layer IV in the somatosensory neocortex of the rat: description and comparison with the mouse. J Comp Neurol 158:437-453.

Woolsey TA, Van der Loos H (1970) The structural organization of layer IV in the somatosensory region (SI) of mouse cerebral cortex. The description of a cortical field composed of discrete cytoarchitectonic units. Brain Res 17:205-242.

Xu L, Anwyl R, Rowan MJ (1998) Spatial exploration induces a persistent reversal of long-term potentiation in rat hippocampus. Nature 394:891-894.

Yao H, Dan Y (2001) Stimulus timing-dependent plasticity in cortical processing of orientation. Neuron 32:315-323.

Zhou Q, Tao HW, Poo MM (2003) Reversal and stabilization of synaptic modifications in a developing visual system. Science 300:1953-1957.

Zucker RS, Regehr WG (2002) Short-term synaptic plasticity. Annu Rev Physiol 64:355-405.

Fig. 2.1: Time course for deprivation-induced depression of L4-L2/3 synapses. A, Arrangement of large whiskers on rat snout. Circles: Intact whiskers. Xs: Deprived D-row whiskers. B, Schematic of across row slice preparation detailing arrangement of L4 whisker barrels and neighboring medial forepaw barrels. Whisker barrels from rows A and E are labeled. Stimulation in L4 and recording in L2/3 with focal bicuculline (BMI) is illustrated in the whisker deprived, D barrel column. C, Representative series of EPSPs at L4-L2/3 synapses in response to increasing stimulation intensity from columns corresponding to spared (top) and deprived whiskers (bottom). Recordings made at 1 to 1.5 times (x) threshold from rats whisker deprived from P12 for 5 days. D, Input-output curve for EPSP amplitude as a function of stimulation intensity after 5 days of whisker deprivation. E, Normalized input-output curves after 3, 5, 7, and 9 days of whisker deprivation. Data are normalized to mean EPSP amplitude for cells in spared column at 1.5x. Asterisks: deprived condition significantly weaker than spared at that stimulus intensity. F, Normalized input-output curve in control conditions. Data from Allen et al. (2003). G, Amplitude of EPSPs from cells in deprived columns relative to spared. EPSP amplitude of cells in deprived columns relative to average response in spared column of same slice. Data were calculated at 1.3-1.5x threshold and averaged for each cell. "Control" and "all 9+" incorporate data from Allen et al. (2003). Numbers in parenthesis are cells in the D column. Bars are SEM.

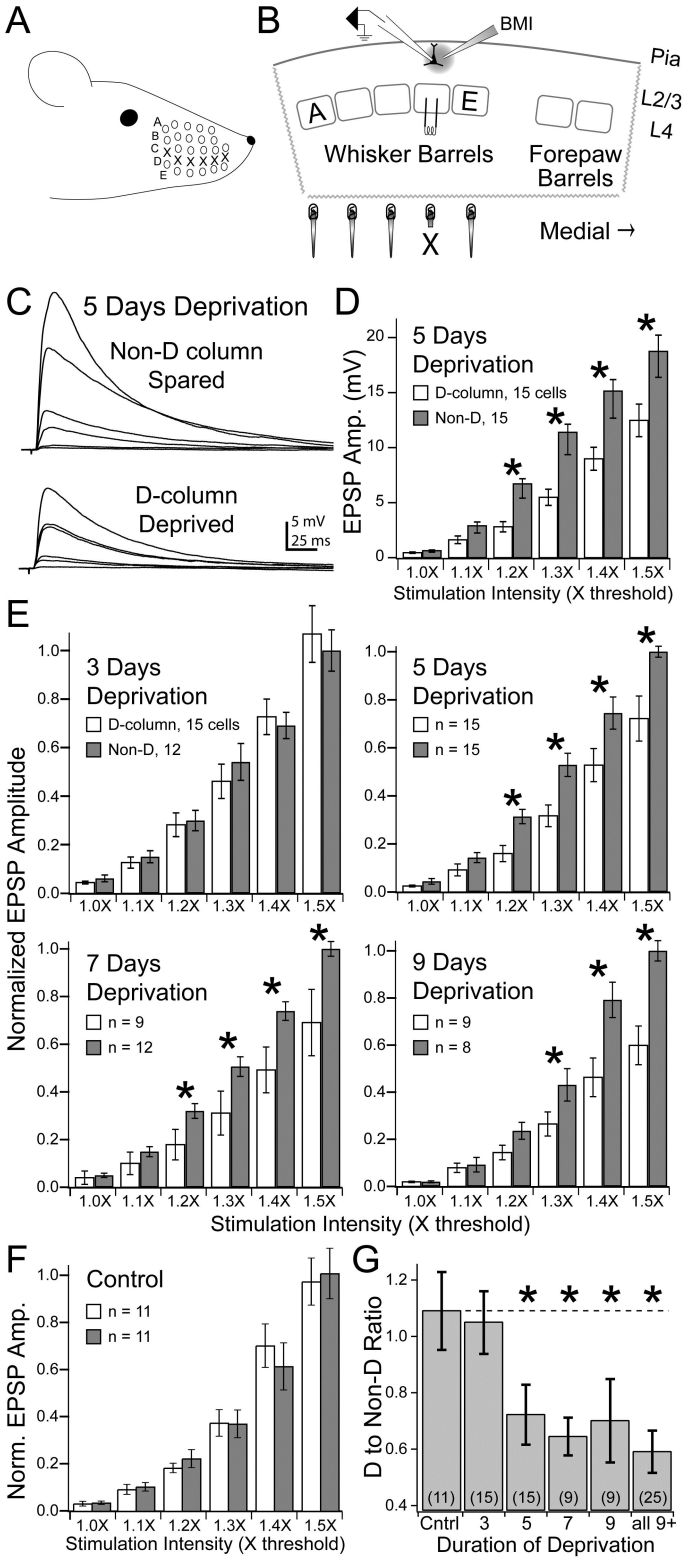
A
B
BMI
Pia
L2/3
L4
A
E
Whisker Barrels
Forepaw Barrels
X
Medial →
C
5 Days Deprivation
Non-D column Spared
D-column Deprived
5 mV
25 ms
D
5 Days Deprivation
D-column, 15 cells
Non-D, 15
EPSP Amp. (mV)
1.0X 1.1X 1.2X 1.3X 1.4X 1.5X
Stimulation Intensity (X threshold)
E
3 Days Deprivation
D-column, 15 cells
Non-D, 12
5 Days Deprivation
n = 15
n = 15
7 Days Deprivation
n = 9
n = 12
9 Days Deprivation
n = 9
n = 8
Normalized EPSP Amplitude
Stimulation Intensity (X threshold)
F
Control
n = 11
n = 11
Norm. EPSP Amp.
Stimulation Intensity (X threshold)
G
D to Non-D Ratio
(11) (15) (15) (9) (9) (25)
Cntrl 3 5 7 9 all 9+
Duration of Deprivation

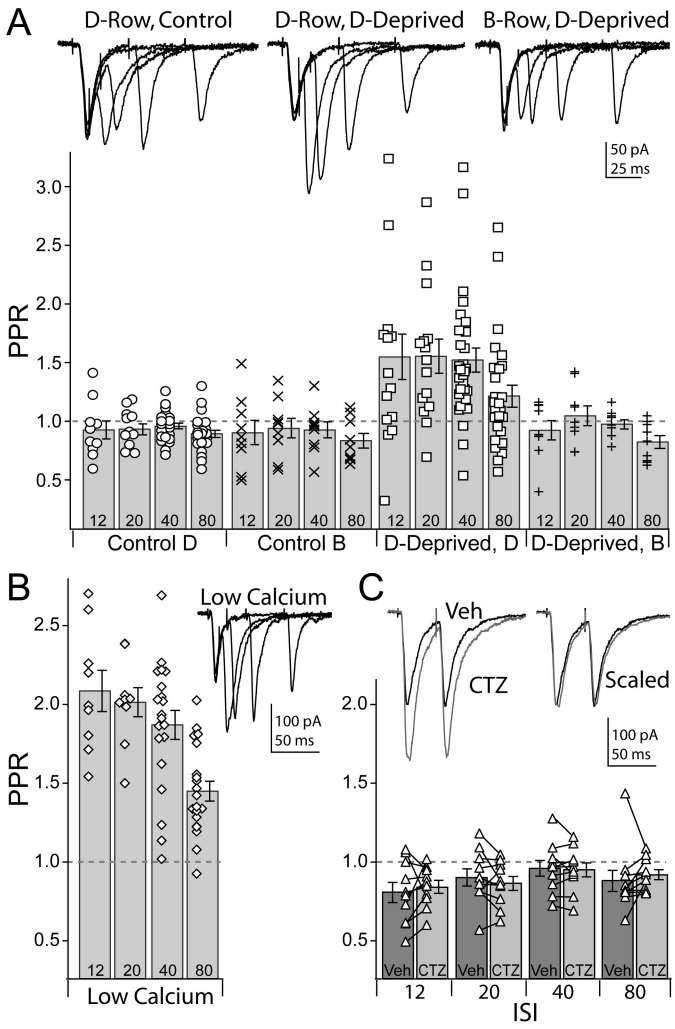

Fig. 2.2: Whisker deprivation increases PPR. A, Top: Representative recordings of pairs of AMPA-mediated EPSCs recorded at ISIs of 12, 20, 40 and 80 msec in D and B columns in slices from control and D-deprived rats. Bottom: Summary of deprivation effects on PPR. Numbers indicate ISI. B, Lowering external calcium from 2.5 mM to 1.25 mM increases PPR at this synapse. C, Cyclothiazide (CTZ) does not alter PPR. Veh: vehicle control. Bars are SEM.

Fig. 2.3: Whisker deprivation slows NMDA-EPSC transmission block by MK-801. A, Example of MK-801—mediated block of transmission. Top left: Averaged NMDAR-mediated EPSC in baseline conditions (1), immediately after resuming stimulation in MK-801 (2), and after ~20 min of stimulation in MK-801 (3). Top right: EPSC (2) scaled to peak amplitude of (1), demonstrating open channel blocking properties of MK-801. Bottom: Time course for individual experiment. Points represent peak EPSC amplitude, input and series resistance for each epoch. B, Average decay in EPSC amplitude for deprived and sham-deprived conditions. Decays are normalized to the amplitude of the first EPSC in MK-801 and fit to double exponentials. C, EPSC decay for sham-deprived and low calcium conditions. Dashed line: fit for deprived condition. Bars are SEM. Insets in B and C: expansion of same data at 0-30 episodes. D, Time to reach half maximal EPSC amplitude. Asterisks indicate $p < 0.05$. E, EPSC decay kinetics in the absence and presence of MK-801 for sham-deprived (circles) and deprived (squares) conditions. MK-801 speeds EPSC decay. Bars are SEM.

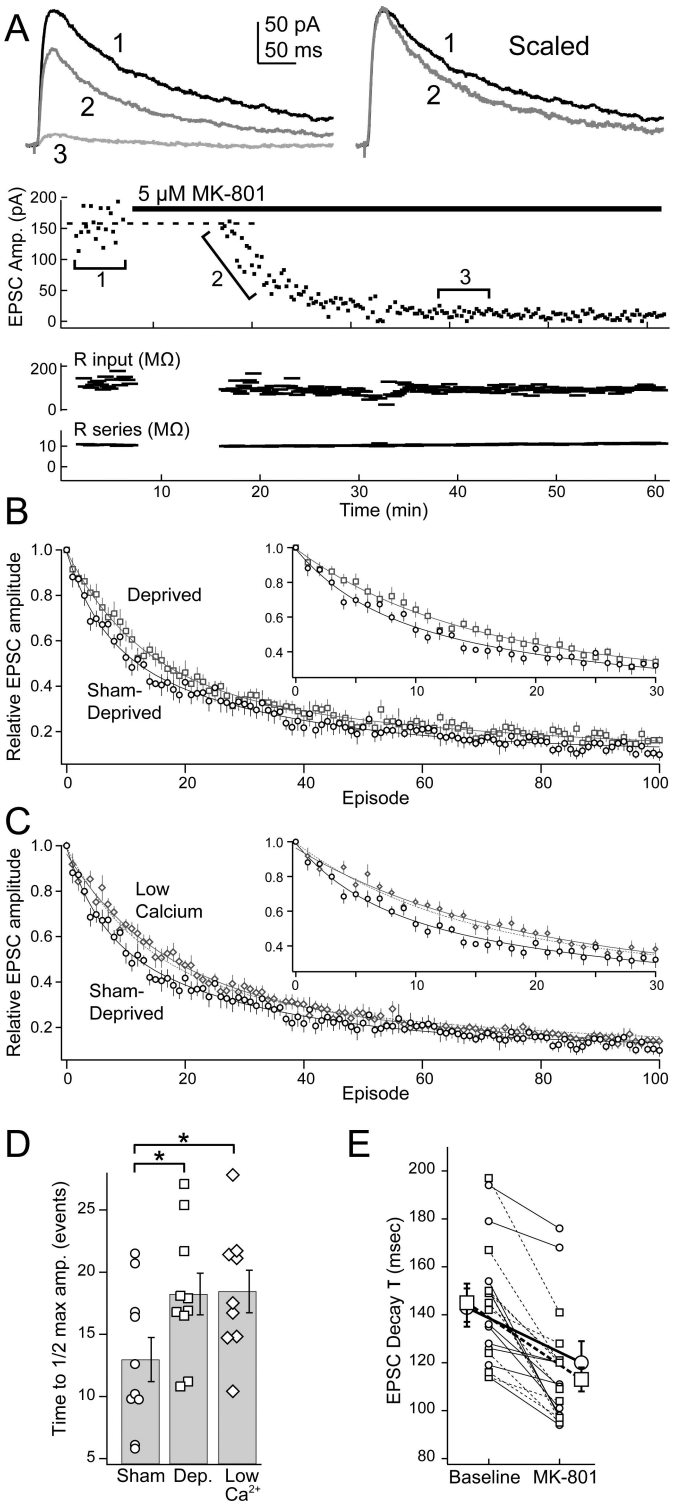
A
50 pA
50 ms
1
2
3
Scaled
5 μM MK-801
EPSC Amp. (pA)
R input (MΩ)
R series (MΩ)
Time (min)
B
Relative EPSC amplitude
Deprived
Sham-
Deprived
Episode
C
Low
Calcium
Sham-
Deprived
Episode
D
Time to 1/2 max amp. (events)
Sham
Dep.
Low
Ca2+
E
EPSC Decay T (msec)
Baseline
MK-801

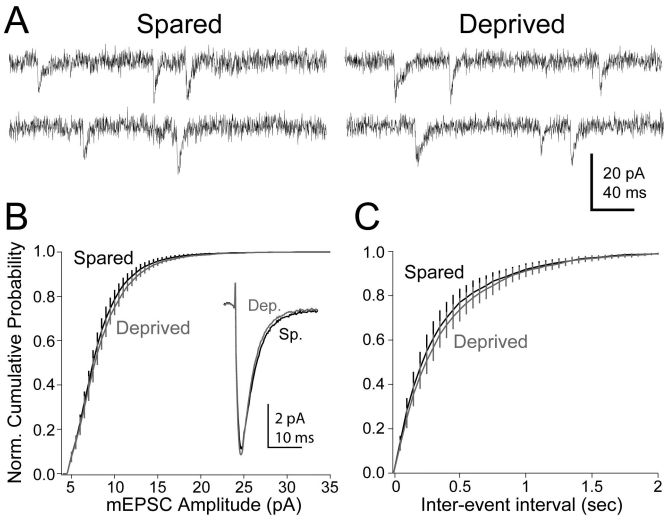

Fig. 2.4: Miniature EPSCs in L2/3 pyramidal cells. A, Representative recordings from L2/3 pyramidal neurons in spared (left) and deprived (right) columns. B. Normalized cumulative probability histogram for mEPSC amplitude. Inset: average mEPSC in deprived and control conditions. Data are normalized to event onset, which is defined by detection software as a peak positivity immediately before the event. C. Normalized cumulative probability histogram for mEPSC inter-event interval. Bars are SEM.

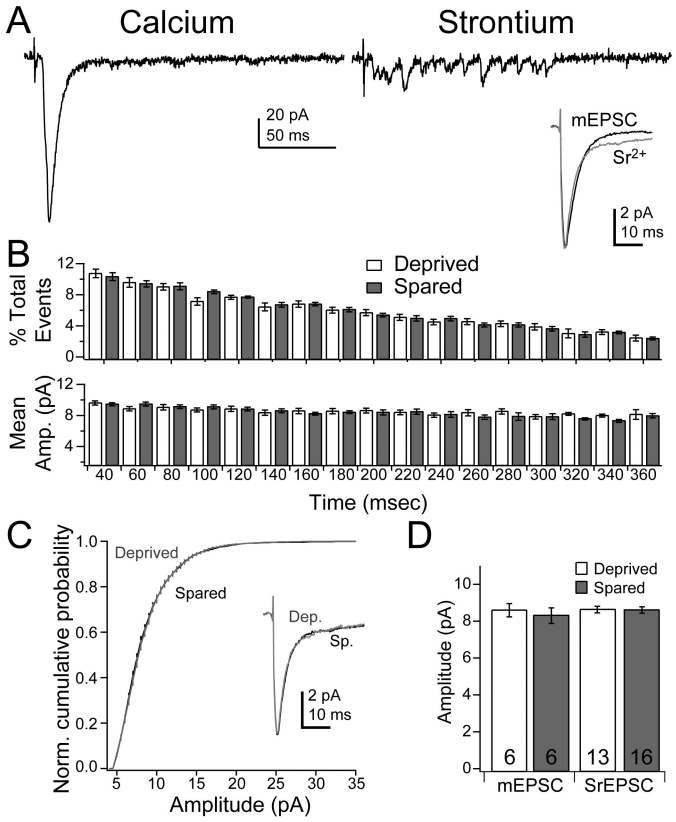

Fig. 2.5: Evoked quantal release in the presence of strontium at L4-L2/3 synapses. A, AMPA-mediated EPSC at L4-L2/3 synapse in the presence of calcium (left). Replacing calcium with strontium produces prolonged release events consisting of individual, presumably quantal events (SrEPSCs). Inset: average SrEPSC compared to average mEPSC from spared column. B, Relative number (top) and amplitude (bottom) of SrEPSCs over time window selected for analysis. Time measured from SrEPSC onset. C, Normalized cumulative probability histogram for SrEPSC amplitude. Inset: average SrEPSC in deprived and control conditions. Data are normalized to event onset, which is defined by detection software as a peak positivity immediately before the event. D. Average mEPSC and SrEPSC amplitude in deprived and spared conditions. Bars are SEM.

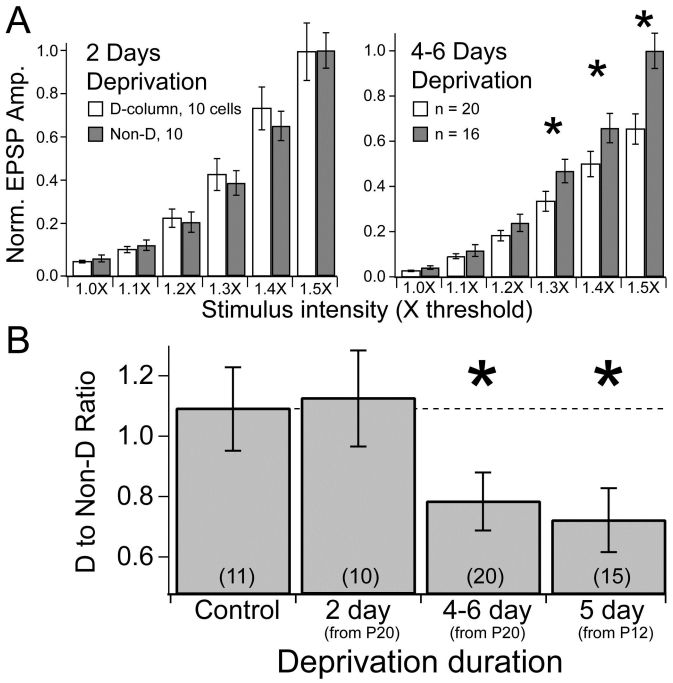

Fig. 2.6: Time course for deprivation-induced depression in more mature animals. A, Normalized input-output curves after 2, and 4-6 days of whisker deprivation beginning at P20. Data are normalized to mean EPSP amplitude for cells in spared column at 1.5 times threshold. Asterisk: deprived condition significantly weaker than spared at that stimulus intensity. B, Amplitude of EPSPs from cells in deprived columns relative to spared, calculated as in Fig. 1D. 4-6 days deprivation mean: 4.7 days. 5 days deprivation from P12 shown for comparison. Numbers in parenthesis are cells. Bars are SEM.

Table 2.1: Effects of deprivation on PPR at L4 to L2/3 synapses

ISI (msec)	12		20		40		80	
Sham deprived								
B row	0.91 ± 0.10 (9)		0.94 ± 0.08 (9)		0.93 ± 0.07 (9)		0.83 ± 0.06 (9)	
D row	0.93 ± 0.08 (10)		0.93 ± 0.05 (12)		0.96 ± 0.02 (25)		0.89 ± 0.03 (24)	
D-row deprived								
B row	0.92 ± 0.08 (9)		1.05 ± 0.08 (9)		0.97 ± 0.04 (9)		0.82 ± 0.06 (9)	
D row	1.55 ± 0.19 (15)	*	1.55 ± 0.15 (15)	#	1.52 ± 0.10 (29)	#	1.21 ± 0.09 (27)	*
Low Calcium	2.09 ± 0.13 (9)	#	2.01 ± 0.09 (9)	#	1.87 ± 0.09 (20)	#	1.45 ± 0.06 (20)	#
Cyclothiazide	0.96 ± 0.05 (10)		0.95 ± 0.04 (10)		0.88 ± 0.07 (10)		0.92 ± 0.03 (10)	

Parenthesis indicate number of cells

* $p < 0.05$ vs corresponding ISI in B row in deprived slices and D row in sham, Fisher's PLSD

# $p < 0.001$ vs corresponding ISI in B row in deprived slices and D row in sham, Fisher's PLSD

Chapter 3

Development of columnar topography in the excitatory layer 4 to layer 2/3 projection in rat barrel cortex

Abstract

The excitatory feedforward projection from layer (L) 4 to L2/3 in rat primary somatosensory (S1) cortex exhibits precise, columnar topography that is critical for columnar processing of whisker inputs. Here, we characterize the development of axonal topography in this projection using single-cell reconstructions in S1 slices. In the mature projection (postnatal day [P] 14-26), axons of L4 cells extending into L2/3 were confined almost entirely to the home barrel column, consistent with previous results. However, at younger ages (P8-11), axonal topography was significantly less columnar, with a large proportion of branches innervating neighboring barrel columns representing adjacent whisker rows. Mature topography developed from this initial state by targeted axonal growth within the home column, and by growth of barrel columns themselves. Raising rats with all or a subset of whiskers plucked from P8-9, manipulations that induce reorganization of functional whisker maps and synaptic depression at L4 to L2/3 synapses, did not alter normal anatomical development of L4 to L2/3 axons. Thus, development of this projection does not require normal sensory experience after P8, and deprivation-induced reorganization of whisker maps at this age is unlikely to involve physical remodeling of L4 to L2/3 axons.

Introduction

The fundamental unit of cortical processing is the cortical column. Columnar processing is achieved in part by precise axonal projections that preferentially connect cells within single, radial columns (Mountcastle, 1957, 1997). In the whisker region of rat primary somatosensory (S1) cortex, each cortical column processes information primarily from one facial whisker (Simons, 1978; Keller, 1995). Neurons in layer 4 (L4) of S1 are arranged in clusters, called barrels, with one barrel corresponding to each whisker in an orderly map (Woolsey and Van der Loos, 1970; Welker and Woolsey, 1974). When a whisker is deflected, thalamic afferents excite neurons in the corresponding L4 barrel, which then relay excitation to layer 2/3 (L2/3) of the radial column centered on that barrel, termed the barrel column (Armstrong-James and Fox, 1987; Petersen and Sakmann, 2001; Laaris and Keller, 2002; Petersen et al., 2003).

In mature S1, the excitatory feedforward relay from L4 to L2/3 is mediated by axons of L4 spiny stellate and star pyramidal cells that project to L2/3 almost exclusively within the home barrel column, forming a topographically precise, columnar projection (Harris and Woolsey, 1983; Lubke et al., 2000; Petersen and Sakmann, 2000, 2001; Feldmeyer et al., 2002). This projection has similar topography in other neocortical sensory areas (Lund et al., 1977; Winer, 1984; Burkhalter, 1989; Callaway and Katz, 1992). In S1, columnar topography is so precise that axons of L4 cells near the edges of barrels project asymmetrically within L2/3, innervating the home column while avoiding neighboring columns (Petersen and Sakmann, 2000). How this precision arises during development is unknown and is the subject of this study.

In the classical model for development of topographic projections, adult precision arises by activity- or age-dependent refinement of initial axons that are either modestly or highly overarborized (Katz and Shatz, 1996; Debski and Cline, 2002; McLaughlin et al., 2003). This basic developmental pattern occurs in neocortex for callosal projections (Innocenti, 1981, 1995), horizontal projections in L2/3 (Luhmann et al., 1986; Callaway and Katz, 1990; Durack and Katz, 1996), and for laminar target selection by L2/3 pyramidal cells (Callaway, 1998; Borrell and Callaway, 2002). Whether thalamocortical axons develop similarly is controversial, with some studies finding initial axons to be poorly segregated or unsegregated into cortical columns (LeVay et al., 1978; Agmon et al., 1995; Finney and Shatz, 1998; Ruthazer et al., 1999; Rebsam et al., 2002), and other studies showing adult-like topography from the earliest stages of axonal development (Catalano et al., 1996; Crowley and Katz, 2002). Thus, whether topographic projections develop by a common process is unclear.

Another unresolved issue is the role of sensory experience in guiding axonal development. Sensory experience is required for late stages of development of horizontal and thalamocortical axons in visual cortex (Callaway and Katz, 1991; Lowel and Singer, 1992; Antonini and Stryker, 1993b), though not for early establishment of thalamocortical axon topography (Horton and Hocking, 1996; Katz and Crowley, 2002). In S1, experience modulates synaptic strength and functional topography of the developing L4 to L2/3 projection (Lendvai et al., 2000; Stern et al., 2001; Allen et al., 2003; Shepherd et al., 2003; Takahashi et al., 2003). However, whether experience exerts these effects by altering the physical arrangement and targeting of L4 to L2/3 axons, as recently proposed (Stern et al., 2001), is unknown.

To characterize development and experience-dependent plasticity of the L4 to L2/3 axonal projection, we filled and reconstructed single L4 cells relative to column boundaries in S1 slices prepared from animals of different ages and sensory experience. We found that at young ages, axons spread across columns more than in mature rats, and that mature, columnar topography was achieved by targeted axonal growth in the home barrel column. Remarkably, axonal development occurred normally even in the absence of normal sensory experience.

Methods

Whisker plucking. All procedures were approved by the UCSD Institutional Animal Care and Use Committee. Whiskers were plucked every 2 days from the right side of the face of Long-Evans rats under isoflurane anesthesia. For unilateral deprivation experiments, all large whiskers (A1-4, B1-4, C1-7, D1-8, E1-9, and the straddler row [α, β, γ, δ]) were plucked beginning at postnatal day (P) 9 and continuing every other day until slices were prepared (P14-17). For D-only deprivation experiments, D1-8 and γ were plucked every other day from P8 until slices were prepared (P23-26).

Slice preparation. Rats (P6-26) were anesthetized with isoflurane and the brain was removed in either chilled normal Ringer's solution (for animals ≤ P13; contains [in mM]: 119 NaCl, 2.5 KCl, 1.3 $MgSO_4$, 1 NaH_2PO_4, 26.3 $NaHCO_3$, 11 D-(+)-glucose, 2.5 $CaCl_2$, pH 7.4, bubbled with 95% O_2/5% CO_2) or low-sodium, low-calcium Ringer's solution (> P13; contains [in mM]: 250 sucrose, 2.5 KCl, 4 $MgSO_4$, 1 NaH_2PO_4, 15 HEPES, 11 D-(+)-glucose, 0.1 $CaCl_2$,). Oblique S1 slices (400 μm) were cut 50° towards coronal from the midsagittal plane (Land and Simons, 1985; Finnerty et al., 1999). In one hemisphere, this plane is parallel to the barrel rows, and produces slices containing multiple barrels from each row ("within-row slices"). In the other hemisphere, this plane is orthogonal to barrel rows, and produces slices with one barrel from each of the 5 rows ("across-row slices"). Slices were incubated for 30 min at 30°C in normal Ringer's solution, then incubated at room temperature 0.5-6 hours before recording.

Electrophysiology. Recordings were made at room temperature in normal Ringer's solution. Whisker barrels were visualized with transmitted light and identified based on location and barrel appearance (Finnerty et al., 1999; Petersen and Sakmann, 2000; Allen et al., 2003). Spiny stellate and star pyramidal neurons at least 100 μm below the surface of the slice were visualized with differential interference contrast optics and filled with biocytin during whole cell recording (Axopatch-200B amplifier [Axon Instruments, Union City, CA], 5-7 MΩ pipettes, 40-60 min recording duration). Internal solution contained (in mM): 116 K-gluconate, 6 KCl, 2 NaCl, 20 HEPES, 0.5 EGTA, 4 MgATP, 0.3 NaGTP, 0.3% biocytin (w/v), pH 7.23. For within-row slices, fills were made in barrels that were flanked by at least one whisker barrel on either side. In across-row slices, fills were made in the D-barrel. Action potentials (APs) were elicited every 30 s by current injection for the duration of the recording. Resting membrane potential (V_m), input resistance (R_{in}), AP threshold, and AP amplitude (from threshold to peak) were measured for each cell. Membrane potential measurements were corrected for a measured junction potential of 10 mV.

Histological procedures. Slices were fixed immediately after recording in 4% paraformaldehyde/20% sucrose in 0.1 M phosphate buffer (PB) overnight. Slices were then transferred to 4% paraformaldehyde/30% sucrose in PB at least 1 hr before resectioning at 100 μm on a freezing microtome. Sections were rinsed in PB and endogenous peroxidases were quenched with 10% methanol and 1% H_20_2 (30 min). Sections were incubated in permeabilization/blocking solution (1% normal rabbit serum, 0.75% Triton X-100 in PB) for 2 hrs, and incubated overnight in primary antibody solution (1:5000 goat anti-biotin, 1% normal rabbit serum, 0.1% Triton X-

100) at 4°C. After rinsing, sections were transferred to a secondary antibody solution (1:200 biotinylated rabbit anti-goat, 1% normal rabbit serum, 0.1% Tritin X-100) for 2 hours. Biotin was then visualized with a standard avidin-biotin-HRP reaction (Vector Laboratories, Burlingame, CA), with diaminobenzidine hydrochloride (DAB, 0.1%) as a chromogen (DeBello et al., 2001). Sections were mounted on Superfrost slides (Fisher, Pittsburgh, PA) and air-dried. Alternate sections were exposed to 1% osmium tetroxide to increase contrast and visualize barrels (Keller and Carlson, 1999). To intensify the reaction product, sections were dehydrated and cleared in xylenes overnight, then rehydrated and incubated in 1.42% silver nitrate at 56°C for 30 min, followed by 0.2% gold chloride at room temperature for 10 min, and fixed with 5% sodium thiosulfate for 5 minutes (Kitt et al., 1988). Finally, sections were dehydrated, cleared in xylenes, and coverslipped using Permount. All antibodies were obtained from Vector.

Reconstruction and quantification of axonal morphology. Neurons with consistently intense staining along the axon length and no obvious truncation of axonal processes were reconstructed from live digital images (40x objective, NA=0.75, resolution: 0.25 μm/pixel) using Neurolucida software (Microbrightfield, Williston, VT) with a Magnafire camera (Optronics, Goleta, CA) on an Axioskop 2 plus microscope (Zeiss, Thornwood, NY). Neurons with somata near the center of the desired barrel were reconstructed for quantitative analysis of axonal topography. Barrel outlines were determined from osmium-stained sections (Keller and Carlson, 1999). Barrel column boundaries were defined by parallel lines bisecting the septa on either side of the barrel containing the filled cell ("home barrel column"), or by two

parallel lines located 220 μm medial and lateral to the soma ("±220 μm column"). This distance corresponds to the mean width of a mature barrel column (440 ± 80 μm for all slices P14-26 in both planes of section, n = 70). A series of line segments connecting the top of the barrels was used to define the L3/4 border (Fig. 3.3A).

Because L2/3 pyramidal cells receive inputs via dendrites located in layers 1-3 (Keller, 1995), topography of the L4 to L2/3 projection was quantified by measuring the location and length of all axon segments in the supragranular layers (L1-3, defined as the region between the pia and the L3/4 border). In practice, ~5% of axon length was located < 150 μm of the pia (presumptive L1), and thus nearly all reconstructed axon within L1-3 was located in L2/3 proper (see Results). Axon length and spatial distribution in L1-3 was calculated using custom image analysis routines in MATLAB (Mathworks, Natick, MA). Distances and lengths were not corrected for the measured 2% shrinkage of fixed, stained tissue relative to living slices. All values are expressed as mean ± standard deviation (SD) unless otherwise noted. Significance was determined using Student's t-test unless otherwise noted.

To determine the tangential distribution of axon in L1-3, L1-3 was divided into 50 μm radially oriented columns with the central column centered on the soma. Axonal length was measured within each column. To determine the sublaminar distribution of axon in L1-3 (i.e., depth profile of axon within L1-3), L1-3 was sub-divided into 10 equal strips oriented parallel to the pia, and axonal length within each strip was measured. The resulting distributions were normalized by the total axon length in L2/3. Differences in the shape of spatial distributions of axon were tested using Kolmogorov-Smirnov statistics.

The measured fraction of axon within L1-3 of the home barrel column was compared to the fraction expected in a simple model of uniform, non-directed axonal growth around the soma. For each age group and plane of section, the radius (*r*) of maximal vertical axonal extent from the soma was calculated as the sum of the average measured distance from the soma to the L3/4 border (*x*) plus the average measured vertical distance (*d*) from the L3/4 border containing 95% of all axon length in L1-3 (Fig. 3.3B). The total area in L2/3 contained within the circle of radius *r* was calculated as $A_{Tot} = \frac{r^2(\theta_1 - \sin\theta_1)}{2}$, where $\theta_1 = 2\cos^{-1}\left(\frac{x}{r}\right)$, which corresponds to the angle between lines KJ and JN in Fig. 3.3B. The area of the circle contained within the home column in L2/3 was calculated as $A_{Home} = \frac{r^2(\theta_2 - \sin\theta_2)}{2} + c\left[r\cos\left(\frac{\theta_2}{2}\right) - x\right]$, where $\theta_2 = 2\sin^{-1}\left(\frac{c}{2r}\right)$, the angle between lines JL and JM in Fig. 3.3B, and *c* equals the average measured width of the barrel column. For a model of non-directional growth in which axonal density is equal in L2/3 throughout the circle of radius *r*, the fraction of axon in the home column would be A_{Home}/A_{Tot}.

Other analyses. For axonal bouton analysis, a section of axon in L2/3 of the home barrel column 200 ± 60 μm in length was chosen randomly. Bouton counts were performed blind to sensory experience at a resolution of 0.16 μm/pixel (63x objective, NA = 1.4). Boutons were defined as swellings visible on either or both sides of an axonal branch, accompanied by increased staining intensity. Dendritic complexity of spiny stellate cells was assessed using Sholl analysis with branch

crossings counted on concentric circles spaced every 25 μm, and centered on the soma (Sholl, 1953). Significance was tested with Kolmogorov-Smirnov statistics. Axon length in L4 was quantified using methods described for L1-3. Here, an additional series of line segments connecting the bottom of the barrels defined the L4/5 border.

Results

Topography of L4 to L2/3 axons in mature S1 slices

To assess the morphology of excitatory L4 to L2/3 axons, single cells in the central 30% of L4 whisker barrels were filled with biocytin during whole-cell recording in S1 slices. Axons and dendrites were visualized with an antibody-based reaction using DAB as a chromogen (Fig. 3.1A). These cells had prominent axons with discernable boutons (Fig. 3.1A, inset) in supragranular layers (L1-3). All axon in L1-3 was analyzed since L2/3 neurons receive inputs in all supragranular layers, including L1 (Keller, 1995). Barrels were visualized in alternate sections by osmium intensification of DAB-stained tissue (Fig. 3.1B), and used to define barrel columns for each slice (Fig. 3.1C). Osmium-stained barrels correspond well to barrels visualized by transillumination in living slices (Keller and Carlson, 1999), which in turn correspond to barrels observed by cytochrome oxidase staining (Petersen and Sakmann, 2000).

All 119 cells (P6-26) reconstructed in this study were excitatory, as defined by presence of dense dendritic spines (Saint Marie and Peters, 1985). Of these, 56 were spiny stellate cells, 40 were star pyramidal cells, and the rest had an incomplete dendritic tree and could not be classified beyond being excitatory. We did not observe any classical (non-star) pyramidal cells, presumably because few exist in the center of barrels (cf. Schubert et al., 2003). The ratio of star pyramids to spiny stellate cells decreased with development (P8-11: 18 star pyramids and 18 stellate cells; P14-26: 18 star pyramids and 36 stellate cells), consistent with reported developmental trends (Peinado and Katz, 1990). No differences in axonal morphology were found between

spiny stellate cells, star pyramids and unidentified excitatory cells, either for immature (P8-11) or mature (P14-26) cell populations (Table 3.1). Axonal measurements were therefore pooled across cell types for all analyses.

Cells were selected based on regular spiking responses to a 500 ms depolarizing current injection (Connors and Gutnick, 1990), and $V_{m\ rest} < -75$ mV. Within our data set, AP threshold and AP amplitude showed modest differences across cell classes (Table 3.1).

Cells were filled in S1 slices cut in one of 2 orthogonal planes of section, either parallel to whisker barrel rows (within-row slices), or parallel to whisker barrel arcs (across-row slices) in order to provide a complete description of axonal topography (see Methods). Each slice contained multiple barrels, with the cell filled in a central barrel (normalized horizontal soma position within central barrel = 0.49 ± 0.1 [0 = lateral edge of barrel, 1 = medial edge of barrel]; normalized depth of soma in barrel = 0.49 ± 0.1 [0 = L3/4 border, 1 = L4/5 border]; P8-26, n = 112). In P14-26 rats, axons of L4 cells projecting into L1-3 were largely restricted to the home barrel column in both planes of section (Fig. 3.1, 3.2A). In across-row slices, 87 ± 14% (n = 25) of axon length in L1-3 was confined to the home barrel column (defined as the column enclosing the home barrel and half the adjacent septa; Fig. 3.3A). In within-row slices, 76 ± 22% (n = 22) of axon length was confined to the home barrel column, significantly less than in the across-row plane ($p < 0.05$). Thus, L4 to L2/3 axons were largely columnar, but showed more divergence to neighboring columns within a row than across rows, as do other axonal projections in S1 (Petersen et al., 2003).

To determine if axonal topography within L1-3 reflected active targeting to the home barrel column, we calculated the percentage of axon expected in the home column assuming uniformly dense, non-targeted axonal growth in all directions from the soma (see Methods and Fig. 3.3B). In the non-directed growth model, only 59.6% and 58.3% of all axons in L1-3 would be expected in the home barrel column in across-row and within-row slices, respectively, given the column width (c) and maximal vertical axonal spread from the soma ($r = d + x$) in these slices (x = 161.5, 153.2 μm; d = 313.5, 330.4 μm; c = 465, 413 μm, across- and within-row, respectively). Because substantially higher fractions of axon were actually observed in the home column than predicted by this model, L4 to L2/3 axonal topography must reflect active targeting of axon to the home barrel column in mature rats.

The sublaminar distribution (i.e., depth profile) of axon within L1-3 was quantified by measuring the percentage of axon length as a function of depth in L1-3 (Fig. 3.3C). Across all mature cells (n = 47), 95% of axon length was contained within the deepest 70% of L1-3. The average pia to L3/4 border distance was 500 ± 70 μm. Thus, 95% of reconstructed axon was contained in the deepest 350 μm of L2/3.

Development of axonal topography in the across-row plane

To characterize development of this projection, neurons were filled in across-row slices from P6, several days after L4 barrels form (Rice et al., 1985), through P26, when cortical circuits are thought to be largely mature. At P6-7, there was little axonal innervation of L1-3, though innervation of infragranular layers was more

extensive. Of 7 cells reconstructed, 4 had no axon in L1-3 (Fig. 3.2, C1) and 3 had extremely sparse projections in L1-3 (Fig. 3.2, C2). By P8, significantly more axonal length was present in L1-3 (Fig. 3.2B), and topography could be measured. This developmental pattern, in which axons extend initially to infragranular layers and subsequently to supragranular layers, has also been observed for L4 spiny stellate cells in cat area 17 (Callaway and Katz, 1992).

At P8-11, when most cells had axon in L1-3, axons (n = 32) exhibited a range of topographic precision, from very columnar, to non-columnar (Fig. 3.2, B1), to exclusive targeting of a neighboring column (Fig. 3.2, B2). On average, axonal topography of these cells within L1-3, measured relative to the home barrel column, was significantly less precise than that of mature cells (Fig. 3.3D, P8-11: 56 ± 30% in home column, P14-26: 87 ± 14% in home column, $p<0.0001$). This percentage is similar to that predicted by the non-targeted growth model (Fig. 3.3B, 58.8%; x = 108.2 μm, d = 259.1 μm, c = 360 μm), suggesting that initial axon growth in L1-3 is non-directed.

Since the width of L4 barrels increases with age (P8-11: 307 ± 55 μm [exclusive of septa], P14-26: 403 ± 73 μm, $p<0.001$), developmental sharpening of topography may reflect growth of the home barrel column, remodeling of the axon itself, or both. To determine if axonal remodeling occurred, we examined axonal topography relative to a constant width column with borders ±220 μm medial and lateral from the soma ("±220 μm column"), which is the mean width of the mature barrel column across both slice planes. We calculated the percent of axon in L1-3 within the ±220 μm column as a function of age for the same cells as in Fig. 3.3D

(Fig. 3.4A). The mean percentage of axon within the ±220 μm column increased significantly with development (P8-11: 64 ± 32%, n = 32; P14-26: 86 ± 15%, n = 25; $p<0.01$), indicating that axonal topography sharpened with age. Thus, both remodeling (spatial sharpening) of axonal arbors and growth of the barrel column occur during development and contribute to developmental sharpening of L4 axonal topography.

To further quantify the developmental sharpening of this projection, we calculated the tangential distribution of axon length in L1-3, relative to the soma position, for mature (P14-26) and immature (P8-11) cells. This tangential distribution of axon showed a strong but non-significant tendency to be sharper in mature than immature cells (Fig. 3.4B: mature vs. immature: $p = 0.17$, Kolmogorov-Smirnoff [KS]-test). When the mean slope of this function was calculated by averaging across both flanks of the distributions, slope was significantly sharper in mature cells (Fig. 3.4B inset, $p < 0.0001$, KS-test). In contrast to these changes in tangential distribution, the sublaminar distribution of axon in L1-3 did not change during development ($p = 0.6$, KS-test). These results demonstrate that L4 to L1-3 axons develop with initial topography that is less precise than in adults, and that adult topography emerges between P11 and P14.

Targeted axonal growth mediates developmental sharpening

Total axon length in L1-3 increased significantly through development (Fig. 3.5A), with mature L4 cells possessing twice as much axon in L1-3 as immature cells (P14-21, n = 19: 4470 ± 2250 μm; P8-11, n = 32: 1950 ± 1710 μm; $p < 0.001$). To

determine whether topographic sharpening involved targeted axonal growth within the home column, regression outside the home column, or both, we measured the absolute length of axon inside and outside the ±220 μm column in across-row slices. Analyses of absolute axonal length were restricted to cells < P22 because older cells tended to have fainter axonal staining that limited our ability to accurately measure axon length.

In young rats (P8-11), total axon length was 1460 ± 1670 μm inside the ±220 μm column, and 490 ± 540 μm outside this column. In older rats (P14-21), total axon length was 4070 ± 2280 μm inside and 400 ± 350 μm outside the ±220 μm column. Thus, axon length within the ±220 μm column increased during development (Fig. 3.5B, $p < 0.0001$, $R^2 = 0.27$), but absolute axon length outside the ±220 μm column did not change ($p = 0.7$, $R^2 = 0.003$). This suggests that topographic sharpening in the across-row dimension occurs via targeted growth in the home column, rather than net retraction of axon outside the column. Correspondingly, the maximal tangential breadth of axon arbors, measured as the distance between the most medial and lateral axonal branches in L1-3, did not change through development (P8-11: 560 ± 280 μm, P14-21: 530 ± 130 μm, $p > 0.5$).

Axonal topography in the within-row plane

To characterize development in the orthogonal plane (within barrel rows), slices were made that contained multiple barrels within a single whisker row (see Methods). Cells were filled in a central barrel flanked by at least one barrel on each side. Axons from mature rats (P17-21, n = 22) showed columnar topography in this plane (76 ± 22% of axon in L1-3 was contained in the home barrel column, defined as

in Fig. 3.3A), though this topography was less precise than in the across-row dimension (87 ± 14% in home column, $p < 0.05$).

To determine why axonal spread into neighboring barrels was greater in this dimension, we compared absolute spatial distribution of axon in the two planes. Neither the absolute tangential distribution of axon length ($p > 0.05$, KS-test), the maximal tangential breadth of axonal arbors (within-row: 650 ± 180 μm; across-row: 550 ± 160 μm; $p > 0.05$), nor the percentage of axon contained in the ±220 μm column (within-row: 82.5 ± 15.8%; across-row: 86.4 ± 14.6%; $p > 0.3$) was different between within-row and across-row planes (Fig. 3.6A). In addition, the sublaminar distribution of axon was identical between the two planes ($p > 0.07$, KS-test). However, barrel columns (defined to include half the adjacent septa) were narrower in the within-row vs. across-row dimension (within-row: 413 ± 90 μm, across-row: 465 ± 82 μm, $p < 0.05$). This discrepancy in column size primarily reflected the fact that septa between rows were larger than within rows (62 ± 35 μm between rows, 36 ± 24 μm within rows, $p < 0.01$), while barrels were roughly the same diameter in both dimensions (403 ± 73 μm in across-row dimension, 377 ± 86 μm in within-row dimension, $p>0.2$) (Welker and Woolsey, 1974; Land and Simons, 1985; Riddle et al., 1992). Since barrel columns were narrower in the within-row dimension, axon segments extending isotropically out of the home column tended to innervate neighboring columns within rows.

No significant changes in topographic precision were found during development in the within-row plane. In immature cells (P8-9, n = 10), 84 ± 23% of axon length in L1-3 was within the home barrel column, comparable to mature cells in

this plane ($p > 0.1$). Topographic precision in immature cells was substantially better than predicted with the non-targeted growth model (61.7%; x = 103.7 μm, d = 203.5 μm, c = 310 μm), suggesting that initial axons are actively targeted to the home column in this dimension. Initial topography was also precise when measured in absolute distance: 89 ± 18% of L1-3 axon was inside the ±220 μm column for immature cells, compared to 83 ± 16% for mature cells ($p > 0.3$). Moreover, the tangential distribution of axon in the within-row dimension was actually sharper for immature than mature cells (Fig. 3.6B, $p < 0.01$, KS-test). The sublaminar distribution of axon length also did not change with development ($p > 0.9$, KS-test).

Developmental maintenance of topography in this plane should require that axon length be added proportionately inside the home barrel column and outside it, in neighboring columns within the row. Indeed, we found that as total axon length in L1-3 increased in within-row slices during development (Fig. 3.6C, P8-11: 1580 ± 1110 μm, P17-21: 3940 ± 2220 μm, $p < 0.01$), axon length increased significantly, and approximately proportionally, within (P8-9: 1390 ± 1060 μm, P17-21: 3380 ± 2110 μm, $p < 0.02$, $R^2 = 0.18$) and outside (P8-9: 190 ± 260 μm, P17-21: 560 ± 540 μm, $p < 0.02$, $R^2 = 0.18$) the ±220 μm column (Fig. 3.6D). Consistent with growth outside the home column, the maximal breadth of this projection increased significantly from 470 ± 270 μm in immature cells to 650 ± 180 μm in mature cells ($p < 0.04$). Thus, unlike in the across-row plane, development in the within-row plane involves net growth of axon both in the home column and in neighboring columns within the row.

Development of L4 axons innervating L4

L4 cells also innervate other L4 barrel neurons, forming a dense local excitatory network. In mature rats, this projection is highly column-specific, with 70-90% of axon length restricted to the home barrel (Harris and Woolsey, 1983; Lubke et al., 2000; Petersen and Sakmann, 2000; Brecht and Sakmann, 2002). To determine how topographic precision develops in the L4 to L4 projection, we analyzed axon segments of L4 cells contained within L4. In mature cells (P14-26, n = 25), 93.1 ± 8.1% of axon length in L4 was contained in the home column (the barrel and half the adjacent septa) in across-row slices, and a similar topographic precision was observed in within-row slices (89.8 ± 9.7%, n = 22). In immature cells (P8-11), significantly less axon was confined to the home column in across-row slices (P8-11: 83.9 ± 14.5%, n = 32, $p < 0.01$ vs. mature), indicating that initial projections were less precise than the adult in this dimension. In contrast, adult-like precision was apparent for immature cells (P8-9) in the within-row dimension (94.6 ± 5.5% in home column, n = 10, $p > 0.15$ vs. mature).

Developmental refinement in the across-row dimension was largely due to growth of the barrel column itself, since the percentage of axon within the ±220 μm column in L4 was not significantly different between mature (93.5 ± 7.4%) and immature (89.2 ± 11.7%) neurons ($p > 0.1$). In addition, developmental refinement also involved targeted axonal growth in L4 of the home column, as axon length increased significantly with development inside the ±220 μm column (P8-11: 2210 ± 1260 μm, n = 32; P14-26: 4440 ± 1640 μm, n = 25; $p < 0.0001$), but axon length remained constant outside the ±220 μm column (P8-11: 250 ± 324 μm; P14-26: 70 ±

310 μm; p = 0.8). Thus, the development of axonal topography in L4 mirrored the pattern of development observed for projections to L1-3.

A summary of axonal topography across development is presented in Figure 3.7. Individual axonal reconstructions were scaled to normalize horizontal and vertical dimension of the home barrel column to their mean values, aligned to column boundaries, and overlaid. Axon length density was calculated per 10 μm^2 pixel (Fig. 3.7, left), and smoothed by a Gaussian filter (50 μm SD) to show the mean shape of the projection (Fig. 3.7, right). It is apparent that the mature projection to L2/3 is largely restricted to a single column in both across-row and within-row dimensions, and that mature topography emerges from a more diffuse projection in the across-row dimension. It is also apparent that this maturation occurs both by addition of axon in the home column and by growth of the barrels themselves. Axons segments in L5-6 are presented here for completeness, but were not analyzed in this study.

Sensory experience does not affect anatomical development

We performed two manipulations to determine whether sensory experience guides development of L4 axons. First, we plucked all contralateral whiskers from P9 to P14-17, a manipulation that drives experience-dependent receptive field plasticity in L2/3 and has been proposed to regulate anatomical connectivity of the L4 to L2/3 projection (Stern et al., 2001). Second, in a separate set of rats, we plucked the D-row of whiskers from P8 to P23-26, a manipulation that drives synaptic weakening of L4 to L2/3 synapses, and thus may cause synaptic elimination on this pathway (Allen et al., 2003). After both manipulations, neurons were filled in the D-barrel of across-row

slices. Passive membrane properties and AP characteristics of L4 neurons were similar in deprived vs. control animals (data not shown).

Neither deprivation paradigm caused any discernable change in topography of L4 to L2/3 axons, either relative to age-matched controls or all mature controls (P14-26) (Table 3.2). The tangential distribution of axon in L1-3 was not different between control rats and either of the whisker deprived groups (Fig. 3.8A, B; Unilateral: $p > 0.9$, D-only: $p > 0.9$, KS-test). Likewise, total axon length and percent of axon in the home column were also unaffected by deprivation (Fig. 3.8C, D; Table 3.2). Sublaminar distribution of axon was also unaffected (Unilateral: $p > 0.9$ vs. control, D-only: $p > 0.3$ vs. control, KS-test), and Sholl analysis of L4 dendritic morphology revealed no effect of deprivation (Table 3.2, Unilateral vs. control: $p > 0.5$, D-only vs. control: $p > 0.4$, KS-test). L2/3 dendrites were not examined in this study.

Finally, we tested for differences in bouton density on L4 axon segments in L2/3 between control and deprived animals. Bouton density has been shown to be relatively constant across different branches within the axonal arbor of single pyramidal cells (Yabuta and Callaway, 1998b), and in our sample, we found no differences in bouton density between central and peripheral axon segments selected randomly from single arbors ($p > 0.5$, paired t-test, $n = 4$ cells, 2 central and 2 peripheral branches per cell). Thus, to measure the effects of deprivation on bouton density, a single axon segment within L2/3 of the home barrel column was selected at random from each cell for bouton analysis. Bouton counts were performed blind to sensory experience. In mature controls, bouton density in L2/3 was 16.9 ± 2.5 boutons per 100 μm ($n = 15$), consistent with previously reported values (Lubke et al.,

2000). Bouton density did not change following either deprivation protocol (Table 3.2). Together, the results in this section indicate that whisker-related sensory activity during the period in which L4 to L1-3 axons are being elaborated does not significantly affect their morphology at the light microscopic level.

Discussion

These results demonstrate that the L4 to L2/3 excitatory axonal projection develops precise columnar topography from an initial state that is significantly less columnar. In the initial state, many cells extend a large number of branches into neighboring columns representing adjacent-row whiskers, and mean topography in this dimension (across rows) is consistent with completely undirected axonal extension in L2/3. In contrast, initial topography in the within-row dimension is as precise as in mature animals (Fig. 3.6, 3.7). Maturation of topography occurs in a 3-day period (P11-14), and involves targeted growth of axon within the home barrel column and growth of the barrels themselves, but no net retraction of axon outside the home column (Fig. 3.5, 3.6, 3.7). The period of topographic refinement coincides with the critical period for experience-dependent regulation of spine dynamics and deprivation-induced, large-scale reorganization of L2/3 receptive fields (Lendvai et al., 2000; Stern et al., 2001). However, development of L4 axonal length, topography, and bouton density occurs normally in whisker-deprived animals (Fig. 3.8). Thus, axonal development and topographic refinement of this projection are independent of sensory experience, at least after P8. These results imply that deprivation-induced map plasticity during this period does not involve large-scale physical remodeling of L4 axons.

Mature axonal topography

The mature columnar topography we observed is consistent with prior studies from cell fills *in vitro* (Kim and Ebner, 1999; Lubke et al., 2000; Petersen and

Sakmann, 2000; Feldmeyer et al., 2002) and *in vivo* (Brecht and Sakmann, 2002), with the columnar relay of excitation from L4 to L2/3 inferred from single unit recording (Armstrong-James et al., 1992), and imaging studies *in vivo* (Petersen et al., 2003) and *in vitro* (Petersen and Sakmann, 2001; Laaris and Keller, 2002). We found that only 13% of axon length crossed into neighboring columns within a barrel arc, and 24% crossed into neighboring columns within a barrel row. This preferential divergence into neighboring columns within a row occurred despite the fact that tangential spread of axon in L2/3 was equal, in absolute distance, in both within-row and across-row dimensions (Fig. 3.6A). Instead, divergence was greater within a row because inter-barrel septa are thinner between barrels within a row, so that more axons reached neighboring barrel columns within a row than within an arc (Fig. 3.6, 3.7). Horizontal axonal projections of L2/3 pyramidal neurons show a similar bias along barrel rows (Bernardo et al., 1990; Hoeflinger et al., 1995; Keller and Carlson, 1999; Petersen et al., 2003), suggesting that convergence of information from neighboring whiskers within a row is an important feature of processing in L2/3.

Because some axon branches are inevitably lost during slice preparation and tissue processing (resectioning for the anti-biocytin reaction reduces total tissue thickness to ~350 μm), the axonal length measurements reported here should be considered minimal estimates of total axon length *in vivo*. We cannot rule out the possibility that long-range axonal projections exist *in vivo* but are missing from our reconstructions, and thus actual topography *in vivo* may be somewhat less columnar than observed here. However, substantially different topography is unlikely because receptive field analysis and imaging studies *in vivo* suggest strongly that L4 to L2/3

projections are functionally column-specific (Armstrong-James et al., 1992; Petersen et al., 2003), and axons of single L4 neurons filled *in vivo* are largely confined to single columns in L2/3, consistent with our findings (Brecht and Sakmann, 2002). Similar topography has been observed for L4 axons in visual and auditory cortices (Lund et al., 1977; Winer, 1984; Burkhalter, 1989; Callaway and Katz, 1992; Yabuta and Callaway, 1998a), suggesting that columnar projections from L4 to L2/3 are a basic building block of neocortical columns (Mountcastle, 1997).

Development of axonal topography

The L4 to L2/3 projection develops columnar topography in the across-row dimension from a relatively coarse initial projection whose topography is consistent with non-directed growth. Topographic refinement of this early projection occurs during a discrete developmental period (P11-14). Such refinement of an early, somewhat coarse projection is consistent with classical models of development of axonal topography, and is similar to the pattern observed for callosal and horizontal intracortical projections (Innocenti, 1981; Luhmann et al., 1986; Innocenti, 1995; Katz and Shatz, 1996; Debski and Cline, 2002). Perhaps because initial overarborization is fairly modest, topographic refinement of L4 to L2/3 axons in the across-row dimension occurs through selective addition and/or retention of axon within the home barrel column and growth of barrel columns relative to the axon arbors, rather than through net retraction of axon from neighboring columns (Fig. 3.5, 3.9). Such targeted growth contributes to development of mature topography in many projections (Callaway and Katz, 1990; Katz and Shatz, 1996; Yates et al., 2001; Rebsam et al.,

2002). In contrast, topography in the within-row dimension was initially precise, and precision was maintained throughout development, apparently by equal growth of axon both within and outside the home column (Fig. 3.6, 3.7). This pattern of axonal development is illustrated schematically in Fig. 3.9.

It has been controversial whether thalamocortical axons, which are also largely restricted to single columns in adults, develop similarly. Some studies found that thalamacortical axons develop by initial overarborization followed by substantial refinement (LeVay et al., 1978; Finney and Shatz, 1998; Ruthazer et al., 1999; Rebsam et al., 2002). Other studies indicate that even the earliest axons are confined to single, column-sized termination zones in L4 of S1 (Agmon et al., 1993; Catalano et al., 1996) and V1 (Crowley and Katz, 2002), and that development involves addition of terminal branches in those zones (Senft and Woolsey, 1991; Agmon et al., 1993; Catalano et al., 1996). Our results suggest that to determine whether early thalamocortical axons are fully precise or somewhat overarborized requires determining not only whether individual axon arbors are the correct size, but also whether they are located in correct termination zones within the target map, and whether this precision is equal in all dimensions.

In our data, the same pattern of developmental refinement observed for L4 to L2/3 axonal projections was also found for L4 axon branches innervating L4, which show a high degree of column-specific topography in mature animals (Harris and Woolsey, 1983; Lubke et al., 2000; Petersen and Sakmann, 2000; Brecht and Sakmann, 2002). At P8-11, immature L4 axons showed significantly less topographic precision than in mature animals, with a greater proportion of axon innervating L4 of

adjacent, neighboring-row barrel columns. This refinement was due both to growth of barrel columns relative to the axonal arbors, and to targeted growth of axon within the home L4 barrel. As in L2/3, initial projections were topographically precise in the orthogonal, within-row dimension.

Axonal development is independent of normal sensory experience

In many projections, patterns of sensory experience or endogenous activity modulate development of axonal topography. For example, visual deprivation alters the size and complexity of thalamocortical axon arbors in V1 (Antonini and Stryker, 1993a, b; Antonini et al., 1998), binocular experience guides tangential clustering of horizontal axons in L2/3 of primary visual cortex (Luhmann et al., 1986; Lowel and Singer, 1992), and spontaneous retinal activity is required for segregation of retinogeniculate axons into layers in the thalamus (Katz and Shatz, 1996). However, activity is not necessary for proper topographic development of all projections (Lin et al., 2000; Butler et al., 2001; White et al., 2001).

Rats begin to actively whisk at ~ P12 (Welker, 1964), coincident with the period of active refinement of the L4 to L2/3 axonal projection. Because trimming whiskers at this age alters spine dynamics and causes large-scale changes in functional connectivity on the L4 to L2/3 pathway (Lendvai et al., 2000; Stern et al., 2001), we hypothesized that whisker experience would regulate development of L4 to L2/3 axonal topography. Interestingly, whisker deprivation had no effect on development of axonal length, topography, or bouton density (Fig. 3.8). This result indicates that unlike thalamocortical and horizontal intracortical projections, development of L4 to

L2/3 axonal projections does not require normal sensory experience, at least during the period when axons begin to innervate L2/3. Whether L4 to L2/3 axonal development is driven by spontaneous activity in the absence of normal whisker input, is completely activity-independent, or is influenced indirectly by experience at younger ages, during the critical period for plasticity in L4 (Fox, 1992), is unknown. Though it is possible that anatomical plasticity was prevented by the transient isoflurane anesthesia used during whisker plucking, such interference seems unlikely because plucking under anesthesia successfully drives robust changes in both functional synaptic efficacy (Allen et al., 2003) and whisker receptive fields in S1 (Fox, 1992; Glazewski and Fox, 1996; E. Foeller and D. E. Feldman, unpublished data).

Implications for experience-dependent plasticity

Because sensory manipulations can induce receptive field plasticity in L2/3 before or in the absence of plasticity in L4 (Glazewski and Fox, 1996; Stern et al., 2001), L4 to L2/3 synapses have long been hypothesized to be a site of experience-dependent plasticity in S1. Consistent with this hypothesis, whisker deprivation induces measurable synaptic depression at L4 to L2/3 synapses (Allen et al., 2003) and significantly alters the functional topography of the L4 to L2/3 projection (Shepherd et al., 2003). However, whether these effects are mediated in part by experience-dependent changes in L4 axonal morphology had not been tested prior to the present study.

Our data show that plucking a single row of whiskers from P8, the manipulation that induced maximal synaptic depression at L4 to L2/3 synapses (Allen

et al., 2003), caused no differences in axonal length, topography, or bouton density compared to age-matched controls (Fig. 3.8). This suggests that deprivation-induced synaptic weakening at these ages is due to physiological weakening of synapses (e.g., long-term synaptic depression), but not physical removal of axon.

Our data also show that depriving all contralateral whiskers from P9-P14, the manipulation that drove robust receptive field plasticity in L2/3 and changes in functional connectivity of the L4 to L2/3 projection as assessed by photostimulation (Stern et al., 2001; Shepherd et al., 2003), also caused no differences in axonal length, topography, or bouton density compared to age-matched controls (Fig. 3.8). This indicates that functional plasticity on this projection is not due to large-scale anatomical restructuring of L4 axons, as had been originally proposed (Stern et al., 2001). However, we cannot exclude changes in axonal ultrastructure below the resolution of light microscopy.

Possible mechanisms for axonal development

Because we did not follow single cells over time, the present results do not address the underlying mechanism for topographic refinement on the single-cell level. In other systems, refinement can involve apoptosis to remove mistargeted neurons from the population (Cellerino et al., 2000), pruning of mistargeted axonal branches without cell death (Innocenti, 1995), and/or targeted growth of axon in correct target areas (Callaway and Katz, 1990; Katz and Shatz, 1996; Yates et al., 2001; Rebsam et al., 2002). Since absolute length of mistargeted L4 axon did not decrease with development, apoptosis of mistargeted cells and pruning of inappropriate branches are

unlikely to be major mechanisms for development of the L4 to L2/3 projection. Our data indicate that sensory experience is not required for topographic refinement. It will therefore be interesting to determine what molecular (Bolz et al., 1996; O'Leary and Wilkinson, 1999) or spontaneous activity cues (Crair, 1999) contribute to refinement of this projection.

References

Agmon A, Yang LT, O'Dowd DK, Jones EG (1993) Organized growth of thalamocortical axons from the deep tier of terminations into layer IV of developing mouse barrel cortex. J Neurosci 13:5365-5382.

Agmon A, Yang LT, Jones EG, O'Dowd DK (1995) Topological precision in the thalamic projection to neonatal mouse barrel cortex. J Neurosci 15:549-561.

Allen CB (2004) Synaptic depression induced by whisker deprivation in rat barrel cortex. PhD thesis University of California, San Diego.

Allen CB, Celikel T, Feldman DE (2003) Long-term depression induced by sensory deprivation during cortical map plasticity in vivo. Nat Neurosci 6:291-299.

Antonini A, Stryker MP (1993a) Development of individual geniculocortical arbors in cat striate cortex and effects of binocular impulse blockade. J Neurosci 13:3549-3573.

Antonini A, Stryker MP (1993b) Rapid remodeling of axonal arbors in the visual cortex. Science 260:1819-1821.

Antonini A, Gillespie DC, Crair MC, Stryker MP (1998) Morphology of single geniculocortical afferents and functional recovery of the visual cortex after reverse monocular deprivation in the kitten. J Neurosci 18:9896-9909.

Armstrong-James M, Fox K (1987) Spatiotemporal convergence and divergence in the rat S1 "barrel" cortex. J Comp Neurol 263:265-281.

Armstrong-James M, Fox K, Das-Gupta A (1992) Flow of excitation within rat barrel cortex on striking a single vibrissa. J Neurophysiol 68:1345-1358.

Bear MF (1996) A synaptic basis for memory storage in the cerebral cortex. Proc Natl Acad Sci U S A 93:13453-13459.

Bear MF, Cooper LN, Ebner FF (1987) A physiological basis for a theory of synapse modification. Science 237:42-48.

Bernardo KL, McCasland JS, Woolsey TA, Strominger RN (1990) Local intra- and interlaminar connections in mouse barrel cortex. J Comp Neurol 291:231-255.

Bolz J, Castellani V, Mann F, Henke-Fahle S (1996) Specification of layer-specific connections in the developing cortex. Prog Brain Res 108:41-54.

Borrell V, Callaway EM (2002) Reorganization of exuberant axonal arbors contributes to the development of laminar specificity in ferret visual cortex. J Neurosci 22:6682-6695.

Brecht M, Sakmann B (2002) Dynamic representation of whisker deflection by synaptic potentials in spiny stellate and pyramidal cells in the barrels and septa of layer 4 rat somatosensory cortex. J Physiol 543:49-70.

Buonomano DV, Merzenich MM (1998) Cortical plasticity: from synapses to maps. Annu Rev Neurosci 21:149-186.

Burkhalter A (1989) Intrinsic connections of rat primary visual cortex: laminar organization of axonal projections. J Comp Neurol 279:171-186.

Butler AK, Dantzker JL, Shah RB, Callaway EM (2001) Development of visual cortical axons: layer-specific effects of extrinsic influences and activity blockade. J Comp Neurol 430:321-331.

Callaway EM (1998) Prenatal development of layer-specific local circuits in primary visual cortex of the macaque monkey. J Neurosci 18:1505-1527.

Callaway EM, Katz LC (1990) Emergence and refinement of clustered horizontal connections in cat striate cortex. J Neurosci 10:1134-1153.

Callaway EM, Katz LC (1991) Effects of binocular deprivation on the development of clustered horizontal connections in cat striate cortex. Proc Natl Acad Sci U S A 88:745-749.

Callaway EM, Katz LC (1992) Development of axonal arbors of layer 4 spiny neurons in cat striate cortex. J Neurosci 12:570-582.

Catalano SM, Robertson RT, Killackey HP (1996) Individual axon morphology and thalamocortical topography in developing rat somatosensory cortex. J Comp Neurol 367:36-53.

Celikel T, Szostak VA, Feldman DE (2004) Modulation of spike timing by sensory deprivation during induction of cortical map plasticity. Nat Neurosci 7:534-541.

Cellerino A, Bahr M, Isenmann S (2000) Apoptosis in the developing visual system. Cell Tissue Res 301:53-69.

Connors BW, Gutnick MJ (1990) Intrinsic firing patterns of diverse neocortical neurons. Trends Neurosci 13:99-104.

Crair MC (1999) Neuronal activity during development: permissive or instructive? Curr Opin Neurobiol 9:88-93.

Crowley JC, Katz LC (2002) Ocular dominance development revisited. Curr Opin Neurobiol 12:104-109.

Dan Y, Poo MM (2004) Spike timing-dependent plasticity of neural circuits. Neuron 44:23-30.

DeBello WM, Feldman DE, Knudsen EI (2001) Adaptive axonal remodeling in the midbrain auditory space map. J Neurosci 21:3161-3174.

Debski EA, Cline HT (2002) Activity-dependent mapping in the retinotectal projection. Curr Opin Neurobiol 12:93-99.

Diamond ME, Huang W, Ebner FF (1994) Laminar comparison of somatosensory cortical plasticity. Science 265:1885-1888.

Dudek SM, Bear MF (1992) Homosynaptic long-term depression in area CA1 of hippocampus and effects of N-methyl-D-aspartate receptor blockade. Proc Natl Acad Sci U S A 89:4363-4367.

Durack JC, Katz LC (1996) Development of horizontal projections in layer 2/3 of ferret visual cortex. Cereb Cortex 6:178-183.

Feldman DE (2000) Timing-based LTP and LTD at vertical inputs to layer II/III pyramidal cells in rat barrel cortex. Neuron 27:45-56.

Feldmeyer D, Lubke J, Silver RA, Sakmann B (2002) Synaptic connections between layer 4 spiny neurone-layer 2/3 pyramidal cell pairs in juvenile rat barrel cortex: physiology and anatomy of interlaminar signalling within a cortical column. J Physiol 538:803-822.

Finnerty GT, Roberts LS, Connors BW (1999) Sensory experience modifies the short-term dynamics of neocortical synapses. Nature 400:367-371.

Finney EM, Shatz CJ (1998) Establishment of patterned thalamocortical connections does not require nitric oxide synthase. J Neurosci 18:8826-8838.

Fox K (1992) A critical period for experience-dependent synaptic plasticity in rat barrel cortex. J Neurosci 12:1826-1838.

Fox K (2002) Anatomical pathways and molecular mechanisms for plasticity in the barrel cortex. Neuroscience 111:799-814.

Frenkel MY, Bear MF (2004) How monocular deprivation shifts ocular dominance in visual cortex of young mice. Neuron 44:917-923.

Glazewski S, Fox K (1996) Time course of experience-dependent synaptic potentiation and depression in barrel cortex of adolescent rats. J Neurophysiol 75:1714-1729.

Glazewski S, Giese KP, Silva A, Fox K (2000) The role of alpha-CaMKII autophosphorylation in neocortical experience-dependent plasticity. Nat Neurosci 3:911-918.

Hardingham NR, Fox K (2004) The relationship between spike timing plasticity and experience-dependent plasticity in αCAMKII-T286A Mutants. Soc Neurosci Abstr 857.21.

Harris RM, Woolsey TA (1983) Computer-assisted analyses of barrel neuron axons and their putative synaptic contacts. J Comp Neurol 220:63-79.

Hebb DO (1949) Organization of Behavior. John Wiley & Sons, New York.

Heynen AJ, Abraham WC, Bear MF (1996) Bidirectional modification of CA1 synapses in the adult hippocampus in vivo. Nature 381:163-166.

Heynen AJ, Yoon BJ, Liu CH, Chung HJ, Huganir RL, Bear MF (2003) Molecular mechanism for loss of visual cortical responsiveness following brief monocular deprivation. Nat Neurosci 6:854-862.

Hoeflinger BF, Bennett-Clarke CA, Chiaia NL, Killackey HP, Rhoades RW (1995) Patterning of local intracortical projections within the vibrissae representation of rat primary somatosensory cortex. J Comp Neurol 354:551-563.

Horton JC, Hocking DR (1996) Anatomical demonstration of ocular dominance columns in striate cortex of the squirrel monkey. J Neurosci 16:5510-5522.

Huber KM, Sawtell NB, Bear MF (1998) Brain-derived neurotrophic factor alters the synaptic modification threshold in visual cortex. Neuropharmacology 37:571-579.

Innocenti GM (1981) Growth and reshaping of axons in the establishment of visual callosal connections. Science 212:824-827.

Innocenti GM (1995) Exuberant development of connections, and its possible permissive role in cortical evolution. Trends Neurosci 18:397-402.

Katz LC, Shatz CJ (1996) Synaptic activity and the construction of cortical circuits. Science 274:1133-1138.

Katz LC, Crowley JC (2002) Development of cortical circuits: lessons from ocular dominance columns. Nat Rev Neurosci 3:34-42.

Keller A (1995) Synaptic organization of the barrel cortex. In: The barrel cortex of rodents (Jones EG and Diamond IT, ed). New York: Plenum:221-262.

Keller A, Carlson GC (1999) Neonatal whisker clipping alters intracortical, but not thalamocortical projections, in rat barrel cortex. J Comp Neurol 412:83-94.

Kim U, Ebner FF (1999) Barrels and septa: separate circuits in rat barrels field cortex. J Comp Neurol 408:489-505.

Kirkwood A, Rioult MC, Bear MF (1996) Experience-dependent modification of synaptic plasticity in visual cortex. Nature 381:526-528.

Kitt CA, Levy AI, Friedman DP, Walker LC, Koliatos VE, Raskin LS, Price DL (1988) Immunocytochemical visualization of cholinergic fibers in monkey: enhanced visualization using silver nitrate. Soc Neurosci Abstr 14:631.

Knott GW, Quairiaux C, Genoud C, Welker E (2002) Formation of dendritic spines with GABAergic synapses induced by whisker stimulation in adult mice. Neuron 34:265-273.

Laaris N, Keller A (2002) Functional independence of layer IV barrels. J Neurophysiol 87:1028-1034.

Land PW, Simons DJ (1985) Cytochrome oxidase staining in the rat SmI barrel cortex. J Comp Neurol 238:225-235.

Lebel D, Grossman Y, Barkai E (2001) Olfactory learning modifies predisposition for long-term potentiation and long-term depression induction in the rat piriform (olfactory) cortex. Cereb Cortex 11:485-489.

Lendvai B, Stern EA, Chen B, Svoboda K (2000) Experience-dependent plasticity of dendritic spines in the developing rat barrel cortex in vivo. Nature 404:876-881.

LeVay S, Stryker MP, Shatz CJ (1978) Ocular dominance columns and their development in layer IV of the cat's visual cortex: a quantitative study. J Comp Neurol 179:223-244.

Lin DM, Wang F, Lowe G, Gold GH, Axel R, Ngai J, Brunet L (2000) Formation of precise connections in the olfactory bulb occurs in the absence of odorant-evoked neuronal activity. Neuron 26:69-80.

Linden DJ, Connor JA (1995) Long-term synaptic depression. Annu Rev Neurosci 18:319-357.

Lowel S, Singer W (1992) Selection of intrinsic horizontal connections in the visual cortex by correlated neuronal activity. Science 255:209-212.

Lubke J, Egger V, Sakmann B, Feldmeyer D (2000) Columnar organization of dendrites and axons of single and synaptically coupled excitatory spiny neurons in layer 4 of the rat barrel cortex. J Neurosci 20:5300-5311.

Luhmann HJ, Martinez Millan L, Singer W (1986) Development of horizontal intrinsic connections in cat striate cortex. Exp Brain Res 63:443-448.

Lund JS, Boothe RG, Lund RD (1977) Development of neurons in the visual cortex (area 17) of the monkey (Macaca nemestrina): a Golgi study from fetal day 127 to postnatal maturity. J Comp Neurol 176:149-188.

Madison DV, Malenka RC, Nicoll RA (1991) Mechanisms underlying long-term potentiation of synaptic transmission. Annu Rev Neurosci 14:379-397.

Manahan-Vaughan D, Braunewell KH (1999) Novelty acquisition is associated with induction of hippocampal long-term depression. Proc Natl Acad Sci U S A 96:8739-8744.

McKernan MG, Shinnick-Gallagher P (1997) Fear conditioning induces a lasting potentiation of synaptic currents in vitro. Nature 390:607-611.

McLaughlin T, Hindges R, O'Leary DD (2003) Regulation of axial patterning of the retina and its topographic mapping in the brain. Curr Opin Neurobiol 13:57-69.

Mountcastle VB (1957) Modality and topographic properties of single neurons of cat's somatic sensory cortex. J Neurophysiol 20:408-434.

Mountcastle VB (1997) The columnar organization of the neocortex. Brain 120 (Pt 4):701-722.

Mulkey RM, Malenka RC (1992) Mechanisms underlying induction of homosynaptic long-term depression in area CA1 of the hippocampus. Neuron 9:967-975.

O'Leary DD, Wilkinson DG (1999) Eph receptors and ephrins in neural development. Curr Opin Neurobiol 9:65-73.

Peinado A, Katz LC (1990) Development of cortical spiny stellate cells: retraction of a transient apical dendrite. Soc Neurosci Abstr 16:1127.

Petersen CC, Sakmann B (2000) The excitatory neuronal network of rat layer 4 barrel cortex. J Neurosci 20:7579-7586.

Petersen CC, Sakmann B (2001) Functionally independent columns of rat somatosensory barrel cortex revealed with voltage-sensitive dye imaging. J Neurosci 21:8435-8446.

Petersen CC, Grinvald A, Sakmann B (2003) Spatiotemporal dynamics of sensory responses in layer 2/3 of rat barrel cortex measured in vivo by voltage-sensitive dye imaging combined with whole-cell voltage recordings and neuron reconstructions. J Neurosci 23:1298-1309.

Rebsam A, Seif I, Gaspar P (2002) Refinement of thalamocortical arbors and emergence of barrel domains in the primary somatosensory cortex: a study of normal and monoamine oxidase a knock-out mice. J Neurosci 22:8541-8552.

Rice FL, Gomez C, Barstow C, Burnet A, Sands P (1985) A comparative analysis of the development of the primary somatosensory cortex: interspecies similarities during barrel and laminar development. J Comp Neurol 236:477-495.

Riddle D, Richards A, Zsuppan F, Purves D (1992) Growth of the rat somatic sensory cortex and its constituent parts during postnatal development. J Neurosci 12:3509-3524.

Rioult-Pedotti MS, Friedman D, Donoghue JP (2000) Learning-induced LTP in neocortex. Science 290:533-536.

Ruthazer ES, Cline HT (2004) Insights into activity-dependent map formation from the retinotectal system: a middle-of-the-brain perspective. J Neurobiol 59:134-146.

Ruthazer ES, Baker GE, Stryker MP (1999) Development and organization of ocular dominance bands in primary visual cortex of the sable ferret. J Comp Neurol 407:151-165.

Saint Marie RL, Peters A (1985) The morphology and synaptic connections of spiny stellate neurons in monkey visual cortex (area 17): a Golgi-electron microscopic study. J Comp Neurol 233:213-235.

Sanes JN, Donoghue JP (2000) Plasticity and primary motor cortex. Annu Rev Neurosci 23:393-415.

Sawtell NB, Frenkel MY, Philpot BD, Nakazawa K, Tonegawa S, Bear MF (2003) NMDA receptor-dependent ocular dominance plasticity in adult visual cortex. Neuron 38:977-985.

Schubert D, Kotter R, Zilles K, Luhmann HJ, Staiger JF (2003) Cell type-specific circuits of cortical layer IV spiny neurons. J Neurosci 23:2961-2970.

Senft SL, Woolsey TA (1991) Computer-aided analyses of thalamocortical afferent ingrowth. Cereb Cortex 1:336-347.

Shepherd GM, Pologruto TA, Svoboda K (2003) Circuit analysis of experience-dependent plasticity in the developing rat barrel cortex. Neuron 38:277-289.

Sholl DA (1953) Dendritic organization in the neurons of the visual cortex and motor cortices of the cat. J Anat (Lond) 87:387-406.

Simons DJ (1978) Response properties of vibrissa units in rat SI somatosensory neocortex. J Neurophysiol 41:798-820.

Singer W (1995) Development and plasticity of cortical processing architectures. Science 270:758-764.

Stent GS (1973) A physiological mechanism for Hebb's postulate of learning. Proc Natl Acad Sci U S A 70:997-1001.

Stern EA, Maravall M, Svoboda K (2001) Rapid development and plasticity of layer 2/3 maps in rat barrel cortex in vivo. Neuron 31:305-315.

Takahashi T, Svoboda K, Malinow R (2003) Experience strengthening transmission by driving AMPA receptors into synapses. Science 299:1585-1588.

Welker C, Woolsey TA (1974) Structure of layer IV in the somatosensory neocortex of the rat: description and comparison with the mouse. J Comp Neurol 158:437-453.

Welker WI (1964) Analysis of sniffing of the albino rat. Behavior 22:223-244.

White LE, Coppola DM, Fitzpatrick D (2001) The contribution of sensory experience to the maturation of orientation selectivity in ferret visual cortex. Nature 411:1049-1052.

Wiesel TN, Hubel DH (1963) Single-Cell Responses in Striate Cortex of Kittens Deprived of Vision in One Eye. J Neurophysiol 26:1003-1017.

Winer JA (1984) Anatomy of layer IV in cat primary auditory cortex (AI). J Comp Neurol 224:535-567.

Woolsey TA, Van der Loos H (1970) The structural organization of layer IV in the somatosensory region (SI) of mouse cerebral cortex. The description of a

cortical field composed of discrete cytoarchitectonic units. Brain Res 17:205-242.

Yabuta NH, Callaway EM (1998a) Functional streams and local connections of layer 4C neurons in primary visual cortex of the macaque monkey. J Neurosci 18:9489-9499.

Yabuta NH, Callaway EM (1998b) Cytochrome-oxidase blobs and intrinsic horizontal connections of layer 2/3 pyramidal neurons in primate V1. Vis Neurosci 15:1007-1027.

Yates PA, Roskies AL, McLaughlin T, O'Leary DD (2001) Topographic-specific axon branching controlled by ephrin-As is the critical event in retinotectal map development. J Neurosci 21:8548-8563.

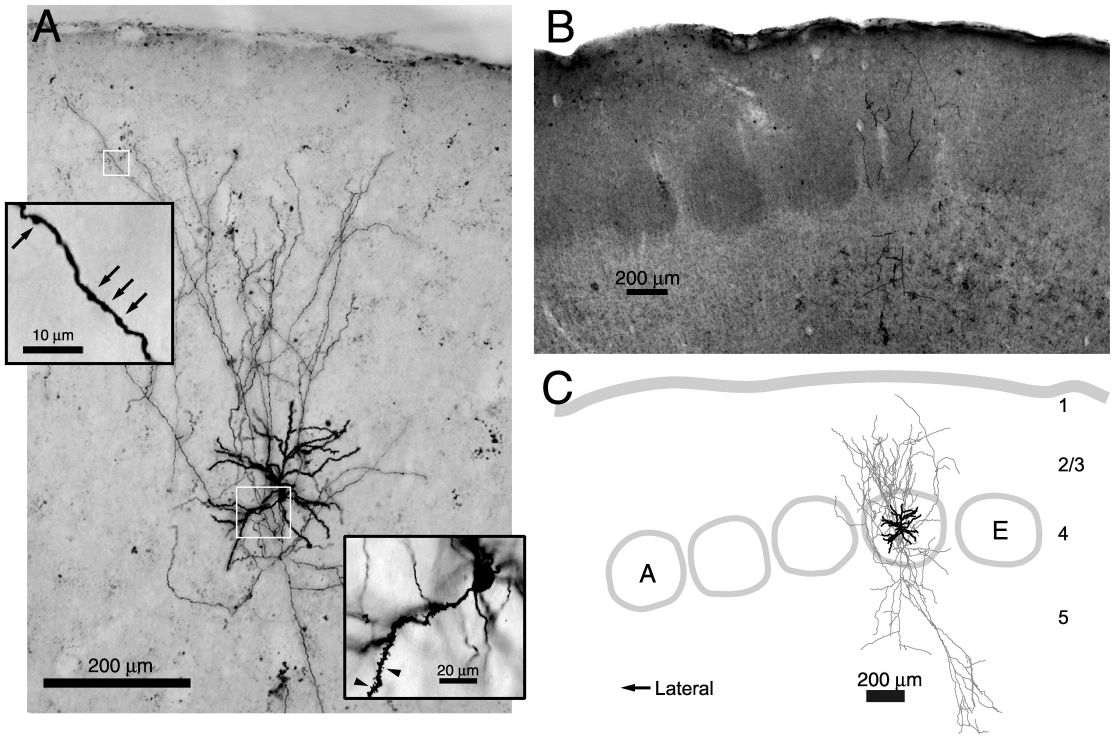

Fig.3.1: Labeling and reconstruction of single spiny stellate cell in L4 of S1. A, Photomontage from a single 100 µm thick section showing a biocytin-labeled L4 spiny stellate neuron in an across-row slice (P21). Insets, dendrite with spines (arrowheads) and axon with boutons (arrows). B, Osmium-intensified barrels in an adjacent section from the same slice. C, Full reconstruction of the neuron in (A-B). Soma and dendrite in black, axon in dark gray, barrels and pia in light gray. Numbers indicate cortical layers.

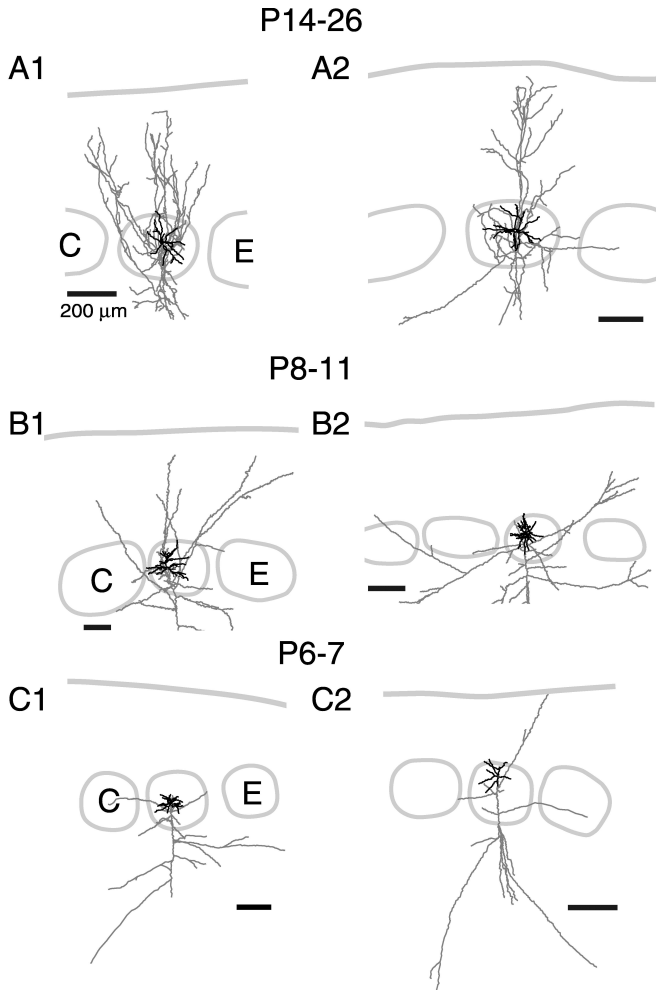

Fig 3.2: Representative examples of L4 excitatory cells in across-row slices at different ages. Lateral is to left. Scale bar, 200 µm. L5 and 6 boundaries are not shown.

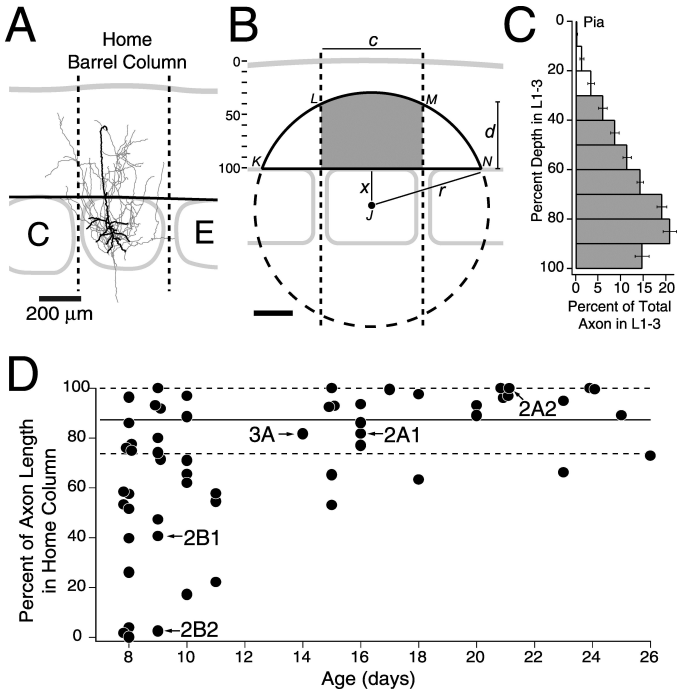

Fig 3.3: Development of columnar topography measured relative to the home barrel column. A, Definition of home barrel column. Dashed lines, midpoints of septa. Horizontal line, L3/4 border. Cell: P14 star pyramid in across-row slice. B, Schematic of non-directed axon growth model. Variables (x, d, c) are measured for each experimental group (see Methods for definitions). ATot is enclosed by solid black lines. AHome is gray. Assuming non-directed growth if uniform density around the soma, the fraction of axon in the home column in L1-3 is AHome/ATot. Vertical scale indicates percent depth in L1-3 from pia. C, Sublaminar distribution of axon length in L1-3 for mature cells (P14-26). 95% of total axon length (gray) occurs in deepest 70% of L1-3. Bars are SEM. D, Percent of axon length in L1-3 contained within home barrel column as a function of age, for all cells. Solid and dashed lines, mean±SD for mature cells (P14-26). Labels indicate cells shown in Fig. 2 and 3A.

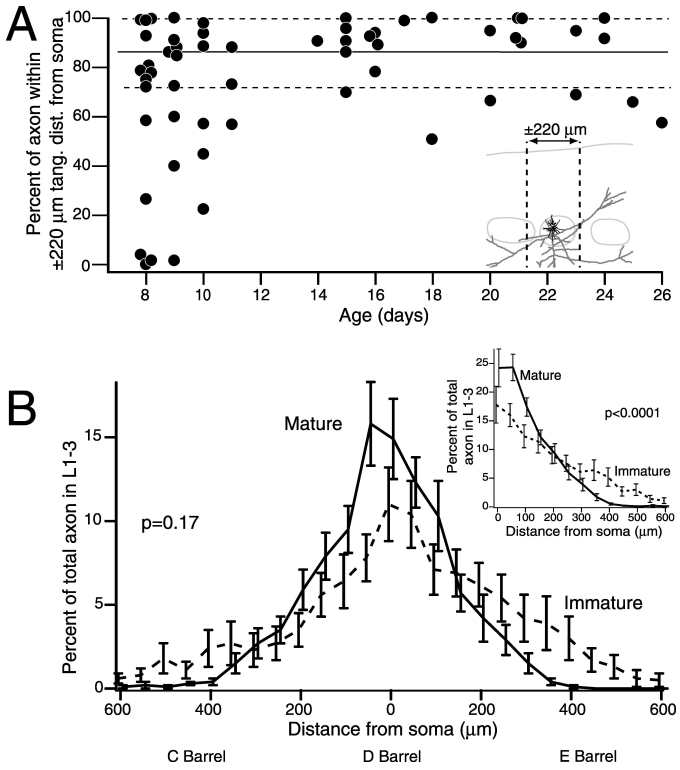

Fig 3.4: Development of columnar topography measured relative to the ±220 µm column. A, Percent of axon length in L1-3 contained within ±220 µm tangential distance from soma as a function of age. Solid and dashed lines, mean±SD for mature cells. B, Distribution of axon length in L1-3 as a function of tangential distance from soma, for immature (P8-11) and mature (P14-26) cell groups. Bars are SEM. Ellipses show approximate barrel boundaries. Inset, Average falloff of the data determined by summing both flanks of the distributions in (B).

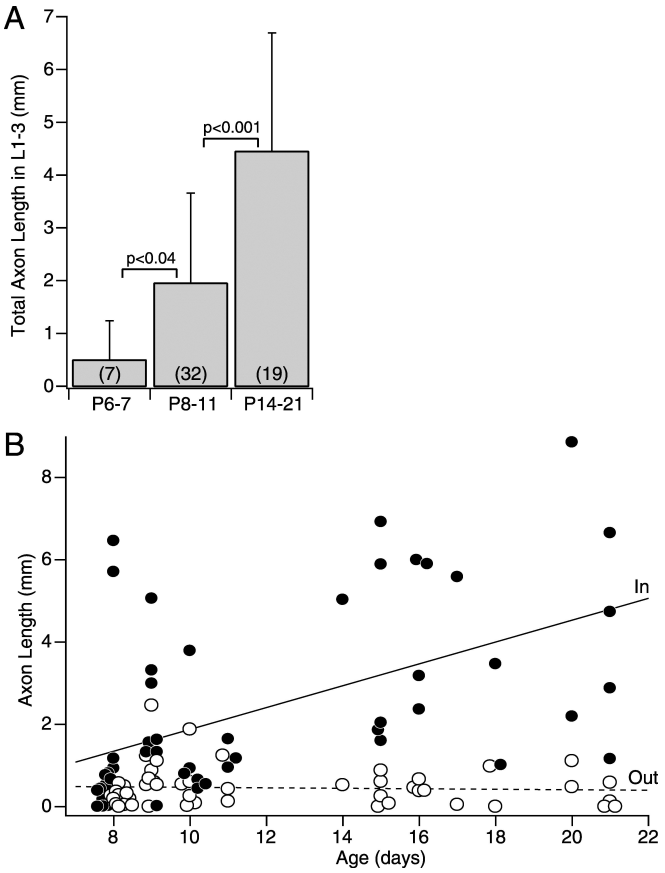

Fig 3.5: Topographic refinement in the across-row plane occurs through targeted axon growth. A, Total axon length in L1-3 as a function of age. Bars are SD. Parentheses, number of cells. B, Axon length within (filled circles) and outside (open circles) the ±220 μm column, as a function of age. Least-squares regression lines show a significant increase in axon length within the ±220 μm column with age ($p = 0.0001$, $R^2 = 0.27$), but no significant regression outside the ±220 μm column.

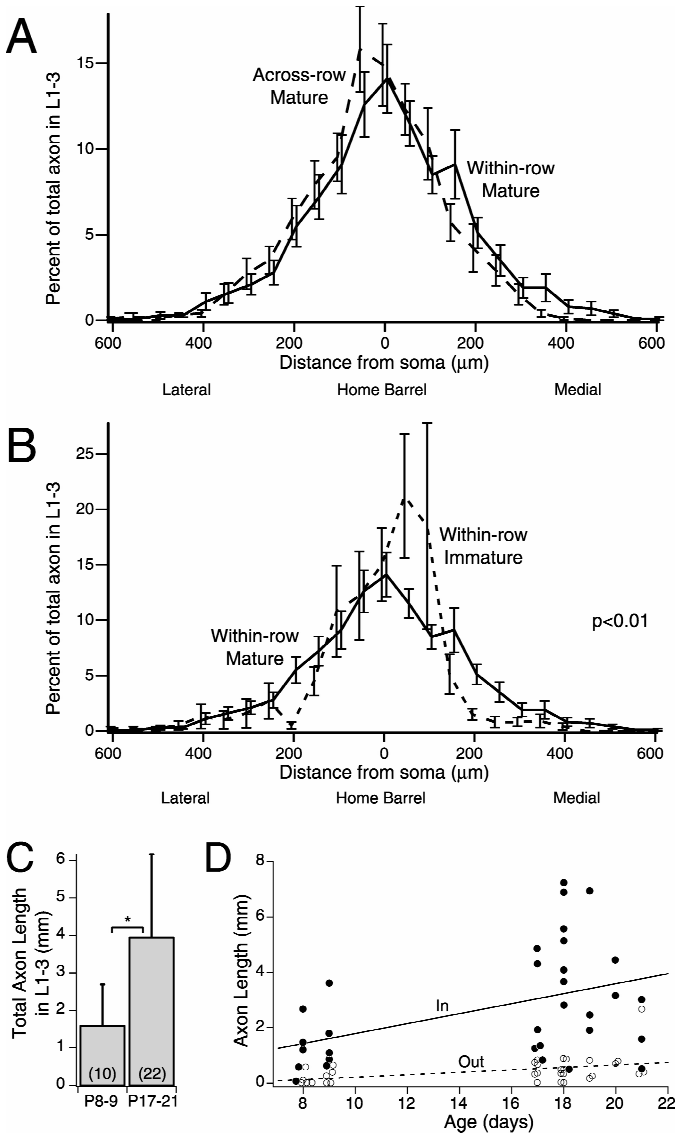

Fig 3.6: Development of axons in the within-row plane. A, Distribution of axon length as a function of tangential distance from soma for mature neurons in within-row and across-row planes of section. B, Distribution of axon as a function of tangential distance from soma for immature (P8-11) and mature (P17-21) cells in the within-row plane. Bars are SEM. Ellipses show approximate barrel boundaries. C, Total axon length in L2/3 as a function of age. Bars are SD. Parentheses, number of cells. D, Axon length within (filled circles) and outside (open circles) the ±220 μm column as a function of age. Regression lines indicate that axon length increased significantly with age both within ($p < 0.02$, $R^2 = 0.18$) and outside ($p < 0.02$, $R_2 = 0.18$) the ±220 μm column.

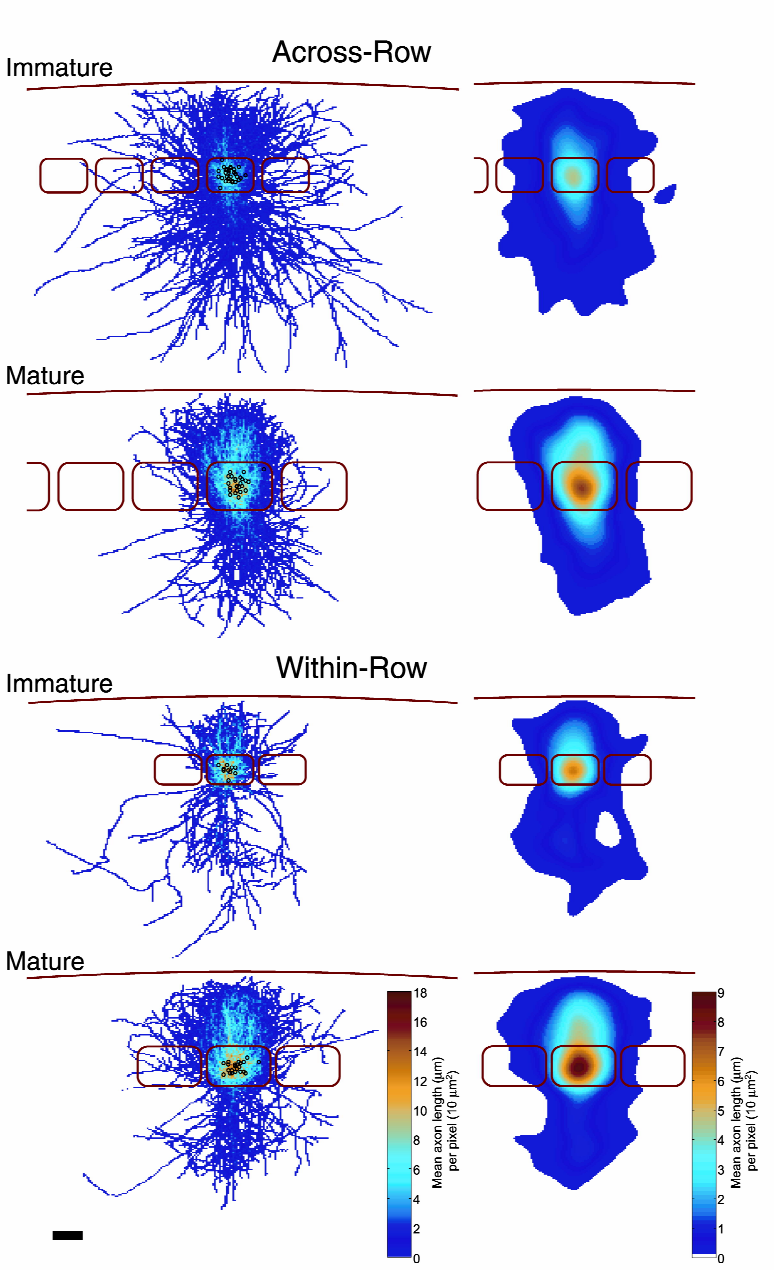

Fig. 3.7: Summary of axonal topography from all reconstructed cells. Left, overlay of all reconstructed axons relative to barrel column. Individual axons were scaled to normalize barrel width and pia to L4/5 distance to mean values, and aligned by barrel boundaries. Black dots: location of somata in L4. Right, same data smoothed using a 2 dimensional, 50 µm SD Gaussian. Barrels and pia in red. Barrels and septa size are drawn to accurately reflect mean size for each developmental age and plane of section. Scale bar: 200 µm for all panels.

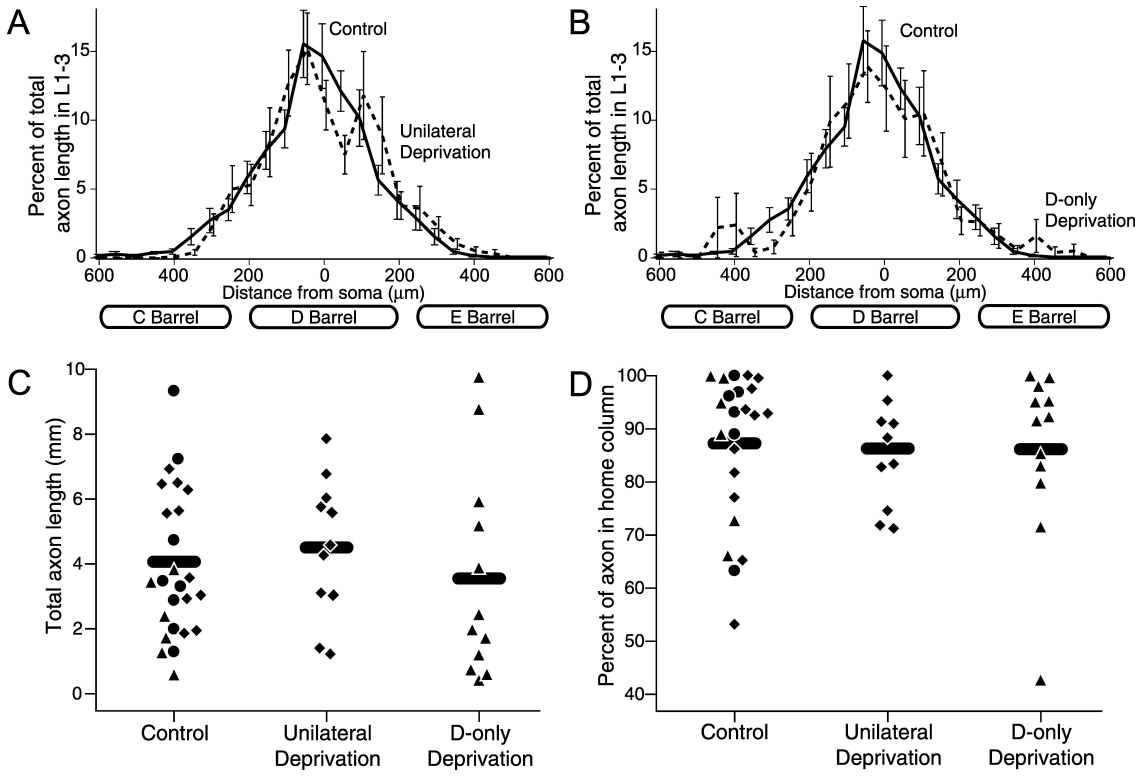

Fig. 3.8: Whisker experience does not alter axonal morphology. A, Tangential distribution of axon length for control rats and rats deprived of all whiskers unilaterally. B, Tangential distribution of axon length for control rats and rats deprived of the D-row of whiskers. Bars are SEM. Ellipses show approximate barrel boundaries. C, Total axon length in L2/3 for all conditions. D, Percent of axon in home column for all conditions. Diamonds, P14-17 rats. Circles, P18-22 rats. Triangles, P23-26 rats. Horizontal bars are means.

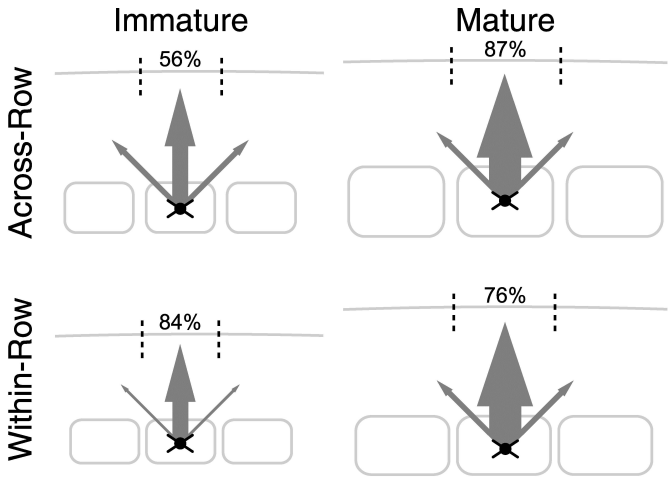

Fig. 3.9: Schematic model of L4 to L2/3 axonal development. Arrow thickness is proportional to mean total axon length in L2/3 of the home column (center arrow) and each of two neighboring columns through development. Numbers indicate percentage of axon in the home barrel column for that age (dashed lines). Barrels and septa are drawn to scale across all conditions, as in Fig. 3.7.

Table 3.1: Morphology of axons and membrane properties of spiny stellate, star pyramidal, and unclassified spiny neurons

	Percent of axon in ±220 µm column	Total axon length in L2/3 (µm)	V_m (mV)	R_{in} (MΩ)	AP Threshold (mV)	AP Height (mV)
Mature controls						
Spiny stellate (n=25)	83.9±13.9	3490±2090	-83.8±4.2	171.6±56.2	-51.0±2.5	78.7±8.4
Star pyramidal (13)	80.0±17.9	4460±2200	-80.6±10.1	177.6±65.0	-48.1±3.4 *	71.6±10.7 *
Unclassified (9)	93.4±10.9	4400±2600	-85.8±4.2	155.6±30.9	-51.3±2.7	81.0±10.3
Immature controls						
Spiny stellate (18)	62.7±35.2	1380±1490	-80.3±3.9	354.2±111.5	-48.1±3.7	65.8±9.2
Star pyramidal (18)	75.6±30.0	2270±1750	-79.1±2.7	349.8±88.8	-49.1±1.7	64.3±7.3
Unclassified (6)	77.4±15.0	2090±1010	-80.3±2.2	334.9±62.6	-50.2±6.6	69.8±12.9

All values averaged over both planes of section

* $p<0.05$ relative to spiny stellate cells (t-test)

Table 3.2: Morphology of axons and dendrites in animals with altered whisker experience

	Total axon length in L2/3 (μm)	Bouton density (Boutons/100 μm)	Percent of axon in L2/3 in home column	Sholl Analysis: Number of dendritic crossings x μm from soma x = 50	x = 100	x = 150
All Mature Controls †	3920±2260 (25)	16.9±2.5 (15)	87.3±13.7 (25)	15.6±4.7 (14)	9.3±4.1	1.6±2.0
Unilateral Deprivation §	4500±2150 (11)	18.1±3.9 (11)	86.3±10.5 (11)	17.0±4.9 (5)	10.6±1.7	0
Aged-Matched Controls §	4600±1950 (11)	16.2±2.2 (10)	83.9±14.5 (11)	16.2±3.7 (9)	9.2±4.1	1.6±1.8
D-only Deprivation ‡	3550±3210 (12)	19.1±4.1 (5)	86.2±16.2 (12)	14.4±3.3 (7)	6.4±2.1	0.1±0.4
Aged-Matched Controls ‡	2210±1260 (6)	18.2±2.9 (5)	87.0±14.4 (6)	16.8±5.1 (4)	11.0±3.4	2.3±2.6

† P14-26 § P14-17 ‡ P23-26 Parentheses indicate number of cells

Chapter 3, in full, is a republication of the material as it appears in Bender, K.J., Rangel, J., Feldman, D.E., Development of columnar topography in the excitatory layer 4 to layer 2/3 projection in rat barrel cortex. *J Neurosci.* 23, 8759-8770 (2003). The dissertation author was the primary investigator and first author of this paper.

Acknowledgements: This work was supported by the Klingenstein Foundation, the McKnight Endowment Fund for Neuroscience, and NINDS 1 R01 NS046652. D.E.F. is an Alfred P. Sloan Research Fellow. We are grateful to Edward Callaway, Marla Feller, and the members of the Feldman lab for critically reading this manuscript, and to Tansu Celikel for MATLAB programming.

Chapter 4

Sensory deprivation does not affect neuron number

in layer 4 of rat somatosensory cortex

Abstract

Whisker deprivation in adolescent rats has been shown to weaken layer 4 (L4) to L2/3 excitatory synapses by reducing presynaptic efficacy, but not to alter the length or bouton density of presynaptic L4 axonal arbors. These experiments do not address whether whisker deprivation decreases the strength of the L4-L2/3 projection by reducing the number of presynaptic L4 neurons. Here, we address this question by examining neuron density in L4 using immunohistochemical techniques. We found that L4 barrels contain roughly 7000 neurons in 23 day old rats, and that whisker deprivation does not alter neuron density. These results, together with findings in previous chapters, suggest that deprivation alters synapse physiology, but not the basic anatomy of S1 circuits.

Introduction

During map plasticity, neurons in pathways that no longer receive relevant sensory information can be eliminated. Deafferentation (Born and Rubel, 1985; Guimaraes and Linden, 2000) and functional silencing of sensory afferents have been shown to increase levels of apoptosis in downstream areas (Born and Rubel, 1988; Catsicas et al., 1992), resulting in activity-dependent decreases in neural number. In the visual system, monocular deprivation eliminates specific populations of neurons in the thalamus (Norton et al., 1977), alters neuron size (Casagrande et al., 1978; Kuppermann and Kasamatsu, 1983; Tigges et al., 1984), and alters thalamocortical axonal length (Antonini and Stryker, 1993b).

In rat somatosensory cortex (S1), deprivation from postnatal day 0 (P0) and enriched environmental experience in adults are known to alter the physical size of barrels in layer 4 (L4) (Fox, 1992; Polley et al., 2004). This suggests that it is possible that experience regulates cell number in barrels, though this has not been tested, to our knowledge.

In S1, whisker deprivation in adolescents causes a measurable weakening of bulk L4-L2/3 inputs, measured by input-output curves, from extracellular stimulation of many L4 fibers (Allen et al., 2003). In chapter 2, we showed that much of this weakening reflects a decrease in L4-L2/3 synaptic efficacy, because deprivation caused changes in paired pulse ratios and the time course of NMDA-EPSC blockade by MK-801, consistent with a decrease in average release probability. Here, we test whether an additional factor in weakening the L4-L2/3 projection is a loss of L4 neurons.

To determine if whisker deprivation lowers neuronal number in deprived barrel columns, we examined cell density in L4 barrels from control and whisker deprived animals by immunohistochemical staining for NeuN, a neuron-specific nuclear protein. We found no differences in neuron density or barrel size with deprivation, suggesting that whisker deprivation does not weaken the L4-L2/3 projection by reducing the number of constituent presynaptic neurons.

Methods

NeuN immunolabelling: Long-Evans rats were raised with either normal whisker experience or were D-row deprived from P12-P23. Animals were perfused at P23 with 4% paraformaldehyde. The contralateral hemisphere was sectioned at 40 μm in the across-row plane (Finnerty et al., 1999), and alternate sections were stained for NeuN, a neuron-specific nuclear protein, or cytochrome oxidase (CO) to visualize barrels. NeuN staining (mouse anti-NeuN, Chemicon, 1:1000 dilution, 18 hr at 4°C) was visualized using a fluorescent secondary antibody (Alexa-488 anti-mouse, Jackson ImmunoResearch, 1:1000, 1 hr at 25°C). NeuN-immunoreactive neurons were marked using Neurolucida software (Microbrightfield) with the experimenter blind to deprivation history and barrel boundaries. Barrel boundaries were then projected from neighboring CO sections. Neuronal density was calculated for B-E barrels in 3 separate slices per animal, and corrected for 2% tissue shrinkage. Tissue shrinkage was assessed by comparing the average distance between C, D, and E barrel centroids in fixed, CO-stained tissue, versus living, transilluminated acute brain slices. Shrinkage values matched previous measurements from our lab (Bender et al., 2003).

Cytochrome oxidase staining: Immediately following sectioning, alternate sections were placed in a cytochrome oxidase reaction solution (0.0375% cytochrome C, 0.0825% diaminobenzidine tetrahydrochloride, 3.75% sucrose in 0.1 M phosphate buffer) at 37 °C for 6 hr to visualize barrels (Wong-Riley, 1979). Chemicals were obtained from Sigma-Aldrich, St. Louis, MO.

Results

We estimated changes in cell number by calculating cell density within L4 barrels in control and whisker deprived animals using immunohistochemical techniques. Animals were raised with normal sensory experience, or were deprived of D-row whiskers from P12 to 23, a manipulation known to drive weakening of the L4-L2/3 projection (Allen et al., 2003, and see chapter 2). Animals were perfused at P23 and neuronal cell bodies in L4 were visualized with an immunofluorescent reaction for NeuN in 40 μm thick across-row sections (Fig. 4.1A). Alternate sections were stained for cytochrome oxidase (CO) to visualize barrels (Fig. 4.1B). Neighboring sections were aligned based on blood vessel and pial contours (Fig. 4.1A, B), and barrel boundaries were projected onto NeuN sections. NeuN-immunoreactive neurons in 3 sections from each animal were analyzed blind to deprivation history and barrel boundaries. NeuN sections were selected for analysis if neighboring CO-stained sections contained whisker barrels B-E (An A barrel was not present in every section). Whisker barrels were identified based on shape and location of CO profiles within each section (Finnerty et al., 1999; Allen et al., 2003). Neuron density was not analyzed in A barrels.

The cross-sectional area of barrels B-E (excluding septa), measured in across-row sections, was similar in control rats (B: 109,000 ± 2000 μm^2; C: 119,000 ± 11,000 μm^2; D: 102,000 ± 500 μm^2; E: 111,000 ± 3000 μm^2; mean ± standard error; n = 3 animals). D-row deprivation did not alter the size of D-barrels, compared to neighboring barrels B and C, or D-row barrels from control animals (B: 114,000 ± 10,000 μm^2; C: 133,000 ± 4000 μm^2; D: 106,000 ± 3000 μm^2; n = 2 animals). E-row

barrels were larger in sections from deprived animals (E: 133,000 ± 4000 μm^2), but due to the size of the population measured, it is unclear whether this difference is a real effect of deprivation.

To control for apparent differences in barrel size across sections, the number of neurons in each barrel was assessed by calculating neuron density. Neuron density was constant across B-E barrels for both control rats (n = 3) and D-row deprived rats (n = 2) (Fig. 4.1C). Across all sections from control animals, the average neuron density within all barrels was 122,000 ± 4000 neurons/mm^3 (B-row: 122,000 ± 6800; C-row: 119,000 ± 9100; D-row: 122,000 ± 8700; E-row: 122,000 ± 7900; 3 sections/animal; mean ± S.E.M.). At this density, an average barrel, approximated as a cube of across-row width of 460 μm, within-row width of 410 μm, and height of 310 μm (Bender et al., 2003), would contain 7130 ± 120 neurons. Neuronal density in the D column from D-deprived rats was not different when compared to neighboring, spared columns, or to the D column in control rats (Fig. 4.1C) (Deprived rats, B-row: 114,000 ± 5300; C-row: 113,000 ± 4000; D-row: 126,000 ± 3200; E-row: 118,000 ± 4200; 3 sections/animal).

Discussion

These data show that whisker deprivation does not alter neuronal density or barrel area in deprived barrels in L4, measured in across-row sections. These findings are consistent with earlier results showing that while univibrissa rearing beginning at P0 can alter barrel size (by 35% in 1/3rd of all animals studied), univibrissa rearing beginning at P2-7 does not alter barrel size (Fox, 1992), suggesting that the critical period for deprivation-induced changes in barrel size ends by P2. These results indicate that while deprivation changes the strength of L4 neuronal projections, the gross size of L4 barrels and neuron density in L4 remains intact. A caveat to this finding, though, is that techniques used here labeled all neurons, and would not detect possible deprivation-induced changes in the relative populations of different L4 neuron classes, including excitatory and inhibitory neurons.

Combined with previous data (Bender et al., 2003), these results suggest that deprivation-induced map plasticity does not involve large scale loss of L4 neurons or axons. Similar results have been observed in the barn owl sound localization system. In the barn owl, auditory-visual misalignment induced by wearing prismatic spectacles causes visually guided learning of sound localization. This learning involves the loss of pre-existing, inappropriate auditory responses, and the growth of new axonal projections to mediate new auditory responses appropriate to the visual displacement. Axonal connections mediating normal auditory responses persist with extended prism experience, even though these responses are physiologically reduced or absent, suggesting that experience weakens functional synaptic efficacy but does not cause gross synaptic withdrawal (DeBello et al., 2001). Similarly, new axonal connections

formed during learning remain anatomically intact even after they are functionally silenced by prism removal (Linkenhoker et al., 2005).

Why deprivation appears to affect synaptic efficacy, but not axonal anatomy of L4 cells is unclear, especially because in visual cortex, axonal restructuring of thalamocortical and L2/3 horizontal axons does occur during deprivation-induced map plasticity (Antonini and Stryker, 1993b; Darian-Smith and Gilbert, 1994; Trachtenberg and Stryker, 2001). Similarly in S1, all-whisker unilateral deprivation modestly alters the branch structure of L2/3 pyramidal cells at these ages (Maravall et al., 2004), indicating that cortical neurons are capable of experience-dependent anatomical plasticity. Perhaps L4 axons could undergo anatomical plasticity given longer deprivation durations.

References

Allen CB, Celikel T, Feldman DE (2003) Long-term depression induced by sensory deprivation during cortical map plasticity in vivo. Nat Neurosci 6:291-299.

Antonini A, Stryker MP (1993) Rapid remodeling of axonal arbors in the visual cortex. Science 260:1819-1821.

Bender KJ, Rangel J, Feldman DE (2003) Development of columnar topography in the excitatory layer 4 to layer 2/3 projection in rat barrel cortex. J Neurosci 23:8759-8770.

Born DE, Rubel EW (1985) Afferent influences on brain stem auditory nuclei of the chicken: neuron number and size following cochlea removal. J Comp Neurol 231:435-445.

Born DE, Rubel EW (1988) Afferent influences on brain stem auditory nuclei of the chicken: presynaptic action potentials regulate protein synthesis in nucleus magnocellularis neurons. J Neurosci 8:901-919.

Casagrande VA, Guillery RW, Harting JK (1978) Differential effects of monocular deprivation seen in different layers of the lateral geniculate nucleus. J Comp Neurol 179:469-485.

Catsicas M, Pequignot Y, Clarke PG (1992) Rapid onset of neuronal death induced by blockade of either axoplasmic transport or action potentials in afferent fibers during brain development. J Neurosci 12:4642-4650.

Darian-Smith C, Gilbert CD (1994) Axonal sprouting accompanies functional reorganization in adult cat striate cortex. Nature 368:737-740.

DeBello WM, Feldman DE, Knudsen EI (2001) Adaptive axonal remodeling in the midbrain auditory space map. J Neurosci 21:3161-3174.

Finnerty GT, Roberts LS, Connors BW (1999) Sensory experience modifies the short-term dynamics of neocortical synapses. Nature 400:367-371.

Fox K (1992) A critical period for experience-dependent synaptic plasticity in rat barrel cortex. J Neurosci 12:1826-1838.

Guimaraes CA, Linden R (2000) Chloramphenicol induces apoptosis in the developing brain. Neuropharmacology 39:1673-1679.

Kuppermann BD, Kasamatsu T (1983) Changes in geniculate cell size following brief monocular blockade of retinal activity in kittens. Nature 306:465-468.

Linkenhoker BA, von der Ohe CG, Knudsen EI (2005) Anatomical traces of juvenile learning in the auditory system of adult barn owls. Nat Neurosci 8:93-98.

Maravall M, Koh IY, Lindquist WB, Svoboda K (2004) Experience-dependent changes in basal dendritic branching of layer 2/3 pyramidal neurons during a critical period for developmental plasticity in rat barrel cortex. Cereb Cortex 14:655-664.

Norton TT, Casagrande VA, Sherman SM (1977) Loss of Y-cells in the lateral geniculate nucleus of monocularly deprived tree shrews. Science 197:784-786.

Polley DB, Kvasnak E, Frostig RD (2004) Naturalistic experience transforms sensory maps in the adult cortex of caged animals. Nature 429:67-71.

Tigges M, Hendrickson AE, Tigges J (1984) Anatomical consequences of long-term monocular eyelid closure on lateral geniculate nucleus and striate cortex in squirrel monkey. J Comp Neurol 227:1-13.

Trachtenberg JT, Stryker MP (2001) Rapid anatomical plasticity of horizontal connections in the developing visual cortex. J Neurosci 21:3476-3482.

Wong-Riley M (1979) Changes in the visual system of monocularly sutured or enucleated cats demonstrable with cytochrome oxidase histochemistry. Brain Res 171:11-28.

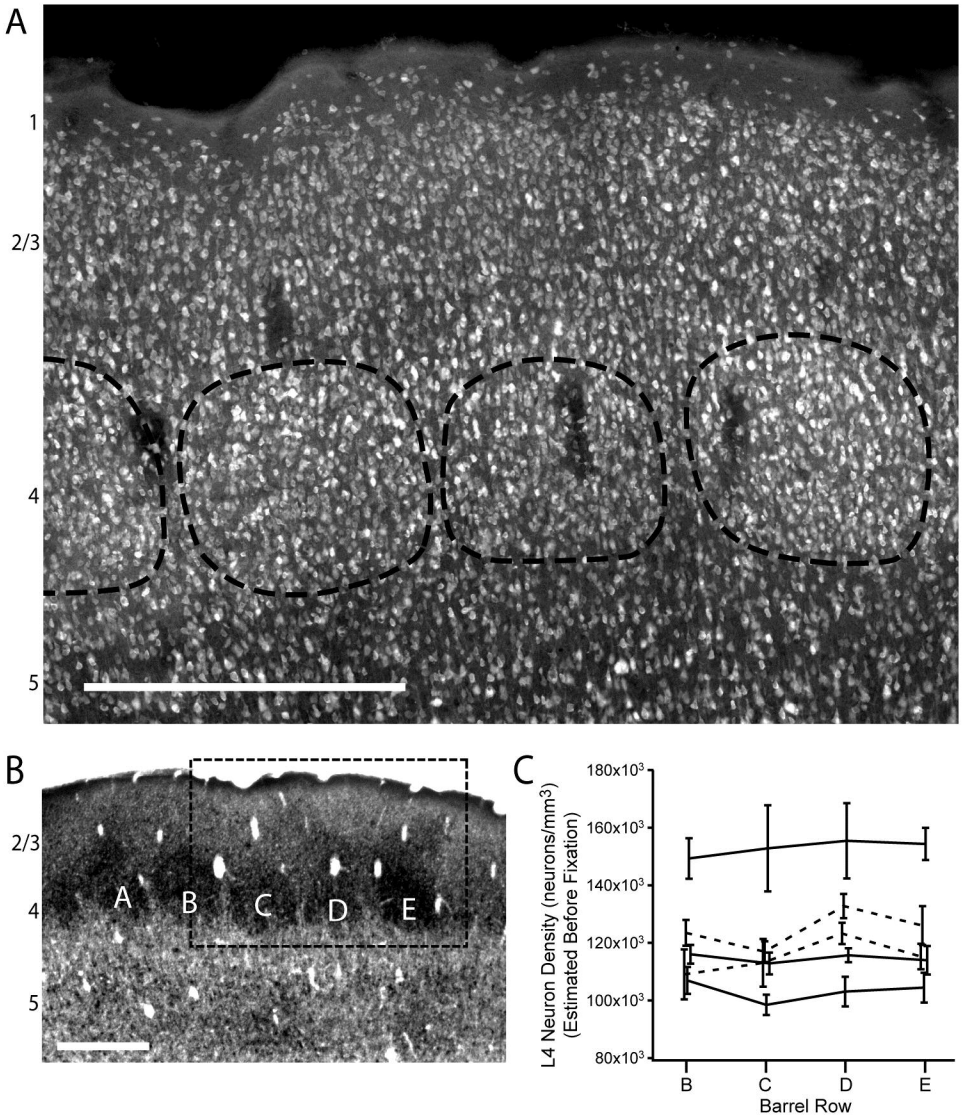

Fig. 4.1: Whisker deprivation does not alter neuronal density in L4 barrels. A, Neu-N staining in single "across-row" section of S1. Barrel borders from neighboring CO-stained section (B) are shown. Dashed rectangle in B shows region corresponding to panel A. Scale bars in (A) and (B) are 500 μm. C, Absolute neuronal density in barrels B-E corrected for tissue shrinkage (see text). Solid lines: control animals. Dashed lines: D-row deprived. Error bars are S.E.M.

Chapter 5

Anatomical characterization of layer 2/3 pyramidal neuron axons

in rat somatosensory cortex

Abstract

Cortical representations of sensory information are often arranged in topographic maps that can be reorganized based on recent experience. During map plasticity in rat primary somatosensory cortex (S1), cortical representations of spared whiskers can expand into neighboring, deprived regions of cortex. In visual cortex (V1), similar map plasticity occurs in response to alterations in visual experience, and involves the remodeling of cross-columnar axonal projections from spared cortical columns into deprived columns. In S1, it is not known whether the expansion of spared whisker representations involves similar cross-columnar axonal remodeling. Here, we examine the axonal arbors of layer 2/3 pyramidal neurons, which are a major source of cross-columnar connectivity, and are known to reorganize during map plasticity in V1. These arbors typically extend beyond single cortical columns in S1, and are thus likely to contribute to neighboring-whisker responses in adjacent cortical columns. We found that patterns of whisker deprivation that are known to induce map plasticity in S1 do not alter the axonal distribution of these neurons, suggesting that the expansion of spared-whisker representations does not involve large-scale reorganization of L2/3 axons.

Introduction

The expansion of cortical representations of behaviorally relevant stimuli is a major component of map plasticity that can involve anatomical restructuring of cortical circuits. Anatomical correlates of map expansion were first shown at thalamocortical projections in visual cortex (V1) following monocular deprivation (Hubel et al., 1977; Shatz and Stryker, 1978; LeVay et al., 1980; Antonini and Stryker, 1993b). More recently, cross-columnar, intracortical projections have also been implicated in the expansion of cortical representations. Evidence exists for experience-dependent reorganization of cross columnar, horizontal layer 2/3 (L2/3) excitatory arbors in visual cortex (Darian-Smith and Gilbert, 1994; Trachtenberg and Stryker, 2001). In other cortical areas, the functional (physiological) strength of horizontal connections has been shown to change with task learning and experience-dependent plasticity (Finnerty et al., 1999; Rioult-Pedotti et al., 2000), though it remains unknown whether these changes in physiological strength involve large-scale restructuring of axon arbors.

Here, we examine whether patters of whisker deprivation that are known to alter the short-term physiological dynamics of horizontal connections modify axonal projections of L2/3 excitatory neurons in rat primary somatosensory cortex (S1) (Finnerty et al., 1999). S1 exhibits robust plasticity following whisker deprivation that includes the expansion of representations of spared whiskers (for review, see Fox, 2002). In rat S1, large facial whiskers are represented by clusters of cells in cortical layer 4 (L4), called barrels, that are arranged in a map isomorphic with the whiskers on the rat's snout (Woolsey and Van der Loos, 1970; Welker and Woolsey, 1974).

Barrels form the center of cortical columns, termed barrel columns, which contain neurons best driven by a single, principal whisker. In animals with normal sensory experience, the receptive fields of neurons in a single barrel column are well tuned to their anatomically appropriate principal whisker. If this principal whisker is plucked or trimmed in adolescent animals, receptive fields of neurons in many cortical layers reorganize. While whisker deprivation has little or no effect in L4, receptive fields of L2/3 cells change in two ways. Neurons in L2/3 of deprived columns first lose responsiveness to the deprived principal whisker (termed principal whisker response depression, PWRD), and later gain responsiveness to neighboring, spared whiskers (termed spared whisker response potentiation, SWRP). Together, these processes shift whisker receptive fields in deprived columns toward neighboring, spared whiskers, thus expanding spared whisker representations (Fox, 1992; Diamond et al., 1994). That this plasticity occurs primarily in L2/3 and not in L4 indicates that these receptive field changes are mediated by functional changes in intracortical, rather than subcortical, circuits.

While much is known about the relevant pathways and mechanisms of PWRD, which involve deprivation-induced weakening of L4-L2/3 synaptic connections (Finnerty et al., 1999; Allen et al., 2003; Bender et al., 2003; Celikel et al., 2004), less is known about SWRP. In L2/3, surround whisker responses require cross-columnar input from neighboring barrel columns, which represent the surrounding whisker (Goldreich et al., 1999; Fox et al., 2003). Thus, cross-columnar projections are hypothesized to mediate surround whisker responses in these layers (Armstrong-James et al., 1992). Anatomically, multiple cross-columnar projections exist from neurons in

L2/3 (Petersen et al., 2003), L4 (Bender et al., 2003), and L5 (Shepherd and Svoboda, 2005). The potentiation of surround whisker responses in deprived columns could be mediated by a strengthening of any of these trans-columnar projections from spared columns to deprived columns. Since the reorganization of L2/3 axonal arbors is such a prominent component of map plasticity in V1, we focused on similar projections in S1.

Here, we examined the horizontal axonal arbors of L2/3 pyramidal neurons, a major projection that mediates long-range connectivity in V1 and intercolumnar connectivity in S1 (Gilbert and Wiesel, 1979; Petersen, 2003). We filled and reconstructed single pyramidal cells in S1 slices from control and whisker deprived rats. We found that these L2/3 neurons extend significant collaterals across cortical columns, supporting a possible role in generating surround whisker responses. However, whisker deprivation did not alter the relative distribution of horizontal projections, suggesting that SWRP does not involve anatomical reorganization of this pathway.

Methods

Single cell labeling and analysis: Protocols for cell fills, immunostaining and reconstruction were as previously reported (Bender et al., 2003). Briefly, Long-Evans rats were raised with normal whisker experience or with D1-6, E1-6, γ, and δ whiskers deprived from P12. At postnatal day (P) 20 to P26, acute slices (400 μm) were cut in an oblique, "across row" plane, such that they contained one barrel from each whisker row (Finnerty et al., 1999; Bender et al., 2003). Barrels were visualized by transillumination, allowing A-E columns to be identified. L2/3 pyramidal neurons at least 100 μm below the surface of the slice were visualized with differential interference contrast optics and filled with biocytin during whole cell recording (Axopatch-200B amplifier [Axon Instruments, Union City, CA], 5-7 MΩ pipettes, 40-60 min recording duration, room temperature). Internal solution contained (in mM): 116 K-gluconate, 6 KCl, 2 NaCl, 20 HEPES, 0.5 EGTA, 4 MgATP, 0.3 NaGTP, 0.3% biocytin (w/v), pH 7.23. Slices were fixed immediately after recording, sectioned at 100 μm, and biocytin was visualized with an avidin-biotin based reaction using diaminobenzidine as a chromogen (DeBello et al., 2001). Alternate sections were treated with osmium tetroxide to visualize barrels (Keller and Carlson, 1999). Cell fills were selected for analysis if axonal staining was consistent along the entire arbor, and no obvious truncation was observed. Neuronal processes were reconstructed using Neurolucida software (Microbrightfield, Williston, VT), and morphometric analysis was performed using custom software in MATLAB (Mathworks, Natick, MA). Axonal bias relative to the soma was calculated as $\left(\frac{2(M)}{T}\right)-1$, where M = all

axon medial to soma, and T = total axon in L1-3. Axonal bias of only axon extending out of home (C) barrel column was calculated as $\left(\frac{2(DE)}{AB+DE}\right)-1$, DE = all axon medial to the home barrel column, and AB = all axon lateral to the home barrel column. Data are shown as mean ± standard error. Student's t-test was used to measure significant differences unless otherwise noted.

Results

To characterize the axonal distribution of L2/3 pyramidal neurons, we filled cells with biocytin during whole cell recordings in 400 μm-thick "across-row" slices of S1 made from rats aged P20-26. Slices were immediately fixed, sectioned at 100 μm, and biocytin was visualized with a DAB-based histochemical reaction. Neuronal morphology was reconstructed across all sections relative to columnar boundaries, defined by the presence of barrels in L4 visualized with osmium tetroxide (Fig. 5.1, 5.2A).

Axonal morphology of L2/3 pyramidal axons

Neurons were filled in L2/3 of the C barrel in across-row slices from control animals (Fig. 5.2B, inset) [normalized horizontal position of filled somata, control: 0.44 ± 0.03 (0 = lateral edge of column, 1 = medial edge); normalized depth from pia: 0.46 ± 0.04 (0 = L3/4 border, 1 = L1/pia border); n = 15]. Neurons extended dense axonal arbors in supragranular layers (L1-3) (e.g., Fig. 5.1C). Cells that extended axon collaterals to deep cortical layers had many branches in L5-6, but minimal arborization in L4, consistent with similar studies in S1 and V1 (e.g., Fig. 5.2A) (Petersen and Sakmann, 2001; Borrell and Callaway, 2002).

To characterize axonal distribution in L1-3, we quantified the length of axon in L1-3 as a function of location tangential to the pial surface (Fig. 5.2B). We also quantified the percentage of the total axon in L1-3 confined to the "home" (C) barrel column (Fig. 5.2C) (column borders were defined as lines extending radially transecting half the distance between adjacent barrel borders; i.e., the midpoint of the

septum), which is a useful measure of columnar axonal targeting (Bender et al., 2003). In control rats, axonal projections were mostly confined to the C barrel column: 82.1 ± 3.4% of all axon in L1-3 was in the home column (Fig. 5.2C) (n = 15). This specificity is lower, but not significantly different than that of axonal branches extending into L1-3 from L4 excitatory neurons [L4 stellate/star pyramid: 91.5 ± 3.2%, n = 12, P20-26; p = 0.06; L4 data from (Bender et al., 2003)]. L2/3 neurons had a larger overall arborization in L1-3 compared to L4 neurons, as measured by total axon length (L2/3 6.7 ± 0.6 mm; L4 total axon: 3.5 ± 0.7 mm; $p < 0.05$), or the absolute horizontal span (AHS) of these projections, defined as the distance between the most lateral and medial axonal branches (L2/3 AHS: 870 ± 70 μm; L4: 580 ± 55 μm, $p < 0.005$). Furthermore, the absolute length of axon in neighboring barrel columns was higher for L2/3 neurons [L2/3: 1190 ± 250 μm; L4: 280 ± 100 μm; $p < 0.005$; L4 data from (Bender et al., 2003)]. These results are consistent with *in vivo* and *in vitro* experiments showing that functional circuits of L2/3 neurons extend beyond column boundaries (Petersen and Sakmann, 2001; Petersen et al., 2003), and suggest that these slices preserve this architecture.

Whisker deprivation does not alter L2/3 axonal topography

To determine if whisker deprivation alters L2/3 axonal topography, we labeled neurons in the C row of across-row slices from animals deprived of D and E row whiskers from P12 to P20-26. Cell position in these slices matched that of cell fills in control rats (normalized horizontal position, DE-deprived: 0.46 ± 0.03; normalized depth from pia: 0.47 ± 0.03; n = 21, $p > 0.4$ vs. control in both axes). This pattern of

deprivation has been shown to alter short-term dynamics of horizontal, L2/3 circuits across the border between spared and deprived cortical areas (Finnerty et al., 1999).

We did not observe any significant differences in axonal distribution or length in DE-row deprived animals. Deprivation did not alter the overall tangential distribution of this projection ($p > 0.9$, Kolmogorov Smirnov test of normalized cumulative tangential axon distributions), the percentage of axon in L1-3 in the C barrel column (Fig. 5.2B, C) (DE-deprived: $79.5 \pm 2.8\%$, $p > 0.5$), or the total axon length within L1-3 (Fig. 5.2D) (5.4 ± 0.3 mm, $p > 0.05$).

Despite the lack of difference in the overall axonal distribution between control and deprived conditions, minor differences in the distribution of axon near the C-D column border are evident in Fig. 5.2B. To examine this possibility in more detail, we examined axonal distribution bias on two levels. First we examined whether all axonal branches in L1-3 were preferentially more medial or lateral than the soma. In control and deprived conditions, axon was equally distributed about the soma (Fig. 5.3A, D) (control axonal bias: -0.01 ± 0.1; DE-deprived: 0.11 ± 0.08; $p > 0.3$; 1 = all axon medial to soma, -1 = all axon lateral to soma). Next, we specifically examined the axonal bias of only those branches that extended into neighboring columns (i.e., axon in A and B barrel columns vs. axon in D and E barrel columns) (Fig. 5.3B, E). No differences were observed in the bias of cross-columnar branches [control: -0.27 ± 0.19, $n = 15$; deprived: -0.1 ± 0.15, $n = 19$ (2 cells had no axon outside home column); $p > 0.4$; 1 = all axon branches extending outside the C barrel column were medial to C column, -1 = all axon branches extending outside the C barrel column were lateral to C column]. Furthermore, the percent of all axon in L1-3 that was medial to the home

barrel column did not change with deprivation (Fig. 5.3C, F) (Control: 5.7 ± 2.0 %; DE-dep: 9.7 ± 1.9 %, $p > 0.1$). These results suggest that DE-whisker deprivation at these ages does not alter the axonal distribution or length of L2/3 pyramidal neurons in the C barrel column.

Discussion

Using single cell reconstruction techniques in across-row slices, we characterized the axonal arbors of L2/3 pyramidal neurons in S1. These axons typically extend beyond single barrel columns, suggesting that they participate in generating surround whisker responses in neighboring barrel columns. Supporting this idea, functional imaging and latency analysis *in vivo* show that whisker-evoked excitatory activity from L4 first activates L2/3 within that barrel column, and only then propagates to adjacent columns (Armstrong-James et al., 1992; Goldreich et al., 1999; Petersen et al., 2003), suggesting that most cross-columnar activity is mediated by horizontal, L2/3 connections.

We did not observe any differences in axonal distribution or length of L2/3 neurons following DE-row deprivation, a manipulation known to drive map plasticity at these synapses (Finnerty et al., 1999). These results stand in contrast with extensive work in V1 demonstrating large-scale experience-dependent axonal plasticity (Darian-Smith and Gilbert, 1994; Antonini and Stryker, 1996; Trachtenberg and Stryker, 2001), but are consistent with an apparent lack of plasticity of L4-L2/3 axonal projections in S1 following whisker deprivation (Bender et al., 2003; Bureau et al., 2004). This may reflect mechanistic differences in map plasticity between S1 and other cortical areas, but alternatively could be a result of a methodological artifact. Typical studies utilizing bulk loading find that axonal rearrangements accompanying map expansion only occurs after several weeks to months of modified sensory experience (Darian-Smith and Gilbert, 1994; Antonini and Stryker, 1996; DeBello et al., 2001), though large-scale remodeling of L2/3 axonal arbors can been seen after as

little as 2 days of altered visual experience (Trachtenberg and Stryker, 2001). Single cell fills using whole-cell techniques, used in S1 studies, can only be made from relatively young animal preparations, and therefore allow only modest sensory deprivation durations (typically 1-2 weeks). Expansion of axonal arbors from spared, C barrel columns has been observed 2 months following vibrissectomy of all but C-row whiskers (Kossut and Juliano, 1999), suggesting that S1 is capable of axonal plasticity, provided long enough deprivation periods.

Our results do not completely rule out anatomical plasticity with such a short deprivation duration. Other forms of anatomical plasticity could have occurred with DE-row deprivation that would not have been detected with current techniques. Experience is known to alter dendritic spine dynamics under some conditions in S1 (Lendvai et al., 2000; Zuo et al., 2005), suggesting that experience does alter anatomy at the ultrastructural level. SWRP is thought to be mediated by long term potentiation (LTP) at transcolumnar excitatory connections, since autophosphorylation-incompetent CaMKII mice lack cortical LTP and have substantially impaired SWRP (Glazewski et al., 2000; Hardingham and Fox, 2004). Since changes in spine size and dendritic complexity have been linked to synaptic plasticity (Tao et al., 2001; Nagerl et al., 2004; Zhou et al., 2004), it is possible that one component of SWRP involves changes in spine size or synaptogenesis at horizontal synapses.

While horizontal L2/3 projections are likely to mediate surround whisker responses, other projections may also contribute to surround receptive field generation and are the primary locus for changes associated with SWRP. Direct, trans-columnar L4-L2/3 excitatory projections exist in S1 and are capable of LTP (Bender et al., 2003;

Hardingham et al., 2003), making them likely alternate pathways for SWRP (Fox, 2002). Furthermore, septal circuits, which have broad, multi-whisker receptive fields, can be modified by full-field unilateral whisker deprivation (Shepherd et al., 2003), raising the possibility that they might be recruited during SWRP. Thus, it is possible that these projections exhibit physiological and/or anatomical plasticity to drive SWRP.

Data presented here indicate that, at these ages, axonal arbors of L2/3 pyramidal neurons in spared barrel columns are not affected by 8-14 day deprivation of neighboring whisker rows. Combined with previous work (Bender et al., 2003), these results suggest that short periods of deprivation drive plasticity via physiological, not large scale anatomical changes (Finnerty et al., 1999; Allen et al., 2003). However, these results do not rule out the possibility that individual arbors reorganize during map plasticity. To determine that, future work should focus on developing techniques that would allow one to image single L2/3 neuronal arbors over long periods of whisker deprivation, similarly to experiments focusing on L5 neurons in S1 (Trachtenberg et al., 2002).

References

Allen CB, Celikel T, Feldman DE (2003) Long-term depression induced by sensory deprivation during cortical map plasticity in vivo. Nat Neurosci 6:291-299.

Antonini A, Stryker MP (1993) Rapid remodeling of axonal arbors in the visual cortex. Science 260:1819-1821.

Antonini A, Stryker MP (1996) Plasticity of geniculocortical afferents following brief or prolonged monocular occlusion in the cat. J Comp Neurol 369:64-82.

Armstrong-James M, Fox K, Das-Gupta A (1992) Flow of excitation within rat barrel cortex on striking a single vibrissa. J Neurophysiol 68:1345-1358.

Bender KJ, Rangel J, Feldman DE (2003) Development of columnar topography in the excitatory layer 4 to layer 2/3 projection in rat barrel cortex. J Neurosci 23:8759-8770.

Borrell V, Callaway EM (2002) Reorganization of exuberant axonal arbors contributes to the development of laminar specificity in ferret visual cortex. J Neurosci 22:6682-6695.

Bureau I, Shepherd GM, Svoboda K (2004) Precise development of functional and anatomical columns in the neocortex. Neuron 42:789-801.

Celikel T, Szostak VA, Feldman DE (2004) Modulation of spike timing by sensory deprivation during induction of cortical map plasticity. Nat Neurosci 7:534-541.

Darian-Smith C, Gilbert CD (1994) Axonal sprouting accompanies functional reorganization in adult cat striate cortex. Nature 368:737-740.

DeBello WM, Feldman DE, Knudsen EI (2001) Adaptive axonal remodeling in the midbrain auditory space map. J Neurosci 21:3161-3174.

Finnerty GT, Roberts LS, Connors BW (1999) Sensory experience modifies the short-term dynamics of neocortical synapses. Nature 400:367-371.

Fox K (2002) Anatomical pathways and molecular mechanisms for plasticity in the barrel cortex. Neuroscience 111:799-814.

Fox K, Wright N, Wallace H, Glazewski S (2003) The origin of cortical surround receptive fields studied in the barrel cortex. J Neurosci 23:8380-8391.

Gilbert CD, Wiesel TN (1979) Morphology and intracortical projections of functionally characterised neurones in the cat visual cortex. Nature 280:120-125.

Goldreich D, Kyriazi HT, Simons DJ (1999) Functional independence of layer IV barrels in rodent somatosensory cortex. J Neurophysiol 82:1311-1316.

Hardingham N, Glazewski S, Pakhotin P, Mizuno K, Chapman PF, Giese KP, Fox K (2003) Neocortical long-term potentiation and experience-dependent synaptic plasticity require alpha-calcium/calmodulin-dependent protein kinase II autophosphorylation. J Neurosci 23:4428-4436.

Hubel DH, Wiesel TN, LeVay S (1977) Plasticity of ocular dominance columns in monkey striate cortex. Philos Trans R Soc Lond B Biol Sci 278:377-409.

Keller A, Carlson GC (1999) Neonatal whisker clipping alters intracortical, but not thalamocortical projections, in rat barrel cortex. J Comp Neurol 412:83-94.

Kossut M, Juliano SL (1999) Anatomical correlates of representational map reorganization induced by partial vibrissectomy in the barrel cortex of adult mice. Neuroscience 92:807-817.

Lendvai B, Stern EA, Chen B, Svoboda K (2000) Experience-dependent plasticity of dendritic spines in the developing rat barrel cortex in vivo. Nature 404:876-881.

LeVay S, Wiesel TN, Hubel DH (1980) The development of ocular dominance columns in normal and visually deprived monkeys. J Comp Neurol 191:1-51.

Nagerl UV, Eberhorn N, Cambridge SB, Bonhoeffer T (2004) Bidirectional activity-dependent morphological plasticity in hippocampal neurons. Neuron 44:759-767.

Petersen CC (2003) The barrel cortex--integrating molecular, cellular and systems physiology. Pflugers Arch 447:126-134.

Petersen CC, Sakmann B (2001) Functionally independent columns of rat somatosensory barrel cortex revealed with voltage-sensitive dye imaging. J Neurosci 21:8435-8446.

Petersen CC, Grinvald A, Sakmann B (2003) Spatiotemporal dynamics of sensory responses in layer 2/3 of rat barrel cortex measured in vivo by voltage-sensitive dye imaging combined with whole-cell voltage recordings and neuron reconstructions. J Neurosci 23:1298-1309.

Rioult-Pedotti MS, Friedman D, Donoghue JP (2000) Learning-induced LTP in neocortex. Science 290:533-536.

Shatz CJ, Stryker MP (1978) Ocular dominance in layer IV of the cat's visual cortex and the effects of monocular deprivation. J Physiol 281:267-283.

Shepherd GM, Svoboda K (2005) Laminar and columnar organization of ascending excitatory projections to layer 2/3 pyramidal neurons in rat barrel cortex. J Neurosci 25:5670-5679.

Shepherd GM, Pologruto TA, Svoboda K (2003) Circuit analysis of experience-dependent plasticity in the developing rat barrel cortex. Neuron 38:277-289.

Tao HW, Zhang LI, Engert F, Poo M (2001) Emergence of input specificity of ltp during development of retinotectal connections in vivo. Neuron 31:569-580.

Trachtenberg JT, Stryker MP (2001) Rapid anatomical plasticity of horizontal connections in the developing visual cortex. J Neurosci 21:3476-3482.

Trachtenberg JT, Chen BE, Knott GW, Feng G, Sanes JR, Welker E, Svoboda K (2002) Long-term in vivo imaging of experience-dependent synaptic plasticity in adult cortex. Nature 420:788-794.

Zhou Q, Homma KJ, Poo MM (2004) Shrinkage of dendritic spines associated with long-term depression of hippocampal synapses. Neuron 44:749-757.

Zuo Y, Yang G, Kwon E, Gan WB (2005) Long-term sensory deprivation prevents dendritic spine loss in primary somatosensory cortex. Nature 436:261-265.

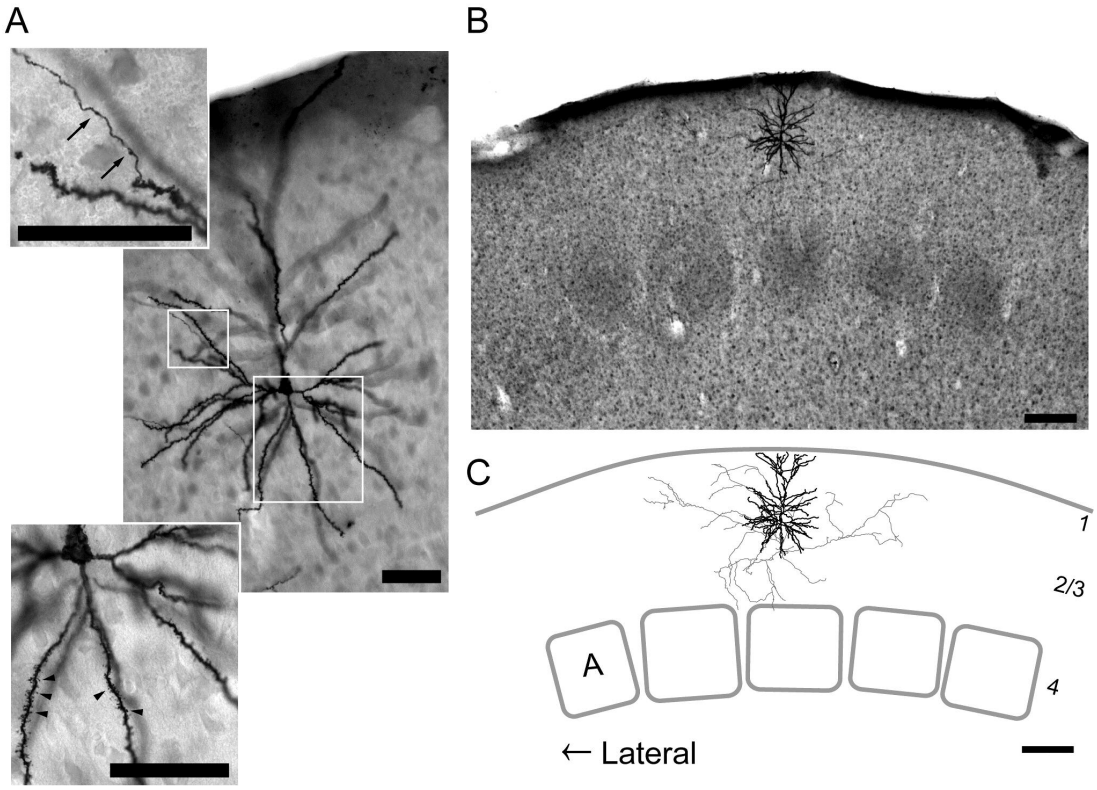

Fig. 5.1: Labeling and reconstruction of a single L2/3 pyramidal cell. A, High power view from single 100 μm section detailing biocytin-filled L2/3 neuron. Insets show axonal boutons (arrows) and dendritic spines (arrowheads). Scale in all panels in (A): 50 μm. B, Low power view of same section showing osmium-intensified barrels in L4. C, Full reconstruction of neuron. Dendrite and soma in black, axon in grey. Barrels and pia in grey. Numbers indicate cortical layers. Scale in (B, C): 200 μm.

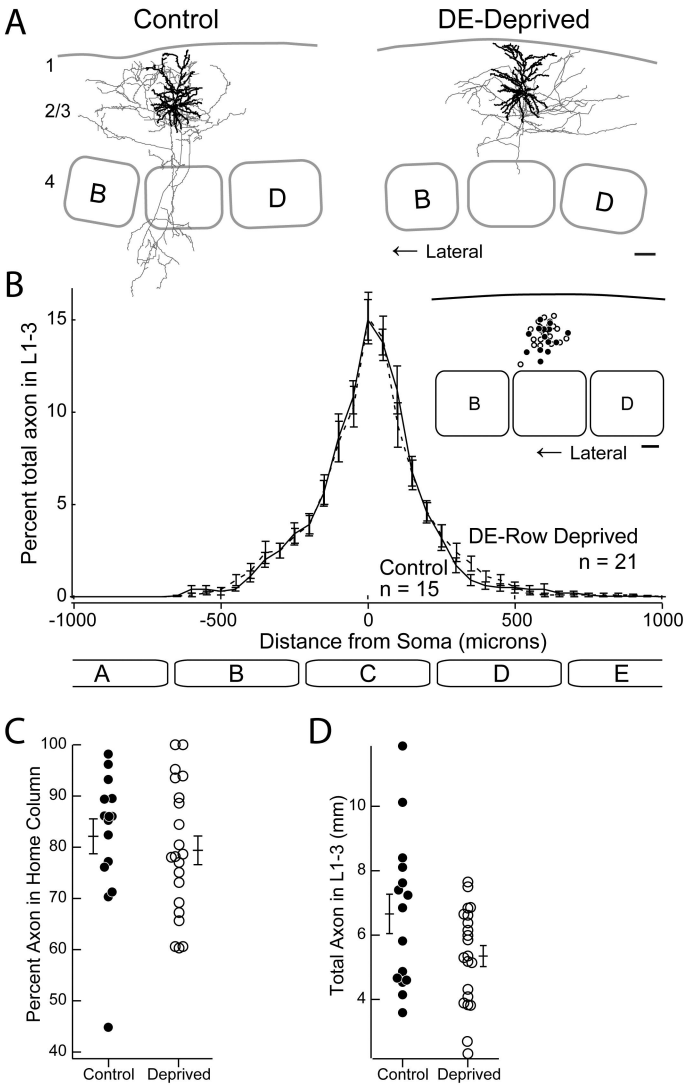

Fig. 5.2: Axonal distribution of L2/3 axons in control and DE-deprived rats. A, Representative reconstruction of L2/3 pyramidal neurons in C barrel column from control (left) and D-E row deprived animals (right). Dendrites and soma in black, axon in grey. Numbers indicate cortical layers. Scale bar: 100 μm. B, Distribution of axon length in L1-3 as a function of tangential distance from average tangential soma position for cells from control (solid) and DE-deprived animals (dashed). Bars are SEM. Ellipses indicate average barrel boundaries. Inset, relative position of soma in C barrel column. Closed circles: control; open: deprived. C, Percent of total axon in L1-3 in the home (C) barrel column. D, Total axon length in L1-3. Bars in C-D are mean ± SEM.

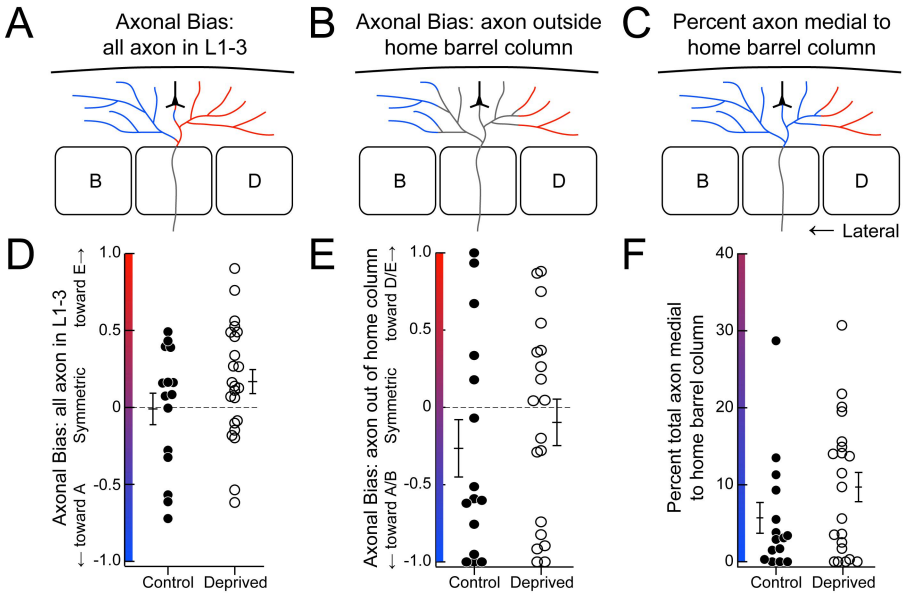

Fig. 5.3: Distribution of axon relative to soma position and column borders. Top: Schematic of L2/3 pyramidal neuron showing axon used in calculating overall axonal bias relative to tangential soma position (A), axonal bias of branches extending outside home column (B), and percent of total axon in L1-3 medial to home column (C). Color code for A-B: Red, medial axon. Blue, lateral axon. Grey, axon not included in analysis. Color code for C: Red, axon medial to home column. Blue, all other axon in L1-3. D-F, quantification of axon bias and percent of total axon medial to home column schematized in A-C, for control and deprived conditions. Bars are mean ± SEM.

Chapter 6

Concluding Remarks

Work presented here characterizes how whisker deprivation drives weakening of layer 4 (L4) to L2/3 synapses. Deprivation decreases presynaptic, but not postsynaptic, efficacy of L4-L2/3 synapses, leading to an overall decrease in the bulk functional efficacy of this projection (Allen et al., 2003; Shepherd et al., 2003). Deprivation does not alter neural number or axonal morphology of L4 excitatory neurons, and produces only minor changes in the dendritic morphology of L2/3 neurons (Maravall et al., 2004). Together, these data suggest that deprivation weakens synapses largely by changing the strength of individual synapses, rather than by changing the physical wiring of L4-L2/3 connections.

Substantial evidence now exists suggesting that L4-L2/3 synapses are weakened during map plasticity by long term depression (LTD) induction *in vivo*. Deprivation-induced weakening and spike timing dependent LTD (t-LTD) are both expressed presynaptically at L4-L2/3 synapses (Bender et al., submitted), and whisker deprivation occludes subsequent attempts to induce LTD (Allen et al., 2003). Furthermore, acute whisker deprivation has been shown to change L4 and L2/3 spike correlations, reversing normal L4-leads-L2/3 spike timing (Celikel et al., 2004). This reversal quantitatively predicts that whisker deprivation induces t-LTD at L4-L2/3 synapses, given the known learning rule for STDP at these synapses (Feldman, 2000; Celikel et al., 2004). Thus, these data provide support for the hypothesis that LTD-mediated synaptic depression is an important component of developmental map plasticity in S1, as well as other sensory cortices (Heynen et al., 2003).

A working hypothesis for how LTD is induced by deprivation is summarized in Fig. 6.1. In this hypothesis, feedforward connectivity from thalamus to L4-L2/3

ensures that during normal sensory use, most L4 spikes occur before L2/3 spikes. Deprivation causes immediate reversal in firing order for L4 and L2/3 neurons (illustrated) and decreases overall firing correlations (not shown), with only modest changes in spike rate (Celikel et al., 2004). What cortical circuits mediate the firing order reversal are not yet clear, although trans-columnar excitatory inputs from surrounding columns with intact whiskers seem well-suited to mediate the residual L2/3 responses in deprived columns (Fox, 2002). We hypothesize that these acute changes in spike timing, over several days, drive spike timing-dependent LTD at L4-L2/3 synapses, and that this LTD is a primary mechanism for weakening of responses to the deprived principal whisker in L2/3.

If whisker deprivation drives LTD *in vivo*, why does deprivation require at least 4 days to significantly depress L4-L2/3 synapses, whereas t-LTD can be induced within minutes *in vitro* (Feldman, 2000; Bender et al., submitted)? One likely factor is that in behaving animals, only a small fraction of total spikes in a given S1 column are driven by whisker deflection, with the rest being spontaneous or driven by whisker self-motion (Fee et al., 1997). Because deprivation only alters the timing of whisker-driven spikes, deprivation may produce only relatively small biases of overall spiking statistics, leading to relatively slow accrual of timing-dependent LTD. Another related factor is that ongoing, spontaneous network activity is known to powerfully reverse recently induced LTP and LTD, which could slow the accrual of these forms of plasticity *in vivo* (Xu et al., 1998; Zhou et al., 2003). Third, receptive field plasticity is known to be faster when whiskers are plucked singly or in a checkerboard pattern, so that each deprived column has many spared neighboring columns (Fox, 2002). In

these studies of deprivation-induced synaptic weakening *in vivo*, we plucked whole rows of whiskers, thus leaving fewer spared whiskers around each deprived whisker.

Differences in the speed of LTD induction and experience-based depression may also indicate that LTD in not involved in map plasticity. Current evidence only shows that deprivation-induced weakening of these synapses resembles LTD; additional experiments testing whether LTD is causally required for plasticity are necessary. In visual cortex, this strategy has produced mixed results, so the causality of LTD in ocular dominance plasticity remains unknown (Hensch and Stryker, 1996; Renger et al., 2002; Fischer et al., 2004). To test causality at L4-L2/3 synapses in S1, it will be necessary to selectively block or manipulate LTD, either pharmacologically or genetically, and to determine if whisker map plasticity is altered or impaired. To do so, it will be critical to expand our current understanding of the molecular basis of LTD at L4-L2/3 synapses, in order to develop more selective and effective reagents that interfere with LTD. These reagents could then be used to probe the role of LTD in cortical map plasticity.

References

Allen CB, Celikel T, Feldman DE (2003) Long-term depression induced by sensory deprivation during cortical map plasticity in vivo. Nat Neurosci 6:291-299.

Bender VA, Bender KJ, Braiser DJ, Feldman DE (submitted) Two coincidence detectors for STDP in somatosensory cortex.

Celikel T, Szostak VA, Feldman DE (2004) Modulation of spike timing by sensory deprivation during induction of cortical map plasticity. Nat Neurosci 7:534-541.

Fee MS, Mitra PP, Kleinfeld D (1997) Central versus peripheral determinants of patterned spike activity in rat vibrissa cortex during whisking. J Neurophysiol 78:1144-1149.

Feldman DE (2000) Timing-based LTP and LTD at vertical inputs to layer II/III pyramidal cells in rat barrel cortex. Neuron 27:45-56.

Fischer QS, Beaver CJ, Yang Y, Rao Y, Jakobsdottir KB, Storm DR, McKnight GS, Daw NW (2004) Requirement for the RIIbeta isoform of PKA, but not calcium-stimulated adenylyl cyclase, in visual cortical plasticity. J Neurosci 24:9049-9058.

Fox K (2002) Anatomical pathways and molecular mechanisms for plasticity in the barrel cortex. Neuroscience 111:799-814.

Hensch TK, Stryker MP (1996) Ocular dominance plasticity under metabotropic glutamate receptor blockade. Science 272:554-557.

Heynen AJ, Yoon BJ, Liu CH, Chung HJ, Huganir RL, Bear MF (2003) Molecular mechanism for loss of visual cortical responsiveness following brief monocular deprivation. Nat Neurosci 6:854-862.

Maravall M, Koh IY, Lindquist WB, Svoboda K (2004) Experience-dependent changes in basal dendritic branching of layer 2/3 pyramidal neurons during a critical period for developmental plasticity in rat barrel cortex. Cereb Cortex 14:655-664.

Renger JJ, Hartman KN, Tsuchimoto Y, Yokoi M, Nakanishi S, Hensch TK (2002) Experience-dependent plasticity without long-term depression by type 2 metabotropic glutamate receptors in developing visual cortex. Proc Natl Acad Sci U S A 99:1041-1046.

Shepherd GM, Pologruto TA, Svoboda K (2003) Circuit analysis of experience-dependent plasticity in the developing rat barrel cortex. Neuron 38:277-289.

Xu L, Anwyl R, Rowan MJ (1998) Spatial exploration induces a persistent reversal of long-term potentiation in rat hippocampus. Nature 394:891-894.

Zhou Q, Tao HW, Poo MM (2003) Reversal and stabilization of synaptic modifications in a developing visual system. Science 300:1953-1957.

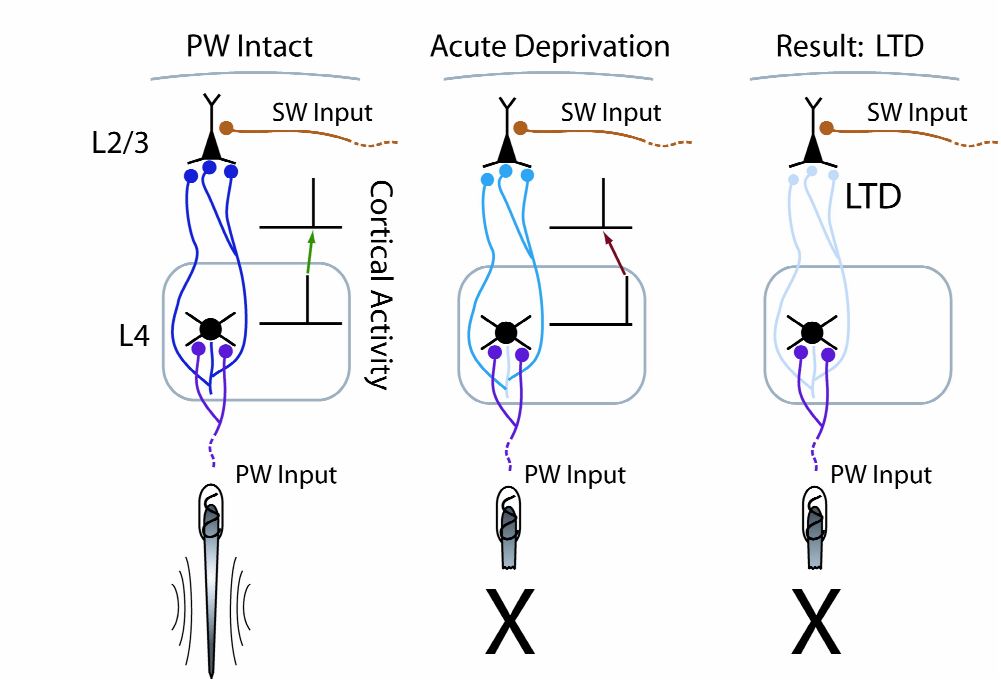

Fig. 6.1: Model for deprivation-driven induction of LTD at L4-L2/3 synapses *in vivo*. Left, When all whiskers are intact, deflection of the principal whisker drives spikes from L4 neurons, which in turn activate L2/3 neurons via ascending, feedforward L4-L2/3 synapses. Thus, L4 neurons tend to spike before L2/3 neurons. Middle, whisker deprivation is known to acutely alter L4-L2/3 firing correlations in two ways: firing order reverses, so that L2/3 neurons tend to fire before L4 neurons (illustrated), and L4 and L2/3 spike trains become decorrelated (not illustrated). Together, these changes in spike timing are hypothesized to drive spike timing-dependent LTD at L4-L2/3 synapses (right panel).